AD-779 628

HYDRAULICS SYSTEM CONTROLS STUDY

Oklahoma State University

Prepared for:

Army Mobility Equipment Research and Development Center

December 1973

FPRC-3M2

HYDRAULIC SYSTEM CONTROLS STUDY

PREPARED BY PERSONNEL OF

FLUID POWER RESEARCH CENTER
OKLAHOMA STATE UNIVERSITY
STILLWATER, OKLAHOMA

December, 1973

ANNUAL REPORT

November 1972 – November 1973

APPROVED FOR PUBLIC RELEASE: DISTRIBUTION UNLIMITED

PREPARED FOR

U.S. ARMY MOBILITY EQUIPMENT RESEARCH
AND DEVELOPMENT CENTER
Fort Belvoir, Virginia 22060

ib

UNCLASSIFIED

SECURITY CLASSIFICATION OF THIS PAGE (When Data Entered)

REPORT DOCUMENTATION PAGE	READ INSTRUCTIONS BEFORE COMPLETING FORM
1. REPORT NUMBER: FPRC-3M2	2. GOVT ACCESSION NO.
3. RECIPIENT'S CATALOG NUMBER: AD 779628	
4. TITLE (and Subtitle): Hydraulics System Controls Study	5. TYPE OF REPORT & PERIOD COVERED: Annual, Section II of 5, 9 Nov. 1972 to 8 Nov. 1973
	6. PERFORMING ORG. REPORT NUMBER: FPRC-3M2
7. AUTHOR(s): Staff of Fluid Power Research Center	8. CONTRACT OR GRANT NUMBER(s): Contract No. DAAK02-72-C-0172
9. PERFORMING ORGANIZATION NAME AND ADDRESS: Fluid Power Research Center, Oklahoma State University, Stillwater, Oklahoma 74074	10. PROGRAM ELEMENT, PROJECT, TASK AREA & WORK UNIT NUMBERS
11. CONTROLLING OFFICE NAME AND ADDRESS: Directorate of Research, Development, and Engr., U.S. Army Mobility Equipment Command, Ft. Belvoir, Virginia 22060	12. REPORT DATE: December, 1973
	13. NUMBER OF PAGES: 142
14. MONITORING AGENCY NAME & ADDRESS (if different from Controlling Office)	15. SECURITY CLASS. (of this report): Unclassified
	15a. DECLASSIFICATION/DOWNGRADING SCHEDULE

16. DISTRIBUTION STATEMENT (of this Report)

Approved for Public Release: Distribution Unlimited

17. DISTRIBUTION STATEMENT (of the abstract entered in Block 20, if different from Report)

18. SUPPLEMENTARY NOTES

N/A

19. KEY WORDS (Continue on reverse side if necessary and identify by block number)

Contamination Control
Contaminant Life Expectation
Contaminant Wear
Component Testing
Computer-Aided Procurement
Digital Simulation
Duty Cycle
Dynamic Thermal Analysis
Filter Evaluation
Fluid Power

(over)

20. ABSTRACT (Continue on reverse side if necessary and identify by block number)

The purpose of the Oklahoma State University-U.S. Army Mobility Equipment Research and Development Center Program is to provide the military with tools for scientific evaluation activity generated and promulgated a number of test procedures for evaluating components like pumps, valves, cylinders, filters, etc. The present phase while continuing this work reports on efforts to evaluate total systems.

This is the second section of the complete annual report which is divided

DD FORM 1 JAN 73 1473 EDITION OF 1 NOV 65 IS OBSOLETE

UNCLASSIFIED

SECURITY CLASSIFICATION OF THIS PAGE (When Data Entered)

Key Words

Heat Exchanger
Hydraulic Pumps
Hydraulic Systems
Modeling
Numerical Representation
Performance Appraisal
Semi-Empirical Models
Service Life
Simulation
System Modeling
Valves

into the following five self-contained sections:

Section I: Hydraulic Cylinder and Seals Specification Study
Section II: Hydraulic System Controls Study
Section III: Hydraulic System Noise Study
Section IV: Hydraulic Hose Specification Study
Section V: On-Board Hydraulic System Monitor Study

A detailed account of the project activities associated with computer-aided procurement is presented in this section.

The first chapter deals with system performance evaluation, and describes how a new concept in modeling--numerical representation--is used for component and system simulation. Results of experimental verification on a typical system are included.

Another chapter details the work accomplished in thermal analysis of hydraulic systems. The development of a semi-empirical model for a heat-exchanger is included along with the dynamic thermal analysis of a total system.

The final chapter is devoted to component service life evaluation and presents the results of various tests on hydraulic pumps, valves, and filters. Based upon this work, techniques have been proposed which are useful under a variety of operating conditions. A comprehensive discussion revealing the influence of a machine's duty cycle on the contaminant sensitivity of components is included.

TABLE OF CONTENTS

LIST OF TABLES

LIST OF FIGURES

LIST OF FIGURES

(Continued)

FOREWORD

This report was prepared by the staff of the Fluid Power Research Center of the School of Mechanical and Aerospace Engineering at Oklahoma State University of Agriculture and Applied Science. The study was initiated by the Mobility Equipment Research and Development Center, Fort Belvoir, Virginia. Authorization for the study reported herein was granted under Contract No. DAAK02-72-C-0172. The time period covered by this report is from 9 November 1972 to 8 November 1973.

The Contracting Officer's Representative was Mr. Hansel Y. Smith, and Mr. John Karhnak served as the Contracting Officer's Technical Representative. In addition, Mr. Paul Hopler has effectively represented the Contracting Officer both administratively and technically in various phases of this contract. The active participation of Messr . Smith, Karhnak, and Hopler during critical phases of this work contributed significantly to the overall success of the program.

In addition to pursuing the goals and objectives of this contract to fruition, members of the Fluid Power Research Center (FPRC) staff have also participated with MERDC personnel in various activities not supported by the program. These efforts were financed through the Basic Fluid Power Research (BFPR) Program, which is a consortium of some 35 industrial fluid power users and suppliers who have sponsored work at the FPRC for the past seven years. These companies have recognized the merits and the derivable benefits of this Hydraulic Specification Study Program and have readily contributed both time and money to its success.

A great many fluid power component test procedures have been developed and verified as a result of this program. The guidance and advice of the fluid power industry were heavily relied upon during all phases of this development and verification work. However, true industrial acceptance can only be achieved when such test procedures receive national and internation adoption by recognized standards-making bodies of the fluid power industry. To this end, members of the FPRC staff have worked closely with the National Fluid Power Association (NFPA), the Society of Automotive Engineers (SAE), the American National Standards Institute (ANSI), and the International Standards Organization (ISO).

Specifically, in behalf of MERDC and the fluid power industry, the FPRC has played an active role in the activities of following committees and sub-committees:

* Filter and Separator Section of NFPA
* Contamination Coordinating Committee of NFPA
* Pump Section of NFPA
* Valve Section of NFPA

* Sound Measurement Coordinating Committee
* Sub-Committee IV (Hydraulic Components) of SAE
* Sub-Committee 6 of TC 131 (Fluid and Contamination Control) of ISO
* Sub-Committee 8 of TC 131 (Component Testing) of ISO
* Working Group 1 of SC-6 (Filter Performance Testing) ISO/TC 131
* Working Group 1 of SC-8 (Sound Measurement) ISO/TC 131

During the reporting period of this document, the main efforts in technical information transfer have been directed toward the areas of filter performance, pump contaminant sensitivity, valve performance, and sound measurement. The results of this work, to date, served as the basis for eight nationally and internationally accepted test procedures. The fruits of such accomplishments should prove very beneficial to MERDC in their quest for adequate component control in the procurement of commercial equipment.

The FPRC team has also assisted MERDC in their effort to effectively monitor and evaluate the results of tests using test procedures developed under this program. For example, a computer program was developed which rigorously examines the data accumulated during a multi-pass filter performance test. This program not only reduces the data to a usable form but also evaluates the recorded data to see that all of the test requirements have been met. The success of this computer program together with the industrial acceptance of the filter test proceudres has allowed MERDC to issue a military filter specification and establish a well received QPL program.

This report represents only one of five major sections of the annual report on the Hydraulic Specification Program. The titles of the various sections are listed below:

SECTION I: Hydraulic Cylinder and Seals Specification Study
SECTION II: Hydraulic System Controls Study
SECTION III: Hydraulic System Noise Study
SECTION IV: Hydraulic Hose Specification Study
SECTION V: On-Board Hydraulic System Monitor Study

The study represented by this report was conducted under the general guidance of Dr. E. C. Fitch, Program Director. Mr. S. K. R. Iyengar not only served as Program Manager for the performance area but also guided the efforts of Mr. D. G. Miller in the thermal area. Mr. R. K. Tessmann was responsible for the technical management of the service life area. These gentlemen were ably supported by the valve, pump, and contamination analysis laboratories as well as the digital computing facilities of the Fluid Power Research Center. Three key individuals making significant contributions to the success of the systems work were Messrs. Bill Koger, Brian Foord, and Stan Wendt.

This report presents a detailed account of the project activities associated with the computer-aided procurement area. The direct numer-

ical representation concept of component and system modeling is discussed together with the experimental verification. Hydraulic component and system thermal models were developed to predict the performance of operating systems under extreme temperatures reflected by actual machine duty cycles. Service life concepts for hydraulic components are presented and used to evaluate the contaminant life expectations of a hydraulic system exposed to realistic field environments.

CHAPTER I

- INTRODUCTION -

From the outset of the OSU-MERDC Hydraulics Program, the main objective has been to provide the product engineer with tools by which he can insure adequate hydraulic component controls and/or appraise the value of a hydraulic system. A great deal of the initial effort was directed toward the development and verification of component test procedures, which are necessary for the desired component control. Eighty test procedures were developed which covered all of the critical operating characteristics of every major hydraulic component.

Based upon the experience derived from the development of these component test procedures, a concept for total hydraulic system appraisal was developed. This concept utilizes computer-aided techniques and was introduced in Section II, Hydraulic System Control Study, in the 1972 Annual Report to MERDC. This program represents a comprehensive analytical approach to fluid power system evaluation, thus aiding the product engineer in making practical and valid procurement decisions during either software or hardware stages of system design.

In order to fully develop and implement the CAP concept, it was necessary to divide it into three parallel efforts -- system performance, thermal analysis, and service life. Each of these areas was investigated during this phase of the current OSU-MERDC Hydraulics Program. This section of the 1973 Annual Report on the Hydraulic Specification Program includes a complete discussion of the activities and accomplishments in each area.

The system performance phase was directed toward the development of procedures and techniques to appraise the operating characteristics of hydraulic systems. In general, previous attempts in this regard have utilized complex mathematical relationships to describe the performance of each component of a system. These component models were interfaced, sometimes with great difficulty, to form an even more complex system model. Basic research in modeling at the Fluid Power Research Center has resulted in the formulation of a new approach to modeling which is ideally suited for the realistic simulation of large hydraulic systems. This technique relies on the basic test data, which stem from performance tests on the components and is thus termed Direct Numerical Representation (DNR). Chapter 2 clearly defines and explains the DNR concept and illustrates its application to specific hydraulic systems.

One of the major concerns in the fluid power industry today is the trend toward higher system operating temperatures, as hydraulic systems

are designed to transmit greater horsepower. In the past, the system designer has utilized the only tool available -- steady-state thermal analysis -- to estimate the temperature which will be prevalent in the system. There is more than sufficient evidence to suggest that this is inadequate. The effort in the thermal analysis phase of this program has produced and verified a technique to perform a dynamic thermal analysis on both a heat exchanger and the total system. Such a procedure is capable of predicting system temperature during the transient operation, such as occurs during short peak power demand periods as well as in evaluating the influence of ambient temperature changes. The activities and accomplishments of the thermal analysis phase are discussed in Chapter 3.

In the evaluation of either hydraulic components or systems, service life is an important consideration. In a hydraulic system, service life is usually dependent upon the degradation in performance of one or more of its components. Therefore, from an engineering standpoint, the service life is the operating time during which the degree of performance degradation is acceptable. Ignoring catastrophic failure, component service life is directly related to both the contaminant wear tolerance of the fluid-exposed elements and the contamination level of the circulating fluid. However, previous work has shown that the contaminant sensitivity of hydraulic components and the contaminant level of the system are both influenced by the dynamic operation of the system. Chapter 4 is concerned with the influence of these duty cycles on the service life of pumps and valves. In addition, the effect of environmental ingression on filter performance is discusses in Chapter 4.

It is felt that the activities and accomplishments of the hydraulic system controls study of the Hydraulic Specification Program have made a considerable contribution toward the realization of a complete and useful computer-aided procedure program. Recommendations have been made in the body of this report where further work or additional studies are required. The implementation of a computer-aided procurement program by anyone who must buy hydraulic components or systems should provide a savings in both time and money.

CHAPTER II

COMPUTER-AIDED PROCUREMENT

(SYSTEM PERFORMANCE ANALYSIS)

- INTRODUCTION -

The system performance phase of the Computer-Aided Procurement (CAP) effort was primarily concerned with ascertaining the variations in diverse physical quantities in a hydraulic system as it goes through a specified duty cycle. Using suitably developed mathematical models for various components of a system, the total system can be simulated to give information which would otherwise require extensive testing. Certain physical quantities -- usually pressures, flows, and displacements--can be shown to characterize a system and secondary quantites like power, efficiency and heat generation can be calculated therefrom. The purpose of a mathematical model is to show how the various physical quantities change as the system is subjected to a certain operating cycle. Mathematical models for systems can be developed in two ways: first, by analyzing the system as a whole and second, by synthesizing the system model using models for components. Both methods have their uses, though the second is much more informative. Mathematical models can also be classified as analytical, empirical, or semi-empirical. Most of the modeling work to date, has been done by the component designer and has usually resulted in analytical models. These are generally cumbersome to use and difficult to interface with other component models. Hence, they are almost unusable for performance appraisal of either the component or of the total system. Basic research in modeling at the Fluid Power Research Center, Oklahoma State University has resulted in the development of a new appraoch to modeling which seems ideally suited for simulating large-scale systems using component models. This has been called "Direct Numerical Representation" or DNR for short.

Numerical methods are often harder to explain than analytic or graphical methods, as it is very easy to get bogged down in the arithmetical calculations. Merely furnishing the algorithms involved, on the other hand, would leave the reader with no appreciation of the nature and extent of data handling. A complete and rigorous treatment of the mathematical foundation of DNR is given in Refs. 1 and 2. The next section gives the results of the mathematical analysis and its implications. As an illustration, a simple dynamic system and its DNR are discussed in Appendix A. The application of the DNR concept to modeling a large system is validated in the section following the mathematical analysis discussion.

Experimental work is the foundation of model verification and is the subject of the final section.

- MATHEMATICAL ANALYSIS -

The purpose of a model, any model, is to convey certain information about a physical object (real or conceptual). There are a number of physical attributes associated with a physical object, and our concern is only with those attributes that are measurable, e.g. length, weight, temperature, pressure, velocity, etc. Examples of unmeasurable ones are smell, aesthetic appeal, etc. The physical variables as attributes of an object are not entirely independent of each other. Thus, the velocity of a moving body (one attribute) depends on the exposed surface (a composite attribute) and its mass. For physical systems, it is extremely useful to have some scheme of describing how certain attributes of the system are affected by changes in other attributes. The former are called inputs and the latter outputs. Circumstances and convenience often dictate which attributes should be (advantageously) treated as inputs and which as outputs. The purpose of the model is to furnish an algorithm whereby the outputs of the physical system can be calculated from a knowledge of the inputs. Since a model essentially conveys information, the "efficiency" of a model may be judged first by its accuracy, second by its information content, and third by its complexity.

The most familiar form of a model is the equation. A second form which is extensively used but not generally recognized as being a model is graphical display. A close examination will reveal that the information content in these two representations is equivalent. However, there are a number of cases where graphical presentations are more useful than equations. On the other hand, equations are particularly compact and often suitable for machine computations. Furthermore, for analytical work, equations can be manipulated in a variety of ways to yield results which would not be apparent at a first glance.

The advent of the high-speed digital computer allows one to investigate yet another mode of presenting information about a physical object -- a numerical mode. In this mode, the outputs of the system can be considered to be the contents of a number of pigeonholes. Each pigeonhole has a unique tag -- the input. Given an input, one can use the tag to locate the output. An example of this form of representation would be a table of inputs and outputs. The advantages of this form of representation are not immediately obvious. On the other hand, its disadvantages are readily seen. It is certainly not as compact as an equation, and it does not give the "big picture" like a graphical display. Its information content is also limited -- an equation can give infinite input-output data and, theoretically, so can a graph, but an array of numbers is finite. Consider now its advantages:

1. A simple algorithm can always be developed to generate data

points from the arrays of numbers; various interpolation and extrapolation schemes are available for this task.

2. An equation or graph is often a "best" fit for data. Thus, mathematical manipulations would be extremely cumbersome if every orifice in a fluid power system was modeled by complex equations rather than the simple square law. Graphs cannot be directly fed as information to a digitial computer; whereas, strings of numbers can be so handled. Also, all test data can be stored as opposed to equations or graphical displays which lose much information and accuracy in the process of fitting.

3. Arrays of numerical data can always be used to produce graphs or equations; the reverse process is not always useful due to the approximations used.

The numerical mode of presenting information about physical objects was conceived at the Fluid Power Research Center and is termed Direct Numerical Representation (DNR). The concept for the DNR stemmed from a state of frustration in working with both the equation and graphical modes. Graphical techniques are not compatible with machine computations. Furthermore, the equations which accurately describe a non-linear fluid power system are by necessity high-order and often defy solution. A DNR is defined as a numerical characterization of the output values of a system as reflected by its inputs and previous time histories.

Digital computers are designed to handle numbers and cannot directly manipulate differential equations which form the basis of most dynamic models. Fortunately however, it is possible to discretize the equations to a form compatible with digital computation techniques. After such discretization any system can be modeled by the following equation:

$$Y(t) = F\left\{ U(t), U(t - \Delta t) \ldots U(t - p\Delta t), Y(t - \Delta t) \ldots Y(t - q\Delta t)\right\} \quad (1)$$

Where:

t = time
Y = output
U = input
F = a functional relationship
Δt = time increment
p, q = integers ($p < q$)

In words, Eq. (1) says that the output at any time t is a function of the input at that time and also the values of the input and output at previous points in time to a total of p and q time increments respectively. Note that Y and U can be vectors. In the more general formulation the number of previous points may be different for each element of the U and Y vectors.

Let:

$U = (u_1, u_2, \ldots, u_r)$ i.e. an r-vector
$Y = (y_1, y_2, \ldots, y_m)$ i.e. an m-vector
q_i = number of previous points for y_i
p_i = number of previous points for u_i

Equation (1) now becomes:

$$\begin{pmatrix} y_1(t) \\ \vdots \\ y_m(t) \end{pmatrix} = F \begin{pmatrix} U_1(t),\ U_1(t-\Delta t),\ldots,\ U_1(t-p_1\Delta t), \\ U_2(t),\ U_2(t-\Delta t),\ldots,\ U_2(t-p_2\Delta t), \\ \vdots \\ U_r(t),\ U_r(t-\Delta t),\ldots,\ U_r(t-p_r\Delta t), \\ y_1(t-\Delta t),\ y_1(t-2\Delta t),\ldots,\ y_1(t-q_1\Delta t), \\ y_m(t-\Delta t),\ y_m(t-2\Delta t),\ldots,\ y_m(t-q_m\Delta t) \end{pmatrix} \quad (2)$$

So far no assumptions have been made about the function F -- which is actually an m-vector of scalar functions $f_1, f_2, \ldots, f_m$. It will now be necessary to assume that F has a Taylor Series expansion which permits linearization of Equation (2) in a certain region of operation to give:

$$\begin{pmatrix} y_1(t) \\ \vdots \\ y_m(t) \end{pmatrix} = \begin{pmatrix} y_1(t-\Delta t) \\ \vdots \\ y_m(t-\Delta t) \end{pmatrix} + \begin{pmatrix} a^1_{11}\cdots a^1_{1p_1} & a^1_{21}\cdots a^1_{rp_r} \\ a^2_{11}\cdots a^2_{1p_1} & \cdots \quad a^r_{rp_r} \\ a^m_{11}\cdots a^m_{1p_1} & \cdots a^m_{r1} \cdots a^m_{rp_r} \end{pmatrix}$$

$$\begin{pmatrix} U_1(t) \\ \vdots \\ U_1(t-P_1\Delta t) \\ U_2(t) \\ \vdots \\ U_n(t-p_n\Delta t) \end{pmatrix} + \begin{pmatrix} b^1_{11}\cdots b^1_{1q_1} & b^1_{21}\cdots b^1_{rq_r} \\ b^2_{11}\cdots b^2_{1q_1} & b^2_{21}\cdots b^2_{rq_r} \\ \vdots & \\ b^m_{11}\cdots b^m_{1p_1}\cdots & b^m_{rq_r} \end{pmatrix} \begin{pmatrix} y_1(t-\Delta t) \\ y_1(t-2\Delta t) \\ y_1(t-q_1\Delta t) \\ y_2(t-\Delta t) \\ \vdots \\ y_m(t-q_m\Delta t) \end{pmatrix} \quad (3)$$

or more concisely,

$$y = [A \vdots B]\, U_A \quad (4a)$$

$$U_A \triangleq \begin{bmatrix} U \\ \vdots \\ Z \end{bmatrix} \quad (4b)$$

where A and B are matrices and U_A is known as the augmented input vector. Note that U_A is comprised of the r-vector and a vector Z, called the augmentation.

If the analytic model of the system or component was available it would be a simple though tedious matter to calculate the elements of the A

and B matrices as functions of the input and output at that point in time. Of much more significance however, is the using of test data to identify these parameters.

Test data typically consists of time histories of the input and output for a component. It is important to emphasize that all inputs and outputs be recorded during a dynamic test. These can be stored in the computer as arrays of inputs and outputs. After some preliminary computation (e.g. multiplying by scale factors to convert transducer outputs to physically meaningful numbers) the arrays be compressed to remove redundancies. These arrays then comprise the DNR for the component and contain all the information collected during the testing. However, this information is not directly usable in simulating either a component or a system. The reason is that the inputs selected for the simulation are rarely those for which test data is available and consequently some interpolation scheme has to be used. Any of the conventional vector interpolation schemes are usable provided the data in the DNR is converted to an algebraic mapping as characterized in Eq. (1). This is achieved by augmenting the input with previous values of the output and input. The number of previous points chosen is a matter of judgment. For low-order models, one or two would be sufficient. Using the DNR, the augmented -- input-output -- arrays can be built-up and it is a relatively simple matter to perform the interpolation. The easiest way of doing this is linear interpolation and involves identifying the A and B matrices in Eq. (4) from the augmented input-output arrays. Once they are identified Eq.(3) can be used to update the output vector. The procedure can then be iterated till the duty cycle is completed.

Though the method is conceptually simple, considerable difficulties may be faced in implementation, especially in the case of nonlinear systems. A few of the factors that affect computerization of the algorithm are:

1. Step size for discretization. Too large a step size can give erroneous results which can increase to very large values as the duty cycles is simulated. On the other hand too small a step size cannot only be wasteful but can also result in poor identification of the A and B matrices. In the case of nonlinear systems step sizes which are satisfactory in one region of operation may be unsuitable in another.

2. Interpolation Region. Test information is stored in only a finite number of data points and consequently some form of interpolation is unavoidable. Interpolation implicitly requires the "fitting" of some geometric 'surface' to the augmented input-output points. Since a global fit is virtually impossible only a local fit is attempted. The selection of the region of fit influences the success and accuracy of the interpolation scheme to a considerable extent. Too small a region can mean recalculating the A and B matrices needlessly and can also introduce errors therein; too large a region will give poorly fitted surfaces.

3. Scaling. The quantities in the DNR arrays are always physically meaningful, e.g. pressure, flows, displacements, etc. However, not all of them attain or change over a similar range of values. Thus, spool displacements of an actuating valve may vary only a quarter of an inch, yet the system pressure may vary over a range of 100 to 3000 psi. Without proper scaling, the interpolation scheme can give wrong results. Inspection of the test data can usually show the kind of scaling required, though no hard and fast rules can be made.

4. Accuracy. Generally speaking, higher accuracy demands smaller step sizes, smaller regions, and smaller allowable errors in identifying the A and B matrices. However, computing time and expense can increase disproportionately and the accuracy of the test data places an upper constraint on the attainable accuracy.

- SIMULATION OF A MULTI-INPUT, MULTI-OUTPUT SYSTEM USING DNR -

A single-input, single-output, linear system and its DNR have been presented in Appendix A of this report. Its extension to Multi-input system requires that the input and augmentation be treated as vectors. For multi-output systems, it is sufficient to consider one output at a time, though the augmentation may involve values of the other outputs at previous points in time (see Eq. (1)). The interpolation scheme can be exactly the same as that described in the previous section.

To illustrate the above features, a multi-input system comprised of a pump, an open-center valve, and actuators is analyzed. The same system will be used to develop static and dynamic models and, later, to synthesize a system model using individual component models.

Fig. 2-1 shows the simplified circuit schematic of the open-center system. The actuators are two single-acting cylinders, mechanically coupled so that they effectively function like a double-acting cylinder with equal areas on either side. The effort needed to operate the directional control valve is considered negligible; thus, the human operator provides the system with a displacement input. However, this is not the only input to the system. There are two energy ports to the system; consequently, there are two inputs -- one at each port. Since the pump is an energy convertor and its efficiency is not under consideration, we can consider the variables at the pump energy port as the flow and the differential pressure across the pump. Similarly, the actuator also serves as an energy convertor, and the port variables there can be considered as the differential pressure between actuators and the net flow to the actuator. The inputs and outputs of the system can now be defined as follows:

Inputs

P_s Supply Pressure

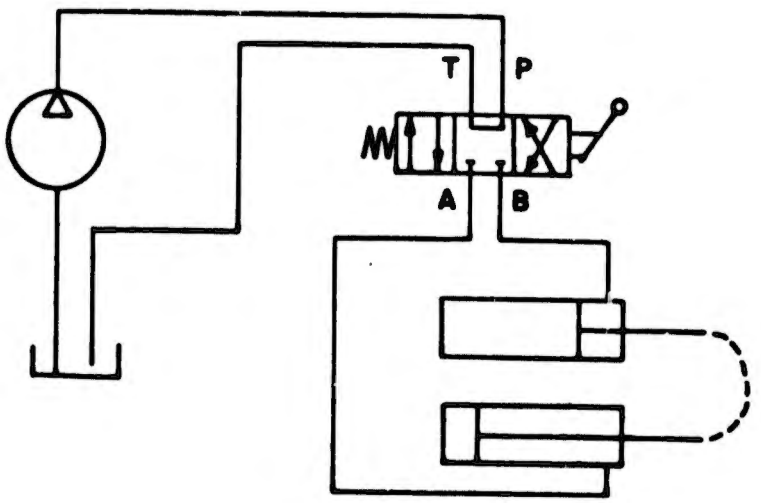

Fig. 2-1. Circuit Schematic for an Open-Center System.

ΔP_{AB}	Pressure Differential Across Actuators
x	Spool Displacement
P_T	Tank Port Pressure

Outputs

P_A	Port A Pressure
P_B	Port B Pressure
Q_s	Supply Flow
Q_A	Flow From P to A

In order to be consistent with the terminology introduced in the section on mathematical analysis, the input will be represented by a four-vector U and the output by a four-vector Y; i.e.,

$$U = \begin{Bmatrix} u_1 \\ u_2 \\ u_3 \\ u_4 \end{Bmatrix} = \begin{Bmatrix} P_s \\ \Delta P_{AB} \\ x \\ P_T \end{Bmatrix} \tag{5a}$$

$$Y = \begin{Bmatrix} y_1 \\ y_2 \\ y_3 \\ y_4 \end{Bmatrix} = \begin{Bmatrix} P_A \\ P_B \\ Q_s \\ Q_A \end{Bmatrix} \tag{5b}$$

For a static model, these quantities are connected by the functional relationship:

$$Y = F(U) \tag{6}$$

Test data giving pairs of values, (U,Y), can be used to identify F. However, in numerical modeling, the objective is to retain the data as such. Thus, the sum total of (U,Y) vectors comprises the static DNR for the system. In using the DNR for simulation, however, there is little chance that the input at any time will be exactly one of those in the DNR. Consequently, to evaluate the output corresponding to an input, it is necessary to perform some type of interpolation between the DNR points. A simple way of doing this is by using the first term

in the Taylor series expansion of F; i.e.,

$$Y = Y_o + \sum_{i=1}^{4} \frac{\partial F}{\partial u_i} \Delta u_1 \qquad (7)$$

Consider the first term in the expanded scalar for of this equation:

$$y_1 = y_{o_1} + \frac{\partial f_1}{\partial u_1} \Delta u_1 + \frac{\partial f_2}{\partial u_2} \Delta u_2 + \frac{\partial f_3}{\partial u_3} \Delta u_3 + \frac{\partial f_4}{\partial u_4}$$

$$= y_{o_1} + c_1 \Delta u_1 + c_2 \Delta u_2 + c_3 \Delta u_3 + c_4 \Delta u_4 \qquad (8)$$

The coefficients c_1, c_2, c_3, and c_4 can be identified from the data in the DNR. If y_o is now chosen to be <u>any</u> of the known outputs, then by putting $\Delta U = (U - U_o)$ the output y corresponding to the input U can ascertained. It should be noted that c_1, c_2, c_3, and c_4 will, in general, differ from point to point in the (U,Y) space. Sufficiently small regions have to be selected in the (U,Y) space for the linearization and identification to be reasonably accurate.

The dynamic model is but an extension of the static model presented above. Eq. (6) now becomes:

$$y(t) = F[U(t), U(t - \ t) \ldots U(t - p\ t), y(t - \ t) \ldots y(t - p\ t) \qquad (9)$$

where the argument t has been included to show the dynamic nature of the model, Δt is a time step, and p is the maximum number of back differences required to model the system. Eq. (9) is seen to be identical to Eq. (1). The introduction of dynamics increases the number of coefficients to be identified to a very large values for multi-input, multi-output systems.

Though the simulation of complete systems using test data has its own uses, a much more powerful analysis and appraisal tool is the simulation of complete systems using individual component test data. The completely general synthesis problem in which there are feedback paths between various components is too complicated to be presented here. It will only be mentioned that the complexity is due to the presence of implicit relationships between the various physical variables which are present irrespective of the <u>form</u> of the individual models; i.e. the representation of components by DNR's does not introduce the complexity.

The open-center system shown in Fig. 2-1 can be considered to be made up of three main components, the pump, the directional control valve and the actuator. These interact as shown in Fig. 2-2. The additional variables introduced here are as follows:

<u>Inputs</u>

N_p	Speed of Pump
W	External Load on Actuator

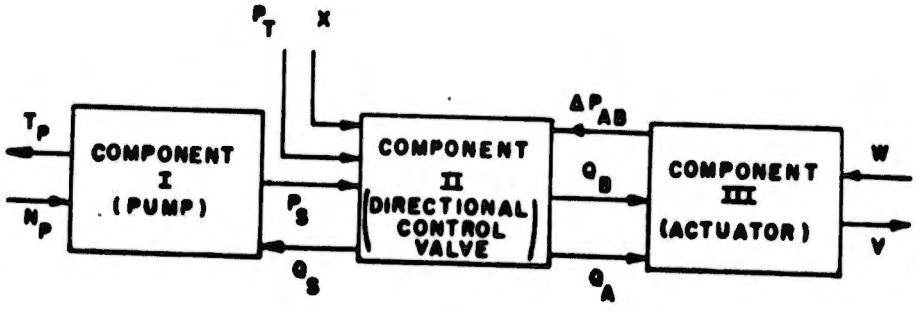

Fig. 2-2. Open-Center System Synthesized from Components.

Outputs

T_p	Torque on Pump
v	Velocity of Actuator

The selection of inputs and outputs depends on the characteristics of the components and the way in which they are interconnected. In this case, the pump is considered to be a constant speed device, and W is a known external load. Since the pump (Component I) and the actuator (Component II) are two-port devices, their characteristics can be uniquely represented by a quadruple comprised of the port variables. Thus, for the pump, the set $[Q_s, N, P_s, T_p]$ over the full range of operating conditions describes the pump completely. It should be noted that power-port theory requires that two of the four quantities be inputs and the other two outputs, with a further restriction that the two inputs cannot be at the same port. The above set, in fact, constitutes the static DNR for the pump. Similarly for the actuator, the set $[W, v, Q_A, \Delta P_{AB}]$ over the full operating range is the DNR.

Now, the great advantage of DNR is in its use of test data where the functional relationships between outputs and inputs cannot be expressed in algebraic terms. In the case of two-port static devices, however, simple formulas usually exist; and, by using them, a few variables can be eliminated. Thus, for the actuator, it is readily seen that:

$$\Delta P_{AB} = \alpha_1 W \tag{10}$$

$$v = \alpha_2 Q_A \tag{11}$$

This set of equations effectively decouples the actuator from the rest of the system and allows ΔP_{AB} to be used as an input.

The static characteristics of a fixed displacement pump are usually given as follows:

$$Q_s = Q_s(P_s, N_p) \tag{12}$$

$$T_p = T_p(P_s, N_p) \tag{13}$$

However, the equations in this form are not compatible with those for the directional control valve (Eqs. (5a) and (5b). Eq. (12) can often be inverted to give:

$$P_s = \Gamma_s(Q_s, N_p) \tag{14}$$

In DNR, this can <u>always</u> be done, as it simply consists of considering Q_s and N_p as the inputs and P_s and T_p as the outputs.

The use of DNR's for the directional control valve and pump to simulate the system is then as follows:

1. Assume a trial value of P_s.
2. Establish the outputs of the valve using the DNR represented by Eq. (5a) and Eq. (5b).
3. Check P_s using the DNR for the pump.
4. If there is a discrepancy, correct the value of P_s and iterate 1 through 3.

- EXPERIMENTAL VERIFICATION -

The open-center system discussed in the previous section forms the nucleus of many mobile hydraulic system actuators. Refinements like cross-over relief valves, cushioning and counterbalance valves are often incorporated but their presence does not invalidate the analysis given earlier. They usually affect only the system transients or become operative during abnormal operation, e.g. overloading. In any case, a low-order model developed by ignoring these effects can always be refined to incorporate them.

Since DNR is still a relatively new concept it was felt that it should be tried out on a working system rather than one in the experimental stages. Consequently a Ford TLB4500 backhoe was selected as the system for simulation and validation of DNR. A simplified circuit schematic is given in Fig. 2-3. All the valves for actuating the various cylinders are contained in one stack. Some of the directional control valves consist only of the metering spool and anti-cavitation check valves, while others have a more complicated construction. Since moving elements are the main source of dynamics, it is evident that the valve stack contains all the components contributing to the dynamics of the system.

Any four-way valve can be modeled as a non-linear wheatstone bridge and is completely described by the metering areas of the different arms of the bridge. These metering areas change with spool displacement, but they can also be functions of the pressures and flows involved. The object of testing the valves was to obtain the metering characteristics as functions of the various port variables, e.g. pressures and flows. For obtaining low-order models, it was considered sufficient to obtain only static characteristics. Appendix C contains selected test results used to develop DNR models. For example, Fig. 2-4 presents the various metering areas, obtained by using the familiar square-law for orifices on the directional control valve for the boom actuator (referred to as the "boon valve"). It may be noted that using DNR does not require the assumption of any kind of orifice relationship, but the use of such a law (if valid) reduces the amount of data to be stored in the DNR. Fig. 2-5 illustrates the results of the metering tests on the directional control valve for the swing cylinders (referred to as the "swing valve"). A special feature of this valve was the arrangement whereby flow could not occur from the pressure port to either of the work ports unless the other work port was pres-

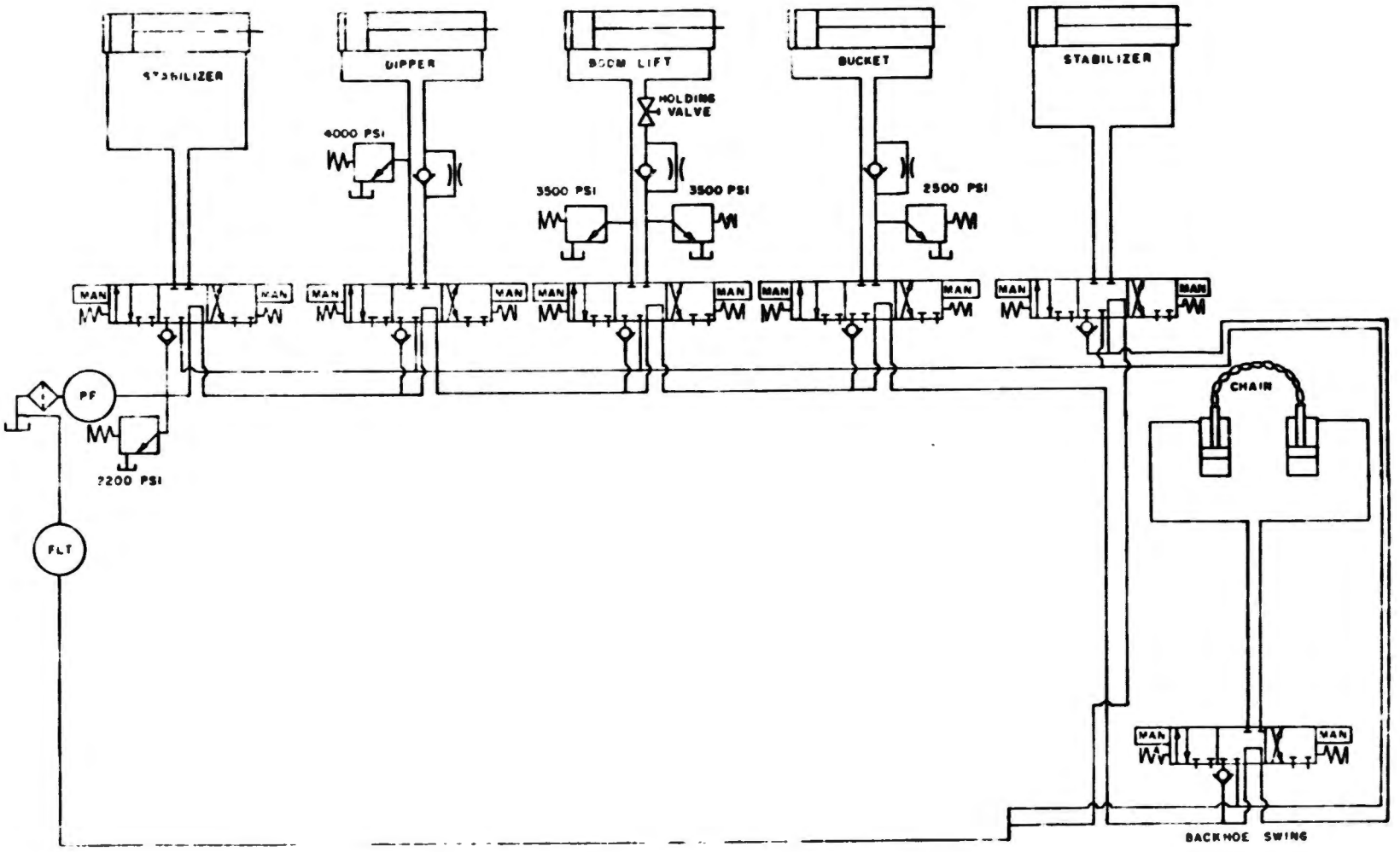

Fig. 2-3. Simplified Circuit Schematic of Backhoe system.

Legend

P Pressure Port

T Tank Port

A Work Port "A"

B Work Port "B"

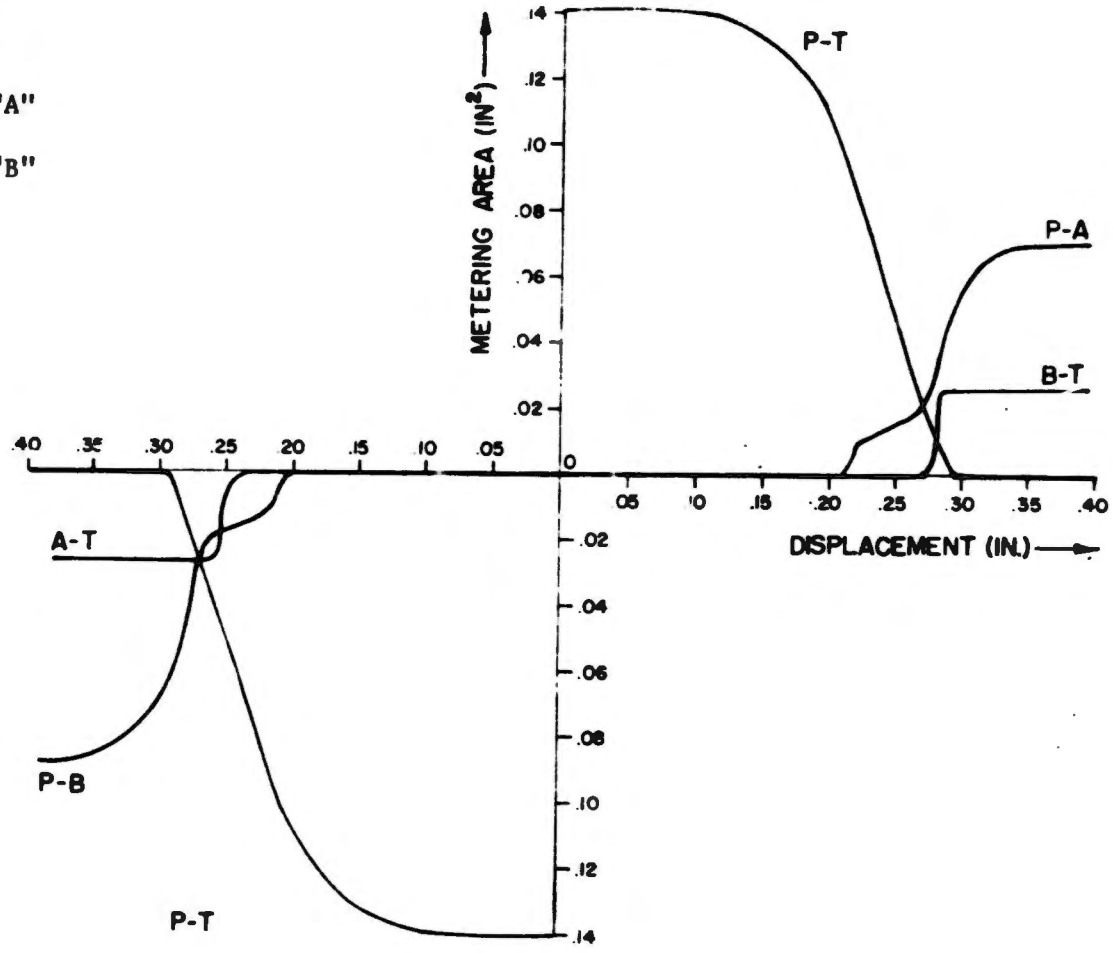

Fig. 2-4. Metering Areas for Swing Valve.

Legend

P Pressure Port

T Tank Port

A Work Port "A"

B Work Port "B"

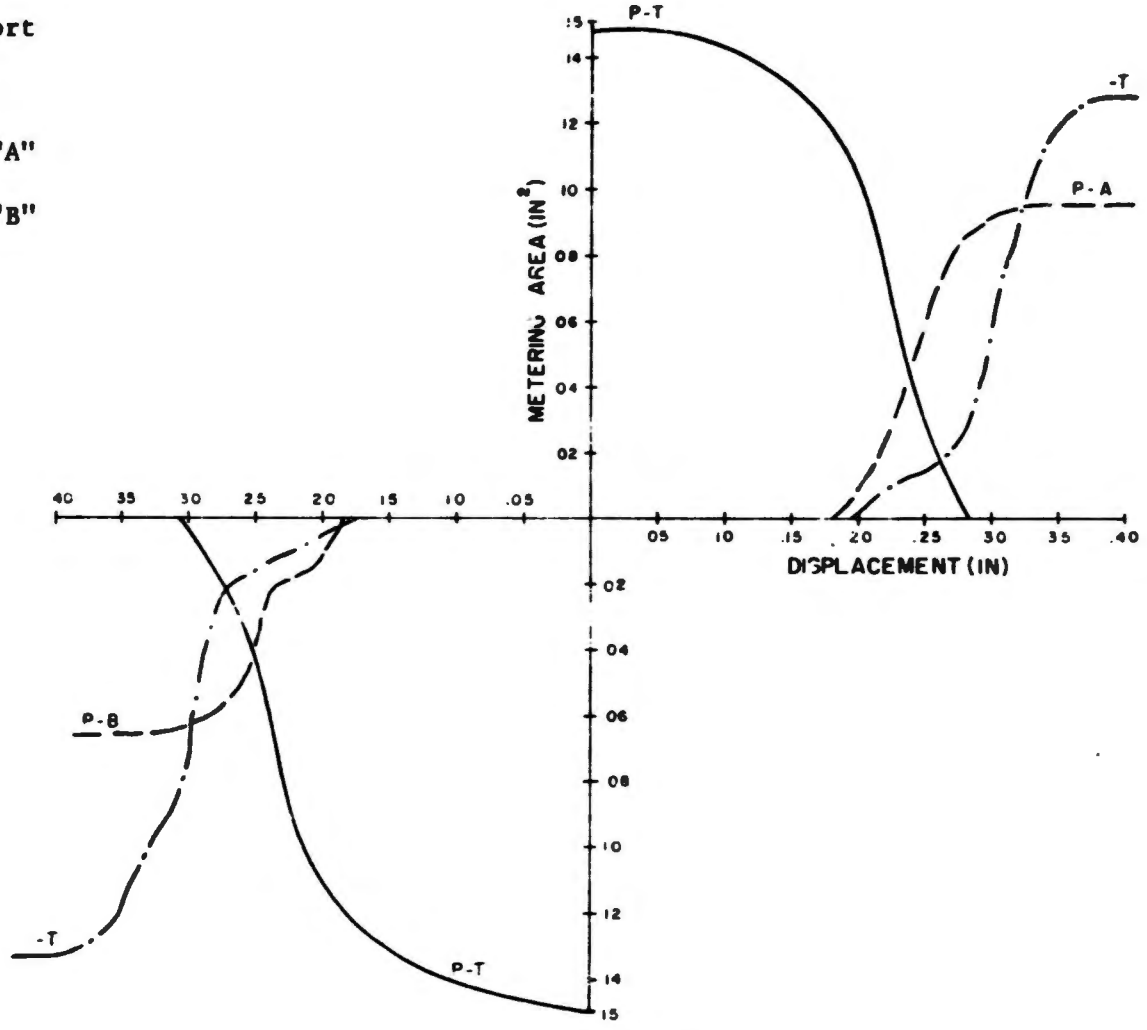

Fig. 2-5. Metering Areas for Boom Valve.

surized. In effect, the metering areas were dependent not only on the spool displacement but also on the port pressures. Figs. 2-6a and b show this effect. The variation, though significant, was considered to be too small for inclusion in a low-order model. Consequently the DNR for the swing valve was also comprised of arrays representing the various metering areas as functions of spool displacement.

Tests were also run on the relief valves incorporated in the swing valve package but were found unnecessary for developing the low-order model of the total system. They are presented in Appendix C.

For simulating the backhoe two modes of operation were selected. The first was the horizontal swing (referred to as the swing mode) and the second, the lift and lowering of the boom (referred to as the boom mode). A study of the circuit schematic shows that though both are open-center systems there are significant differences between them. To name only a few: the swing mode uses symmetrical actuators while the boom uses a single-ended cylinder; gravitational forces are insignificant for swing operation in level ground but play an important role in boom operation.

The test system was instrumented to measure the following quantities for each mode of operation:

1. Pump outflow
2. Pump supply pressure
3. Displacement of directional control valve spool
4. Pressure difference across work ports of directional control valve.

As indicated earlier in the verification of multi-input multi-output systems there is usually some flexibility in choosing inputs and outputs, when all significant variables are measured. For the present simulation it was considered that the following lists comprise the inputs and outputs.

Inputs

1. Spool Displacement
2. Tank Port Pressure
3. Pressure Difference Across Work Ports
4. Supply Pressure

Outputs

1. Supply Flow
2. Pressures in Ports 'A' and 'B' of Valve
3. Flows to and From Actuators
4. Actuator Velocity
5. External Load on Actuator

Since the selection of inputs and outputs affects the simulation algorithm it is useful to review the two lists. The spool displacement is the external signal furnished to the system by the human operator and

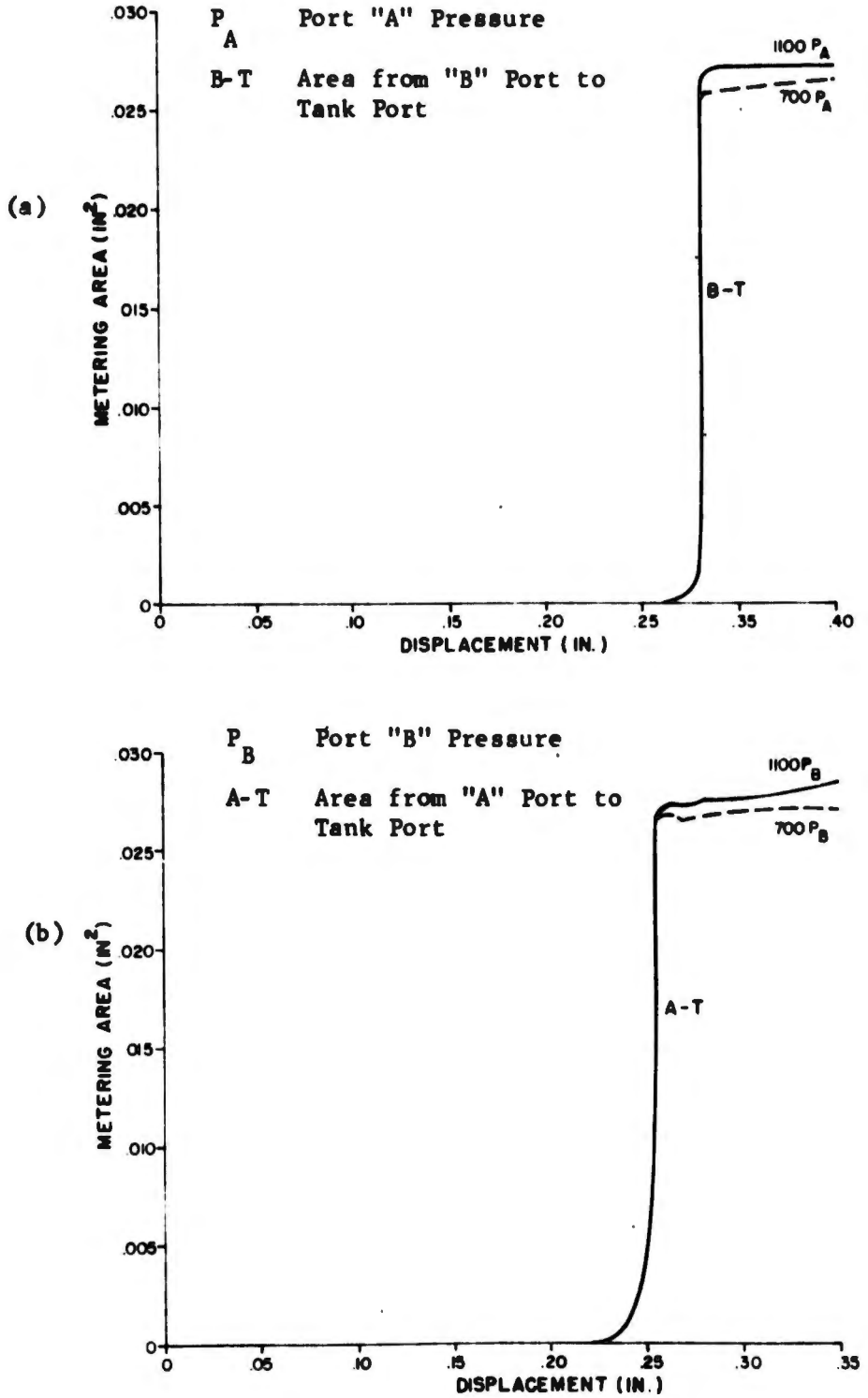

Fig. 2-6. Metering Test Results for Swing Valve Showing Effect of Work Port Pressurization.

its inclusion in the input is not only natural but also essential. Similarly the tank port pressure depends only on the resistance of the piping from the directional control valve to the reservoir and for this open-center system was substantially constant. The selection of the differential pressure across the work ports is valid in view of the effective decoupling of the actuator from the rest of the system (see Eqs. (10) and (11)). One reason for taking advantage of this feature was that it was easier to measure the differential pressure than the actual load on the actuator. The selection of the last input involved a choice between the supply pressure and the supply flow. Due to the presence of the pump ripple the flow trace was harder to digitize and consequently the supply pressure was chosen as the input.

The measured inputs and the DNR for the directional control valve are sufficient to predict the supply flow and the port pressures. The dimensions of the actuators were used to calculate the actuator velocity and the external load. Figs. 2-7 to 2-10 show the variation of the pressures and flows for some modes of operation. It is instructive to compare them with Figs. 2-11 to 2-13 which are reproductions of the measured inputs and outputs as recorded with an oscillograph. One of the first characterisitics of a low-order model is immediately noticed, viz. the high frequency changes in the output (in this case the supply flow) are not portrayed by the model. This should be considered a decided advantage in favor of low-order modeling as high-order models would require step sizes of 1 m.sec. or less, in comparison to that of 0.1 sec. used for the low-order model. Of the four inputs to the system, namely P_s, ΔP, x, and P_T only the first has been included in Figs. 2-7 to 2-9. Fig. 2-10 shows that ΔP follows approximately the same trajectory as P_s as long as the spool displacement, x, is kept large. For the zero spool displacement at the end of an operation the actuator becomes effectively decoupled from the rest of the system and the oscillation in the ΔP do not affect the output under consideration. Significant deviations from the measured output are noticed only at the beginning and end of the spool movement. Since these are positions of a duty cycle where transients are expected to be dominant, the results are not unexpected. The large deviation at approximately 12 milliseconds in the swing mode simulation needs further investigation. Since it shows up in both sample trajectories, measurement error cannot be the culprit. Since, however the large discrepancy exists over a very short time (about 4 m.secs.) the accuracy of the low-order model over the entire duty cycle is not impaired. A higher order model could conceivably simulate the trajectory more accurately, though with an appropriate increase in simulation cost and time.

- SIMULATION OF SECONDARY QUANTITIES -

Typically dynamic models of fluid power components and systems involve physical quantities like pressures, flows, velocities, and displacement. Often, however, one is interested in secondary quantities like power, efficiency and averages of these over a duty cycle. Until very recent times the common practice was to use static models in which a

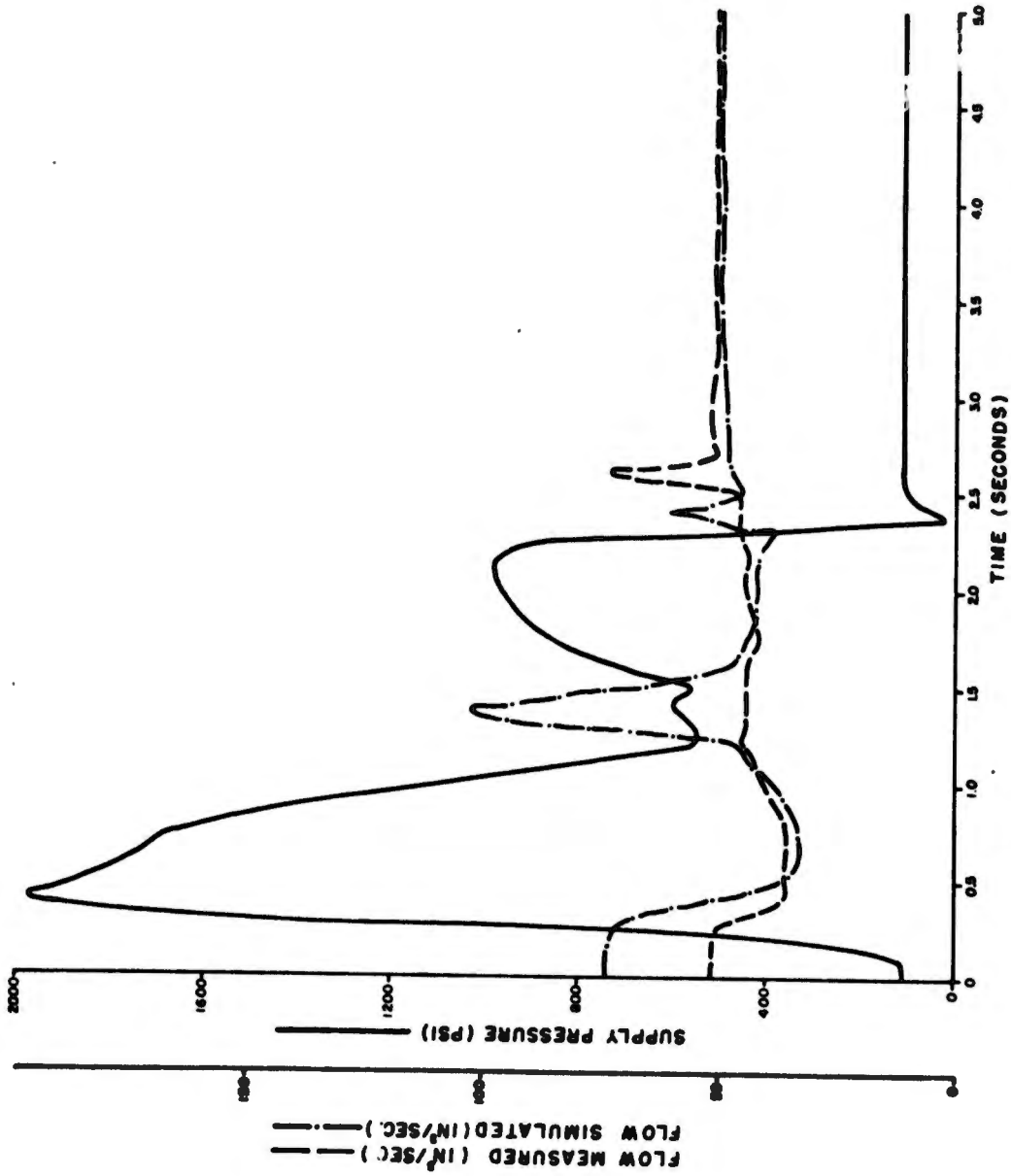

Fig. 2-7. Simulation of Swing Mode; Run #16/28.6.73.

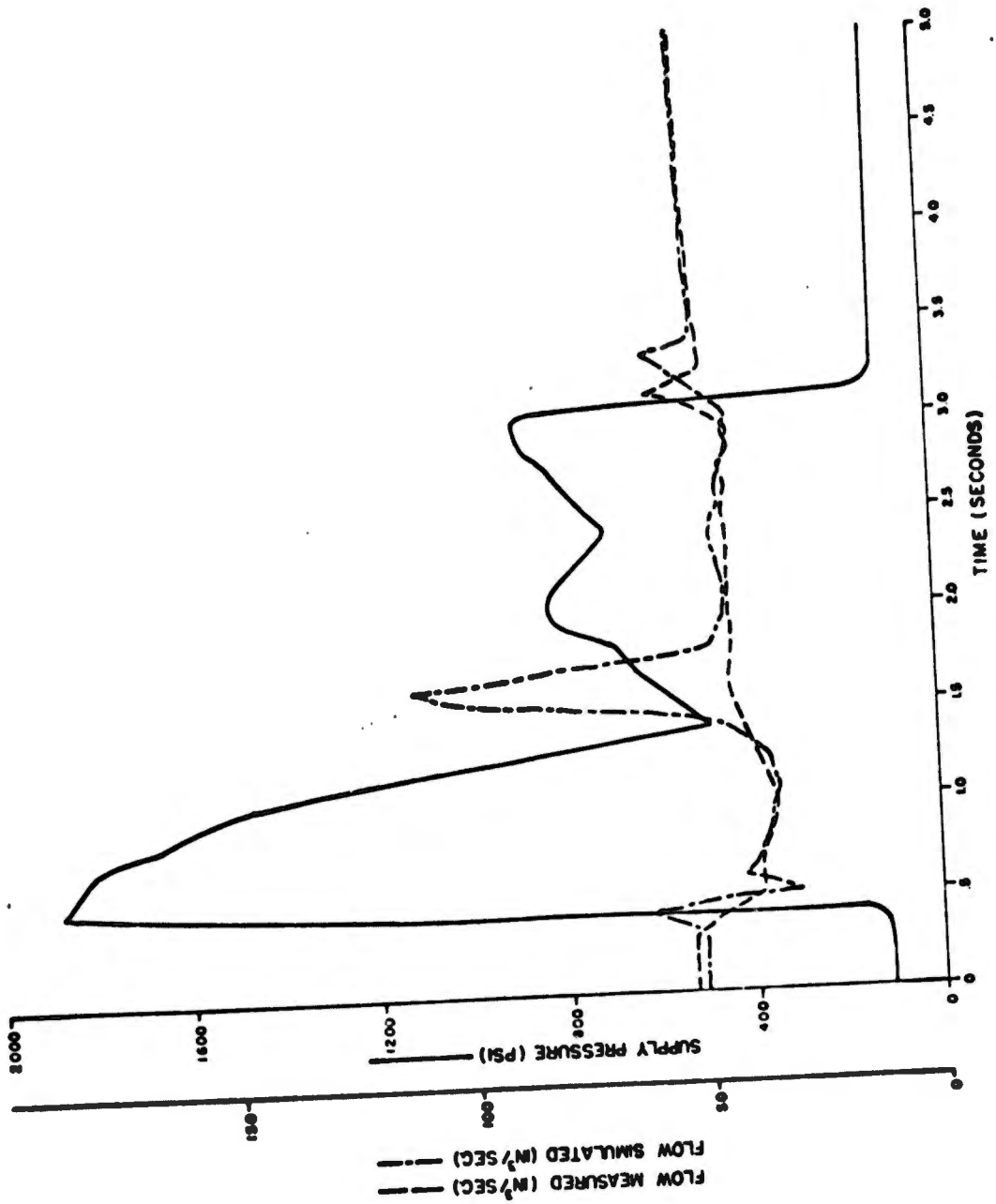

Fig. 2-8. Simulation of Swing Mode; Run #13'26.o.73.

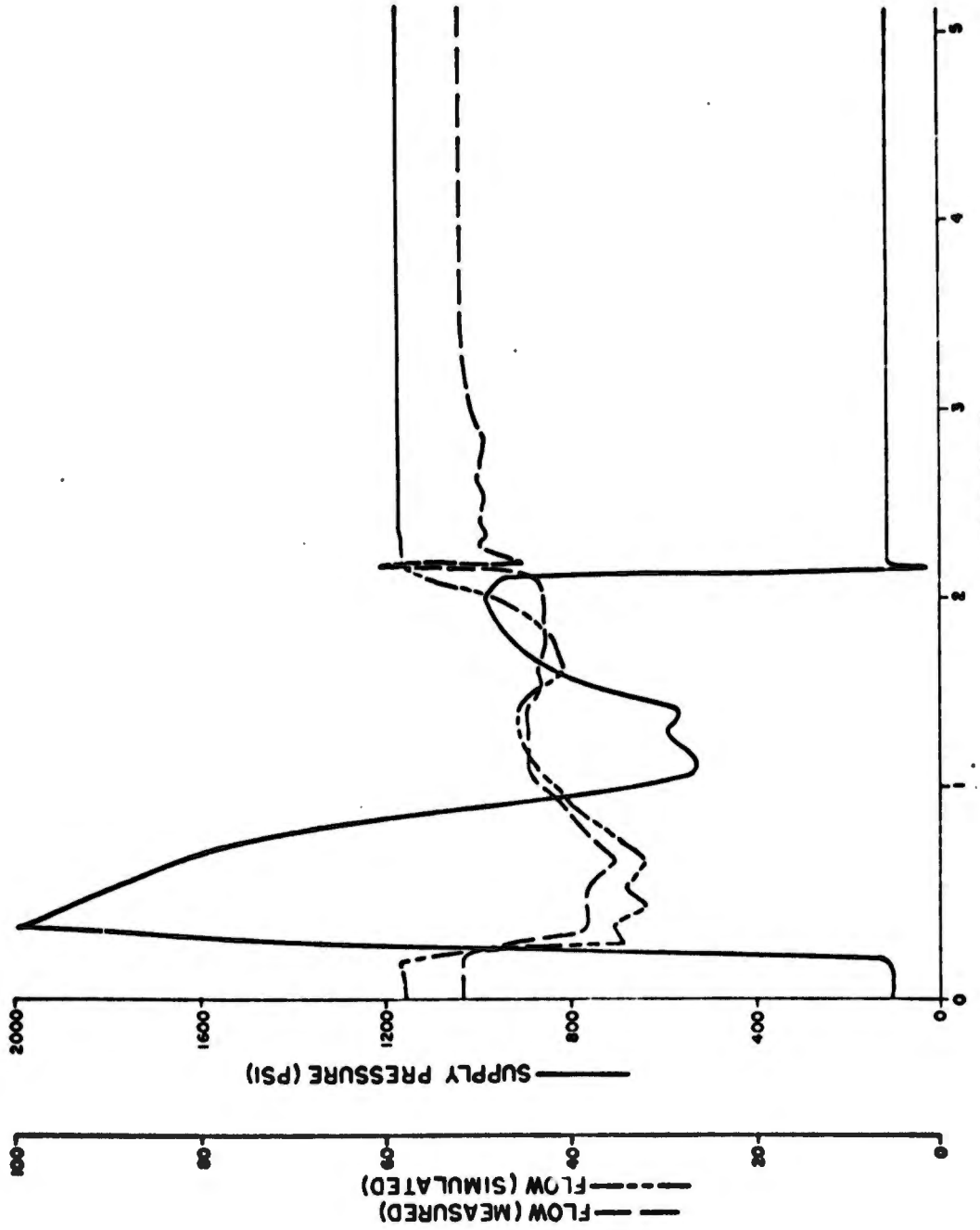

Fig. 2-9. Simulation of Boom Mode; Run #7/2R...73.

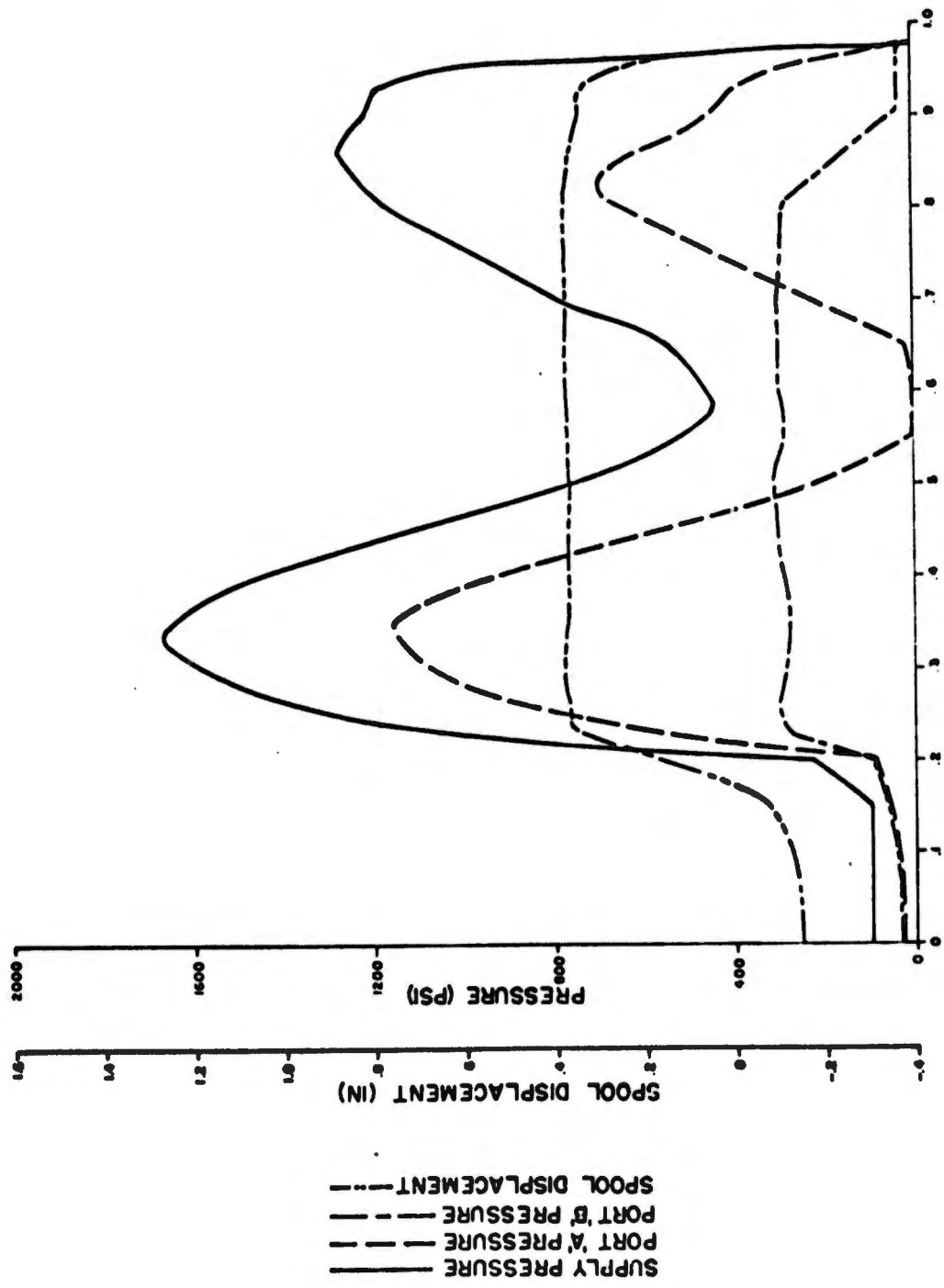

Fig. 2-10. Simulation Results on Backhoe Boom; Run #5.

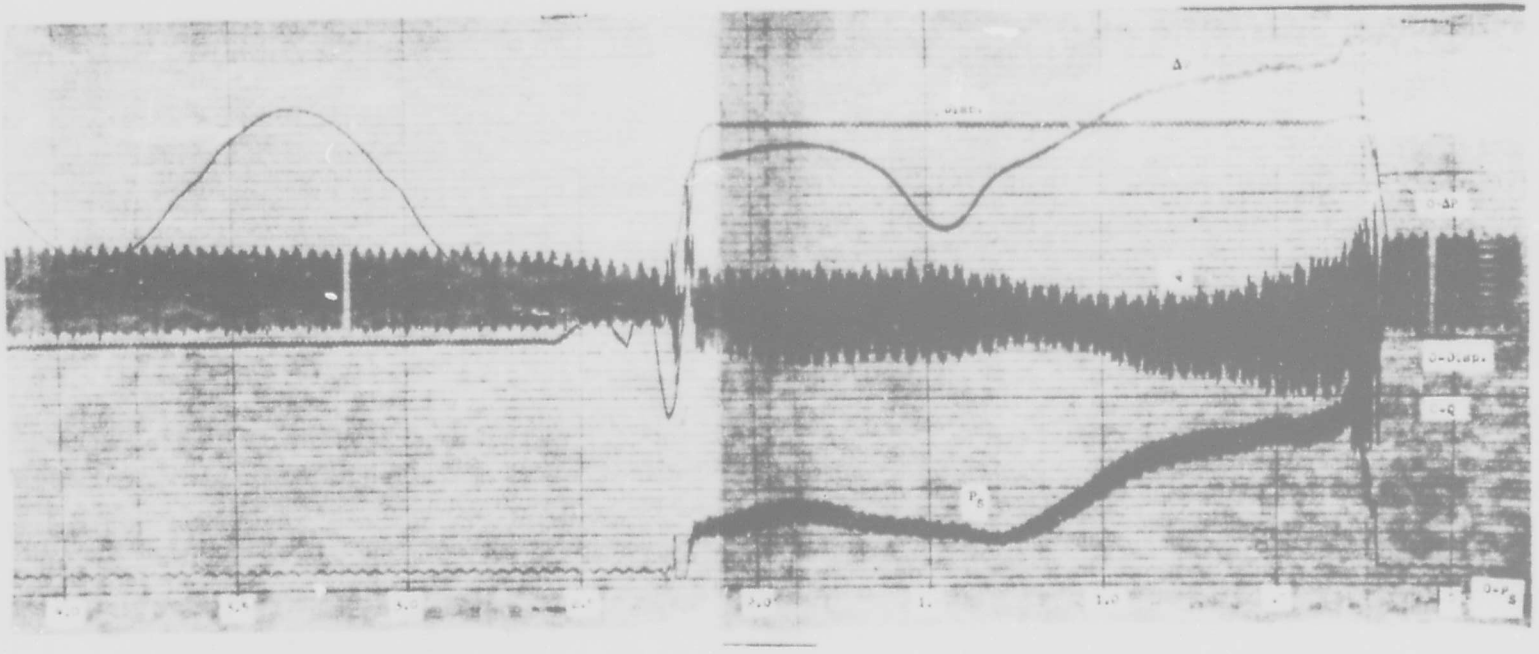

Fig. 2-11. Oscillograph Recording for Swing Mode; Run #16/28.6.73.

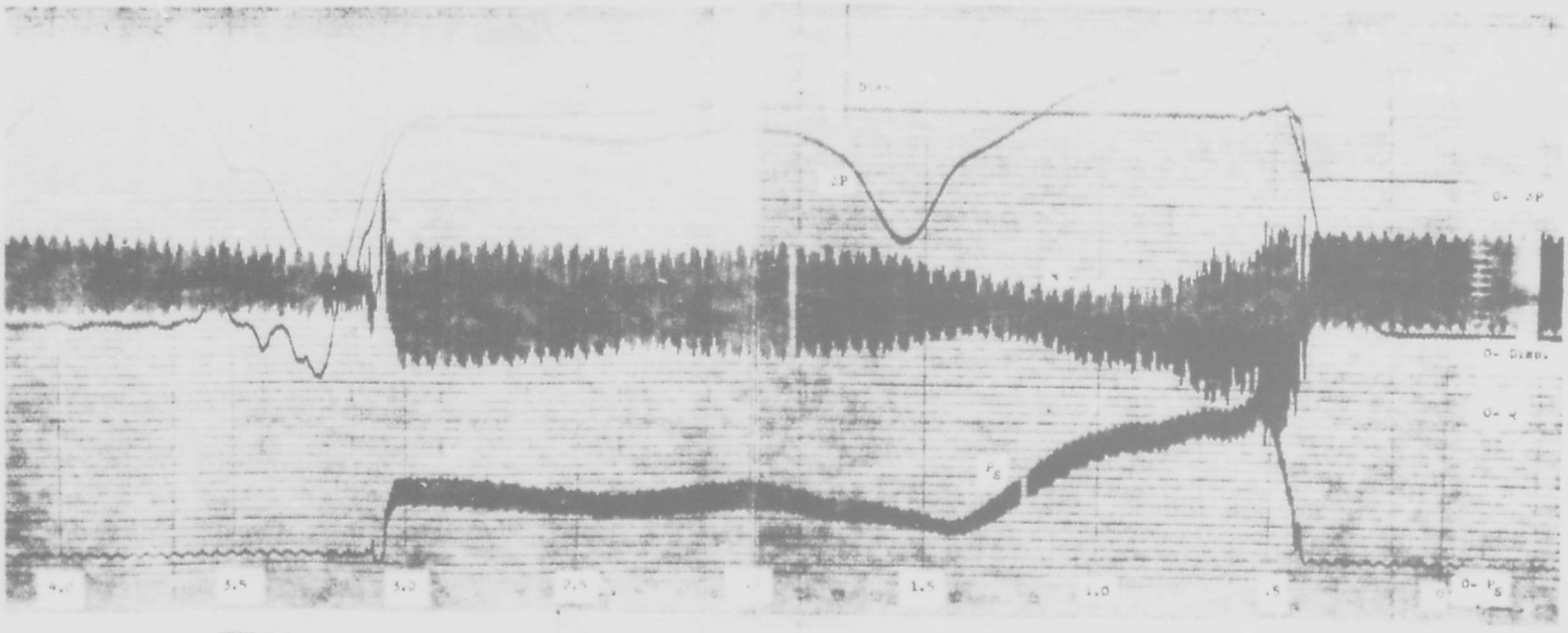

Fig. 2-12. Oscillograph Recording for Swing Mode; Run #13/28.6.73.

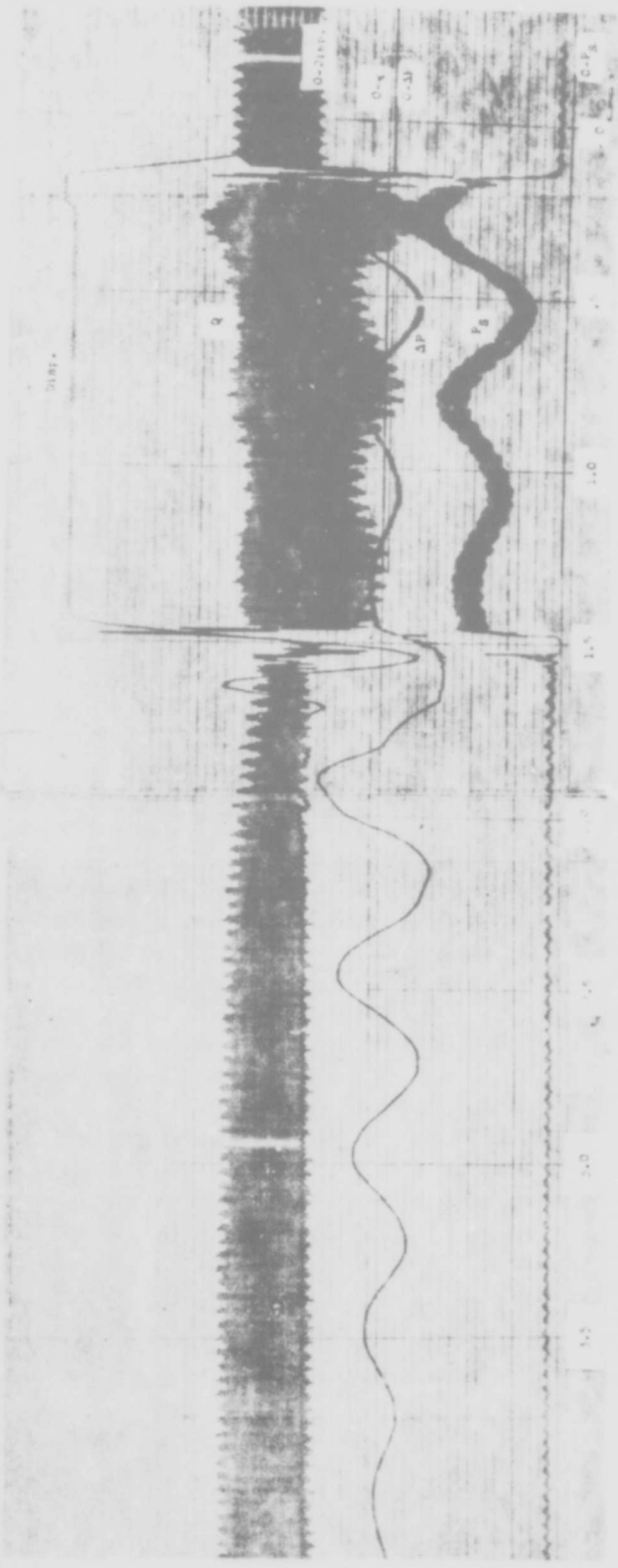

Fig. 2-13. Oscillograph Recording for Boom Mode; Run #5/28.6.73.

number of assumptions would be made, e.g. the pump outflow is constant, the system pressure is substantially constant for part of a duty cycle, etc. Even if the actual values of the physical quantities were known, they were not used other than to obtain average pressures and flows. Consequently the accuracy associated with estimates of power requirements and utilization and duty cycle efficiency is rather low.

With low-order model as developed earlier it is a very easy task to calculate not only the instantaneous power and efficiency but also average values for any specified duty cycle. Figs. 2-14 and 2-15 show the variations of the power and efficiency for the swing mode of operation, corresponding to the trajectories shown in Fig. 2-7 and 2-8. A few points are worthy of comment. First, the input horsepower is that introduced into the open-center system by the pump. Dividing this by the pump efficiency would give the hydraulic output power from the prime mover. It is seen that this quantity is always positive, and the lowest value corresponds to idle conditions when the pressure drop is in the open center valve and the piping. The output power of the system was calculated using the pressure difference between the work ports and the flow into and out of the actuator. A significant point brought out by the simulation is that this output power can be negative; i.e. over part of the duty cycle, the load is regenerative. A close look at the mechanism of operation of the system furnishes the explanation for this as follows: when the valve is first moved over to (say) swing the boom, energy is used to accelerate the moving parts. In the later part of the duty cycle the kinetic energy of the moving parts is returned to the system, thus accounting for the negative sign of the output power. Once the spool is centered at the end of the swing movement, the actuator is effectively decoupled from the rest of the system. Since the actuator may still be undergoing oscillations (see Fig. 2-13) there will be energy interchange between the fluid in the actuator and connecting lines, on one hand and the moving parts, on the other. These are, however, insignificant when the complete duty cycle is considered. Appendix C includes the computer printout of the power input and output as well as the efficiency.

- CONCLUSIONS AND RECOMMENDATIONS -

The main objective of the system performance phase of the CAP Program was to develop and verify a technique for simulating the operation of a hydraulic system using test data on individual components. A new concept of modeling -- Direct Numerical Representation -- was used to process experimental data on the components of a test system and to present the information as numerical components models. In addition, tests were then run on the total system and the data obtained used to verify the model of the system obtained by interfacing the component models. Physical variables, such as pressure and flow, were simulated for a given operation of the test machine, and secondary quantities, like velocity, power, and efficiency, were calculated for each operation cycle. The simulation results confirm the validity of numerical representation of models and illustrate

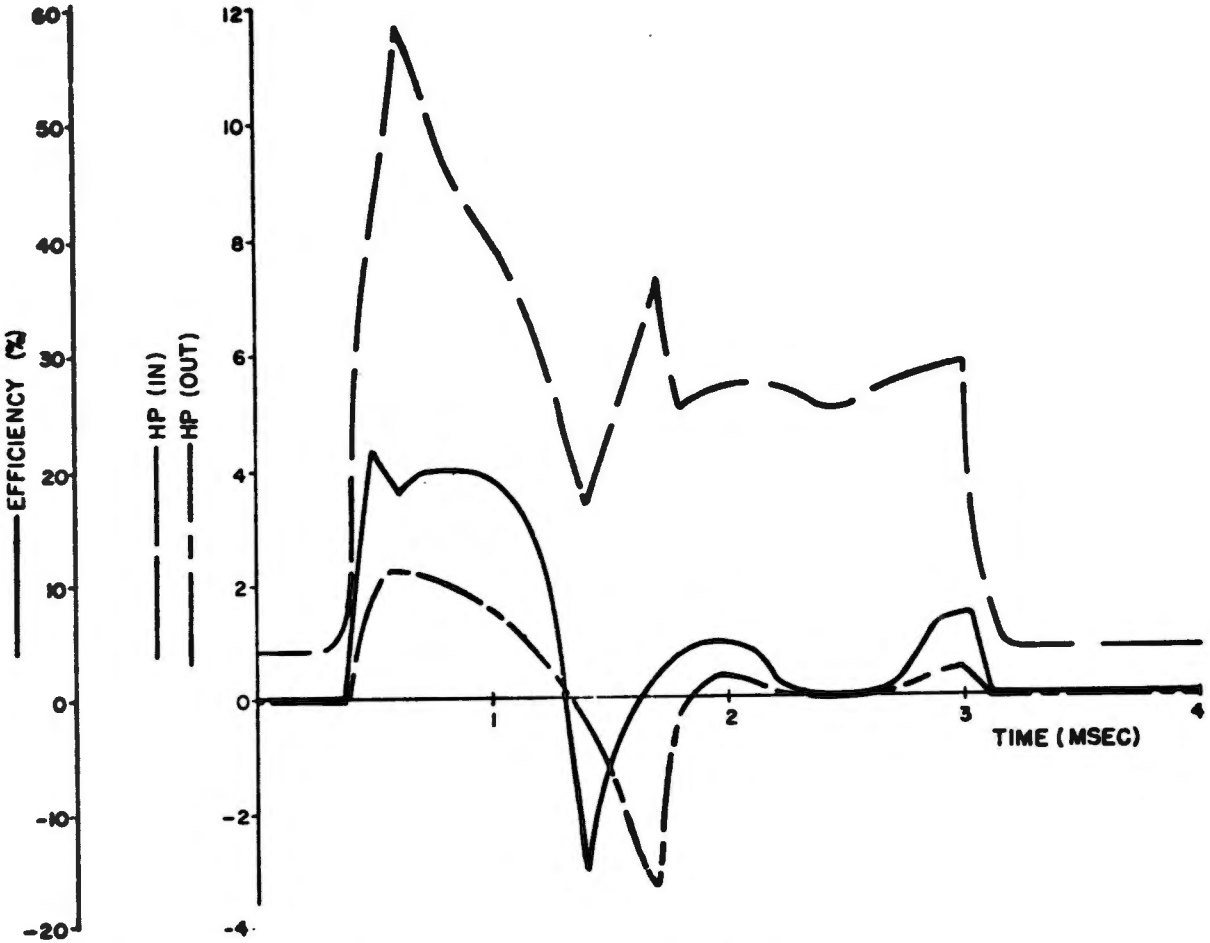

Fig. 2-14. Power and Efficiency for Swing Mode; Run #16/28.6.73.

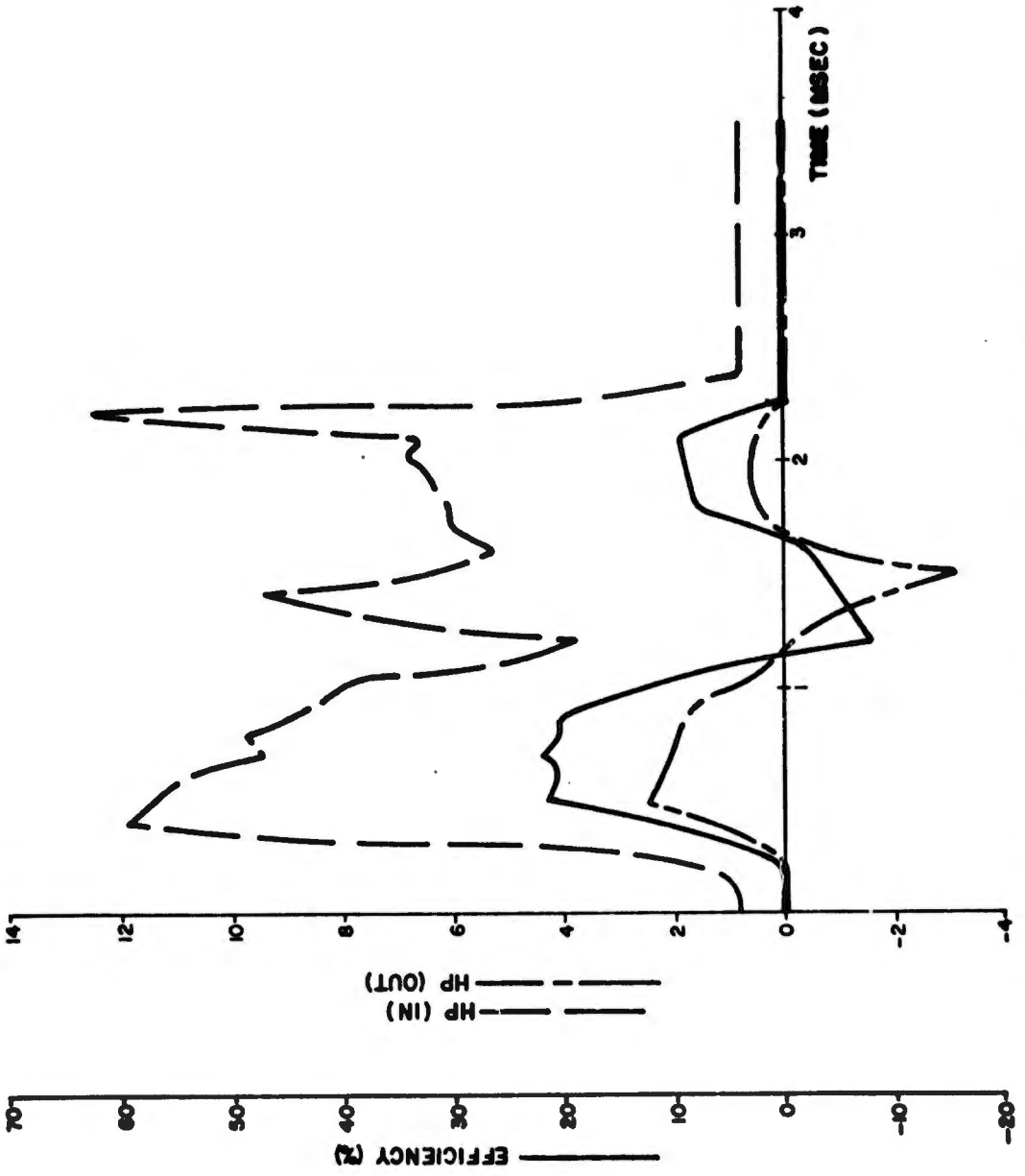

Fig. 2-15. Power and Efficiency for Swing Mode; Run #13/28.6.73.

the feasibility of developing low-order models of systems using such representations.

Direct Numerical Representation is a completely new concept; and, though it holds great promise for efficient simulation of large hydraulic systems, some areas of its theoretical development need additional investigation. Before it can be released as a user-oriented computer program, it is necessary, for example, to acquire test data on different types of hydraulic components and develop a library of DNR models. It is alsc necessary to incorporate error-checking algorithms into the computer programs for accuracy assurance. Finally, and probably most important, it is imperative to improve the speed and efficiency of the software. These are considered to be realizable improvements and well worth the time and effort that should be devoted to them. The simulation of even large complex systems will then be practicable. The information obtained by such sim ulation would be useful for not only hydraulic system appraisal but also for developing realistic performance specifications. The cost of simulation using low-order models will be much less than that of conducting extensive field tests on the actual system in hardware form.

- REFERENCES -

1. Iyengar, S.K.R., "Modeling Fluid Power Components Without Equations," Paper No. P73-SP-2, Seventh Annual Fluid Power Research Conference, Fluid Power Research Center, Oklahoma State University, Stillwater, Oklahoma, October 1973.

2. Iyengar, S.K.R., "Direct Numerical Representation (DNR) -- Mathematical Foundation, Model Development, and Experimental Verification," Report No. R73-SP-2, Basic Fluid Power Research Program, Fluid Power Research Center, Oklahoma State University, Stillwater, Oklahoma, December 1973.

CHAPTER III

COMPUTER-AIDED PROCUREMENT
(Thermal Analysis)

- INTRODUCTION -

Increasing desires for high-powered, highly efficient, high pressure fluid power systems have introduced corresponding increases in system operating temperatures. Such a result is undesirable because it brings with it a multitude of temperature-induced problems which were not prevalent before. Higher incidence of material failures, more rapid degradation of fluids and overall system performance, an increase in personal safety hazards, and an amplification of combustion and explosion hazards represent just a few of the many complications which arise from high system operating temperatures (greater than 250-300°F). All of these are direct results of inherent component energy or power losses, which serve only to convert system pressure energy to thermal energy.

Heat generation in any hydraulic component or system is generally an unwanted and unavoidable phenomenon. Continuous interaction with the environment is often the only measure which is relied upon to alleviate the buildup of thermal energy in an operating system. In many cases, this natural cooling of the system is insufficient in the limitation of system temperatures. When this occurs, heat exchangers are employed to limit and sometimes to control system temperatures. However, the desire for compact and efficient hydraulic systems with high operating pressures frequently imposes severe restrictions upon a heat exchanger solution to thermal problems. One method to circumvent these difficulties is the utilization of a component as well as an overall system thermal analysis during design stages.

The dynamics of a heat exchanger have the most influential effects other than reservoir dynamics on the thermal characteristics of the overall system. It is precisely this influence which warrants a thorough thermal analysis of heat exchangers. A basic systems approach combined with fundamental laws of heat transfer and thermodynamics is well suited for such a development. Thus, a major part of the following discussion concentrates on the development and experimental verification of a multi-input, multi-output, semi-empirical, dynamic thermal model for a heat exchanger. The analysis is done for a liquid-to-liquid heat exchanger. The results of this study are presented in the first part of this paper.

Before an overall system thermal model can be synthesized, individual

component thermal models must be developed. However, to obtain a simplified system model, it is advantageous to use a lumped-parameter approach. This can be achieved by lumping all of the thermal capacitance and resistance into a single component. The application of such a technique is illustrated in an analysis of an open-center system. The results of this treatment are given in the last section of this paper.

- THERMAL MODEL OF A HEAT EXCHANGER -

When natural cooling is no longer sufficient to limit system temperatures, it becomes necessary to employ auxiliary devices such as heat exchangers to perform this task. Liquid-to-liquid exchangers are generally more desirable than liquid-to-air exchangers due to higher efficiencies and better responses. However, in mobile systems, practical considerations restrict the use to the latter type.

In the following development, a liquid-to-liquid heat exchanger is analyzed. Basic concepts of modern control theory, thermodynamics, and heat transfer laws for liquids are used to derive a semi-empirical, non-linear, first-order, dynamic thermal model for this heat exchanger. A completely analogous development can be done for a liquid-to-air exchanger, in which case free convection and forced convection heat transfer laws for gases would be used in place of those for liquids. For certain types of models, this would create considerably more algebraic manipulation than exists in the study given below.

Heat exchanger analysis in general are based on log mean temperature differences (LMTD); but, when certain criteria are met, the arithmetic mean temperature difference (AMTD) can be used as an approximation to the LMTD. The foremost constraint which must be met in order to justify the AMTD approximation is as follows (see Table 3-1 for a complete list of symbols):

$$\frac{T_{fi}}{T_{fi} - T_{co}} > 9 \qquad (1)$$

This criterion assures that less than a ten percent deviation exists between the LMTD and the AMTD [1,2,3,4].

Thermal analysis of large hydraulic systems would be intractable unless certain simplifying assumptions are made. The principal assumption used here is that lumped-parameter models are sufficiently accurate approximations for the physical system. This assumption leads to the following relations for a first-order semi-empirical non-linear, dynamic thermal model to predict the AMTD and the outlet temperatures of a heat exchanger.

1. For the ranges of flow rates and temperatures, the heat transfer from the working fluid to the coolant fluid can be expressed as follows:

TABLE 3-1 - LIST OF SYMBOLS -

A	effective heat transfer area, sq. ft.
A_o	orifice area, sq. in.
C_d	orifice discharge coefficient
C_{eq}	equivalent thermal capacitance, Btu/°F
C_{pc}	specific heat of coolant, Btu/lb_m/°F
C_{pf}	specific heat of fluid, Btu/lb_m/°F
H_{gen}	heat generation rate, Btu/min
H_{in}	rate of heat entering, Btu/min
H_{out}	rate of heat take away, Btu/min
H_{st}	heat storage rate, Btu/min
H_{trans}	heat transfer rate, Btu/min
k_1	constant for dimensional consistency, Btu/sec/in/lb_f/min
ΔP	pressure drop across component, psi
ρ_c	coolant density, lb_f sec^2/in^4
Q	flow rate through component, cu in/sec
Q_c	coolant flow rate, gpm
Q_f	fluid flow rate, gpm
T_{amb}	ambient temperature, °F
T_{ci}	coolant inlet temperature, °F
T_{co}	coolant outlet temperature, °F
T_{fi}	fluid inlet temperature, °F
T_{fo}	fluid outlet temperature, °F
T_{res}	reservoir temperature, °F
U	overall heat transfer coefficient, Btu/hr/sq ft/°F

$$H_{trans} = UA \left(\frac{T_{fi} + T_{fo}}{2} - \frac{T_{ci} + T_{co}}{2} \right)$$

2. The thermal storage characteristics of the heat exchanger can be written as shown below:

$$H_{st} = C_{eq} \left(\frac{\dot{T}_{fi} + \dot{T}_{fo}}{2} - \frac{\dot{T}_{ci} + \dot{T}_{co}}{2} \right)$$

3. All the heat energy brought in by the fluid is carried away by the coolant and the fluid (i.e., there is no other method of heat dissipation).

Utilizing the first law of thermodynamics, a thermal energy balance is applied to the exchanger. The results are given by the following expressions:

$$H_{st} = H_{in} - H_{trans} \qquad (2)$$

$$H_{trans} = H_{out} \qquad (3)$$

$$H_{in} = Q_f C_{pf} (T_{fi} - T_{fo}) \qquad (4)$$

$$H_{out} = Q_c C_{pc} (T_{co} - T_{ci}) \qquad (5)$$

Eqs. (2) and (3) in conjunction with the assumptions given above, form the suitable basis for both steady-state and dynamic thermal analyses. The results shown below summarize a more detailed derivation [5].

Steady State Analysis

At steady-state conditions, Eqs. (2) and (3) reduce to the following equality:

$$H_{in} = H_{trans} = H_{out} \qquad (6)$$

With a knowledge of input temperatures and flow rates into the heat exchanger, this equality yields analytical expressions which predict the outlet coolant and fluid temperatures for the exchanger. These equations can be written as follows:

$$T_{co} = T_{ci} + \frac{Q_f C_{pf}}{Q_c C_{pc}} \left[1 - \left\{ \frac{UA}{Q_f C_{pf}} T_{ci} + \left[1 - \frac{UA}{2 Q_f C_{pf}} \left(1 - \frac{Q_f C_{pf}}{Q_c C_{pc}} \right) \right] T_{fi} \right\} \right] \qquad (7)$$

$$T_{fo} = \frac{\left\{ \frac{UA}{Q_f C_{pf}} T_{ci} + \left[1 - \frac{UA}{2 Q_f C_{pf}} \left(1 - \frac{Q_f C_{pf}}{Q_c C_{pc}} \right) \right] T_{fi} \right\}}{1 + \frac{UA}{2 Q_c C_{pc}} \left(1 + \frac{Q_f C_{pf}}{Q_c C_{pc}} \right)} \qquad (8)$$

It should be noted that, for low flow rates ($Q_f \tilde{=} Q_c \tilde{=} 0$), these equations are invalid. For this situation, both the AMTD and the LMTD analyses of a heat exchanger break down. However, most hydraulic systems which employ heat exchangers do not have operating conditions close to this singular point.

Dynamic Analysis

Although a steady-state analysis is important, it is time independent and cannot provide any information concerning a changing input until a new steady-state point is reached. A dynamic analysis does yield this continuous information, either on a component or system basis. Consideration of a heat exchanger as a component is advantageous for a dynamic analysis. Before this analysis can be done, however, the inputs to the component must be identified and a suitable state vector defined. The state vector for this case yields inlet and outlet temperatures for any point in time.

The following quantities can conveniently be considered as inputs to the component:

1. Q_f working fluid flow rate, gpm
2. T_{fi} inlet fluid temperature, °C
3. Q_c coolant flow rate, gpm
4. T_{ci} inlet coolant temperature, °C

With no loss of generality for this analysis, one or more of these inputs can be held constant. A convenient definition of the state vector of the component can now be made. The state of the system is provided by the arithmetic mean temperature difference:

$$\Delta T = \frac{T_{fi} + T_{fo}}{2} - \frac{T_{ci} + T_{co}}{2} \qquad (9)$$

This is used in place of the more generally used log mean temperature difference:

$$LMTD = \frac{(T_{fo} - T_{ci}) - (T_{fi} - T_{co})}{\ln[\frac{T_{fo} - T_{ci}}{T_{fi} - T_{co}}]} \qquad (10)$$

Note that this is acceptable for any liquid-to-liquid heat exchanger configuration providing that the conditions of Eq. (1) prevail.

Solution of Eqs. (2,3,4) and (5) yield the following equations for the predictions of outlet coolant and fluid temperatures. Each of these expressions is explicitly a function of the component inputs and the

state vector:

$$T_{co} = T_{ci} + \frac{UA\Delta T}{Q_c C_{pc}} \qquad (11)$$

$$T_{fo} = 2T_{ci} + (2 + \frac{UA}{Q_c C_{pc}}) \Delta T - T_{fi} \qquad (12)$$

Using relation 1 given earlier, together with eqs. (2), (4), (11), and (12) yields the following result:

$$\dot{\Delta T} = \frac{2Q_f C_{pf}}{C_{eq}} (T_{fi} - T_{ci}) - \frac{\Delta T}{C_{eq}} \left[UA + Q_f C_{pf} (2 + \frac{UA}{Q_c C_{pc}}) \right] \qquad (13)$$

Eq. (13) is the dynamic thermal model for the liquid-to-liquid heat exchanger that is considered here.

For the given set of inputs, this first-order equation is non-linear and thus does not have a closed-form solution. However, a particular solution can be obtained by a numerical integration method. This is most conveniently done on a digital computer. Also, initial approximations for the equivalent thermal capacitance, C_{eq}, and the UA parameter must be made before any simulation can be done. The equivalent thermal capacitance can be initially approximated by setting it equal to the internal volume of the heat exchanger shell. The UA parameter can be estimated from the values of U and A given in the manufacturer's specifications for the heat exchanger. Also, "best" estimates of C_{eq} and UA can be obtained from any of a host of computer programs for parameter identification and optimization [6,7] by using appropriate test data.

Equations (11), (12), and (13) were simultaneously solved numerically by the DYSIMP computer program package [8].

Experimental Verification of Dynamic Model

The only method to prove or disprove the validity of any mathematical model is experimental testing. For the case of interest here, dynamic tests are required. However, in conducting any dynamic measurements, there is one major pitfall. That is as follows: Is the dynamic response of the sensing and recording equipment considerably faster than the time variation of the measured phenomena? If not, the test results are invalid and of no significance. If it is, the results that are recorded are usable and accurate.

The heat exchanger used for this verification was of significant physical dimensions to cause it to have a relatively slow response time, approximately 15 seconds. Continuous-output, platinum-resistance, temperature sensing equipment with dynamic response times of two to three seconds was used to measure the inlet and outlet temperature of the two

fluid stream of the heat exchanger. In general, most recording equipment has response times of the order of several milliseconds or less. But, since the response time of the exchanger was comparatively slow, a digital readout device was used to record the temperatures at the various ports of the exchanger. The flow rates of both the working fluid and the coolant were recorded simulatneously with the temperatures. A turbine meter was used to record the fluid flow rate, and a calibrated orifice flowmeter was used to record the cooling water flow rate. Knowledge of the non-linear orifice equation to calculate the coolant flow rate [9].

$$Q_c = A_o C_d \sqrt{2/\rho_c \Delta P} \qquad (14)$$

All of the tests were run such that the starting point of each one was at steady-state conditions (i.e., all temperatures and flow rates constant). A temperature or flow rate input change was then imposed on the exchanger, and the corresponding responses of the outlet temperatures were recorded until another steady-state condition prevailed.

For the series of tests that were conducted, the coolant inlet temperature and the fluid flow rate were held constant. Changes in inlet fluid temperature and coolant flow rate were made independent of each other, and the corresponding temperature responses to these changes were recorded. Increasing and decreasing inlet fluid temperatures were imposed on the test heat exchanger for a variety of coolant flow rates; and, for a constant inlet fluid temperature, the effects of a sudden change in coolant flow rate were also recorded.

The test data acquired from these dynamic tests were them digitized and used in the computer simulation of the mathematical model for the exchanger to calculate the resulting outlet fluid and coolant temperatures. The input data to the computer program were the inlet coolant and fluid temperatures and the measured values of the coolant and fluid flow rates. Figs. 3-1(a) and 3-1(b) show typical results for calculated versus experimentally determined results for an increase or decrease in inlet fluid temperature. Fig. 3-2 illustrates the effect that a dynamic change in coolant flow rate has on the outlet temperatures of the heat exchanger.

It was stated earlier that the "best" approximations to the equivalent thermal capacitance and the UA parameter can be obtained by one of many computer programs for parameter identification. The results depicted in Figs. 3-1 and 3-2 are the "best" estimates to these two parameters. The close agreement of the predicted and experimental values reflects the accuracy of the estimation of these two parameters.

Also incorporated into the simulation program is an error analysis. Table 3-2 is a summary of this. The average, maximum, and final value errors are given between the AMTD and the LMTD. The same error summary is also given for the comparison of the experimental and predicted results for the outlet coolant and fluid temperatures. This table and the results shown in Figs. 3-1 and 3-2 indicate that the non-linear dynamic thermal

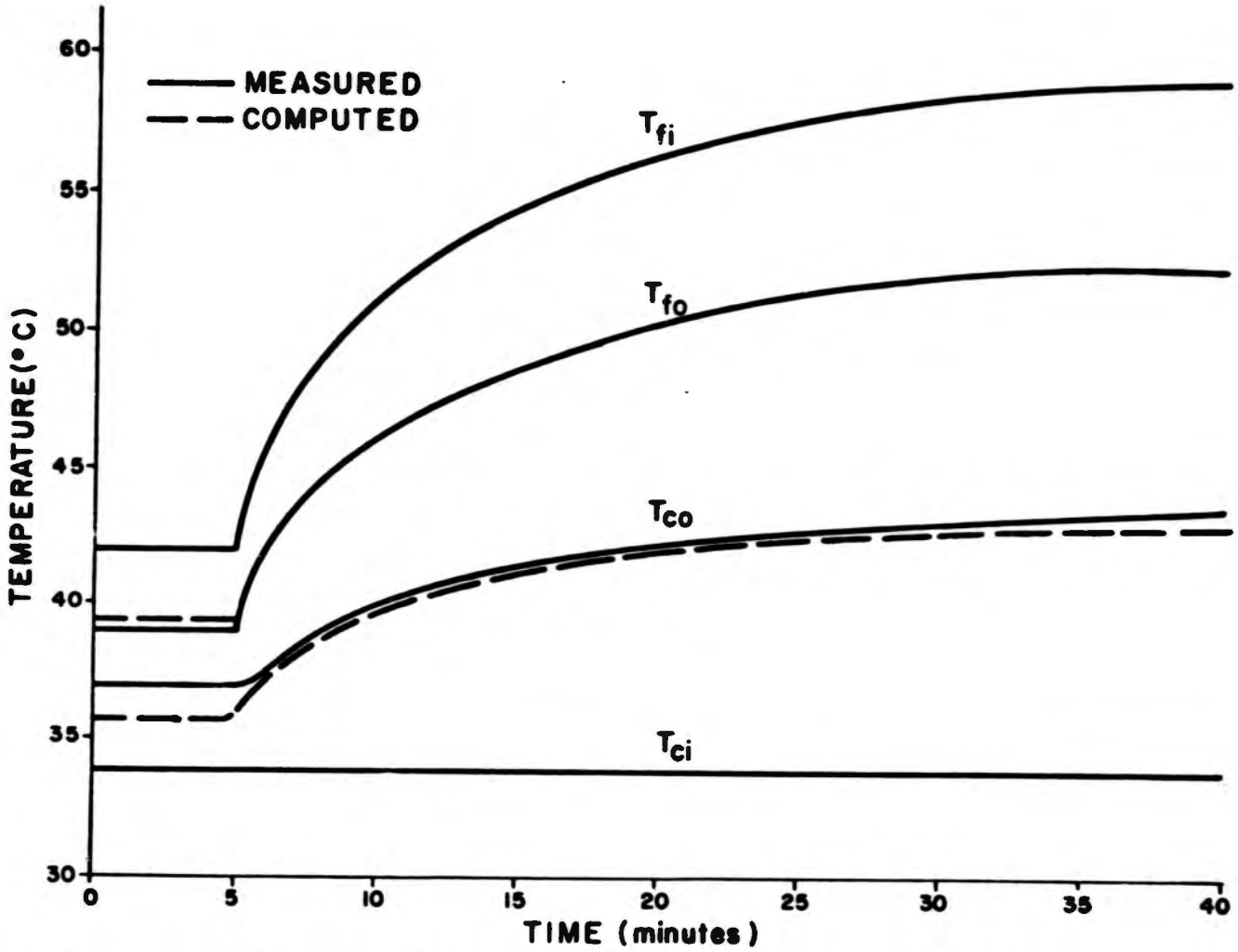

Fig. 3-1(a). Typical Results for an Increase of Inlet Fluid Temperature. Q_c=18.94LPM, Q_f=92.5LPM.

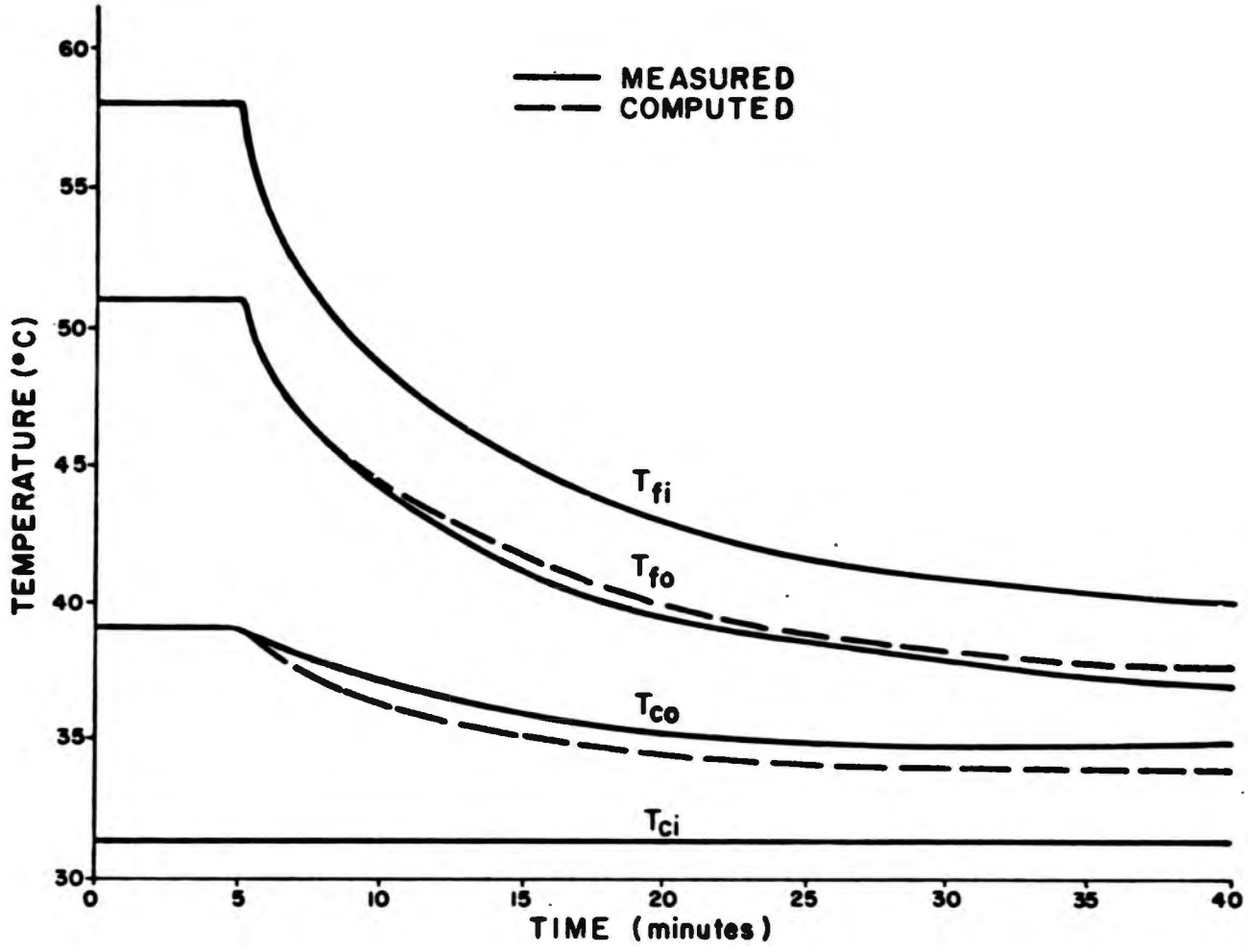

Fig. 3-1(b). Typical Results for a Decrease of Inlet Fluid Temperature. Q_c=31.39 LPM; Q_f=92.5 LPM.

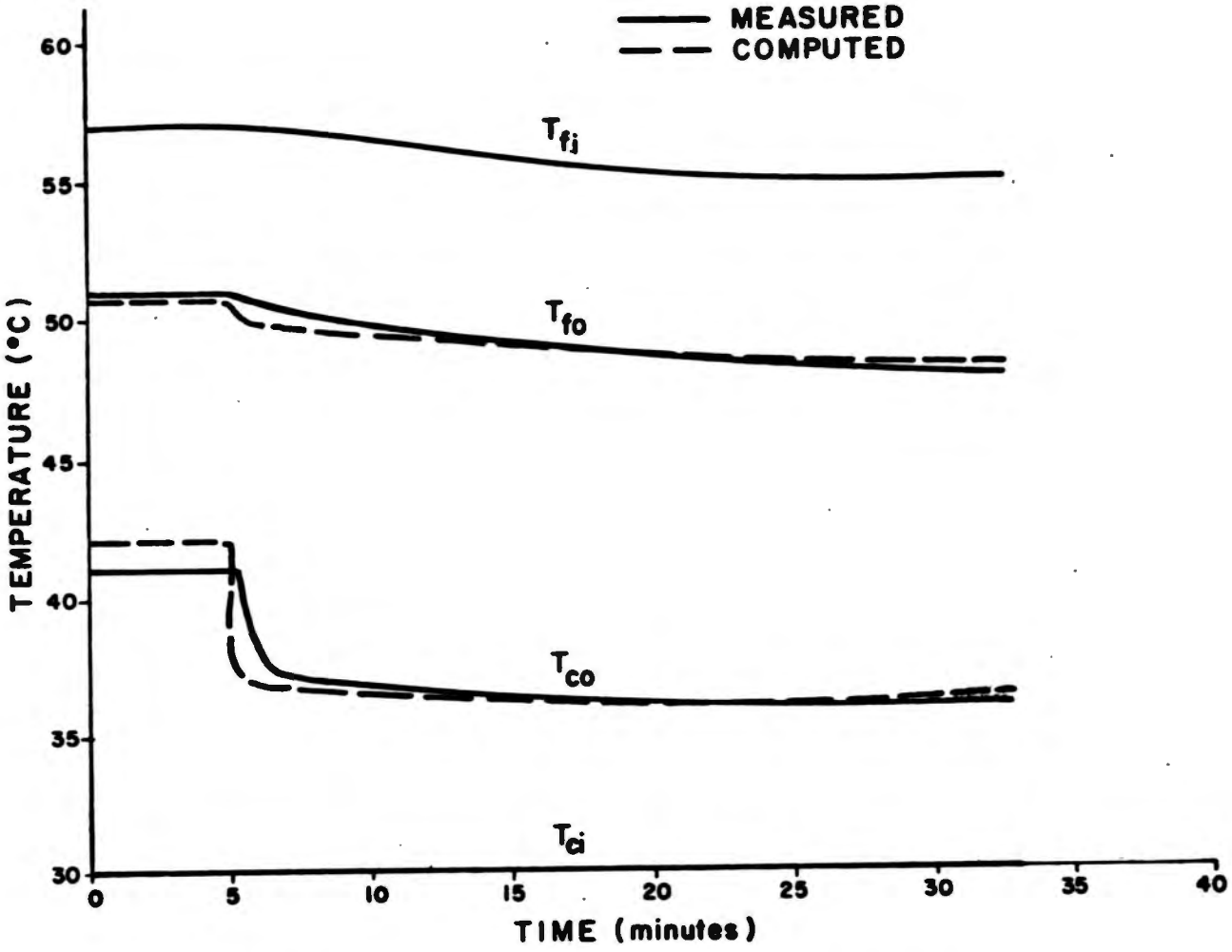

Fig. 3-2. Effects of a Dynamic Change in Coolant Flow Rate Through the Heat Exchanger.
Q_c = 20.87 LPM Initially, at t = 5 Minutes.
Q_c = 42.78 LPM; Q_f = 93 LPM

TABLE 3-2: Error Between Experimental Data and Predicted Results

Run No.	Differences Between AMTD and LMTD			Outlet Coolant Temperature			Outlet Fluid Temperature		
	Average % Error	Maximum % Error	Final Value % Error	Average % Error	Maximum % Error	Final Value % Error	Average % Error	Maximum % Error	Final Value % Error
1	0.147	0.414	0.118	0.737	1.698	0.062	4.488	5.558	5.558
2	0.710	0.873	0.745	0.743	2.282	0.060	4.940	7.908	3.879
3	1.259	1.521	1.204	2.613	4.845	3.226	0.796	1.606	0.632
4	1.479	1.666	1.666	2.862	4.342	3.435	1.020	2.320	0.685
5	0.630	0.721	0.546	0.971	2.330	2.155	0.530	1.121	1.121
6	0.121	0.158	0.118	0.672	2.644	0.095	0.593	2.224	0.626
7	0.128	0.183	0.129	1.022	2.124	1.455	0.872	2.211	1.378
8	0.009	0.068	0.006	0.840	3.030	0.542	0.334	1.531	0.069
9	0.005	0.032	0.000	1.213	2.049	2.048	0.814	2.261	1.445
10	0.152	1.105	0.002	0.753	3.267	0.742	0.573	1.610	0.547

model for the heat exchanger considered here is extremely realistic.

The analysis presented above is generally applicable for liquid-to liquid heat exchangers and, with some modifications, can be applied in thermal analysis of liquid-to-air exchangers.

- THERMAL MODEL OF A COMPLETE SYSTEM -

Although modern control system theory is well suited for individual component analyses, the end objective is to provide an overall system model. This is also the ultimate goal in the thermal analysis of fluid power systems. As an example to this, an open-center system consisting of a positive-displacement pump. a directional control valve, a hydraulic motor, and a reservoir is analyzed. (Schematic is shown in Fig. 3-3).

The simplifying assumptions used in the analysis are, in part, similar to those used in the heat exchanger analysis. They are as follows:

1. All frictional losses due to component inefficiencies can be considered as heat addition to the system.

2. All heat is transferred to the surroundings from the reservoir. A constant overall heat transfer coefficient is applicable to the system.

3. The value of the equivalent lumped thermal capacitance of the system is approximated by the volume of the fluid in the reservoir.

4. All internal component leakages are negligible.

Application of a thermal energy balance to the system yields results that are similar to those obtained in the heat exchanger analysis:

$$H_{st} = \sum H_{gen} - H_{trans} \tag{15}$$

Each of these terms can be defined mathematically. The heat storage rate within the system is given by the following expression:

$$H_{st} = C_{eq}\dot{\Delta T} \tag{16}$$

where $\dot{\Delta T} = d/dt(T_{res} - T_{amb})$. The heat transfer rate can be written as follows:

$$H_{trans} = UA(T_{res} - T_{amb}) \tag{17}$$

The heat generation rate is a summation of the individual generation rates of the components constituting the system. For the orifices in the valve, this can be written as:

$$H_{gen} = k_1 Q \Delta P \tag{18}$$

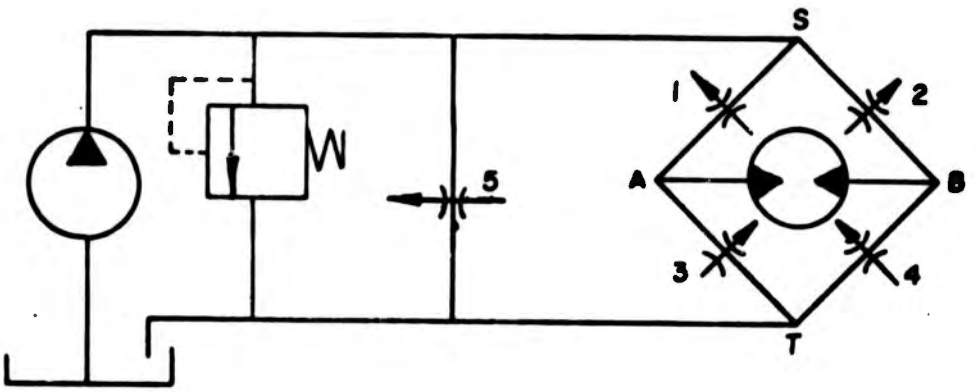

Fig. 3-3. Schematic of Open-Center System.

where: k_1 = conversion factor for dimensional consistency

= 0.006427 Btu sec/in/lb_f/min

ΔP = differential pressure across the component, psi

Q = flow rate through the component, cu in/sec

Combining these equations yields the following result:

$$\dot{\Delta T} = (\sum H_{gen} - UA(T_{res} - T_{amb}))/C_{eq} \qquad (19)$$

which is the dynamic thermal model for the overall system. Solution of this model predicts the reservoir temperature for any point in time.

At steady-state conditions, Eq. (19) can be explicitly solved for the UA parameter, which is the lumped thermal resistance for the entire system.

$$UA = H_{gen} / (T_{res} - T_{amb}) \qquad (20)$$

Eq. (19) is inherently non-linear due to the first term on the right-hand side of the equation. As a result, no exact solution for this equation exists for the dynamic case, but an approximate solution can be obtained by numerical integration techniques. A digital computer can conveniently be used to reach these ends.

The thermal model for this system was simulated on a digital computer by using a modified version of the computer program for open-center directional control valves [10]. Appendices D and E give brief descriptions of the algorithms used to solve both open and closed center systems. A simple Eulerian integration scheme is used to numerically solve the dynamic thermal model. All of the simulation runs are based on actual experimental data from metering tests of an open-center directional control valve. It should be noted that the computer program performs the thermal analysis on a component-to-component basis, which includes all of the components of the system. As it is assumed that there are no thermal energy losses between the component, the output of one component serves as the input to the next.

Fig. 3-4 shows the results for a simulation which includes the assumptions of constant pump and motor efficiencies, constant fluid viscosity, flow rate, motor load, spool displacement, and an ambient temperature of 85°F. Although the results obtained for these conditions are valuable for design and "worst case" specifications, they can be improved. Most hydraulic systems perform some sort of duty cycle. The simulation schemes were drafted with the flexibility to incorporate a duty cycle. To illustrate this the system was simulated for a duty cycle of positive

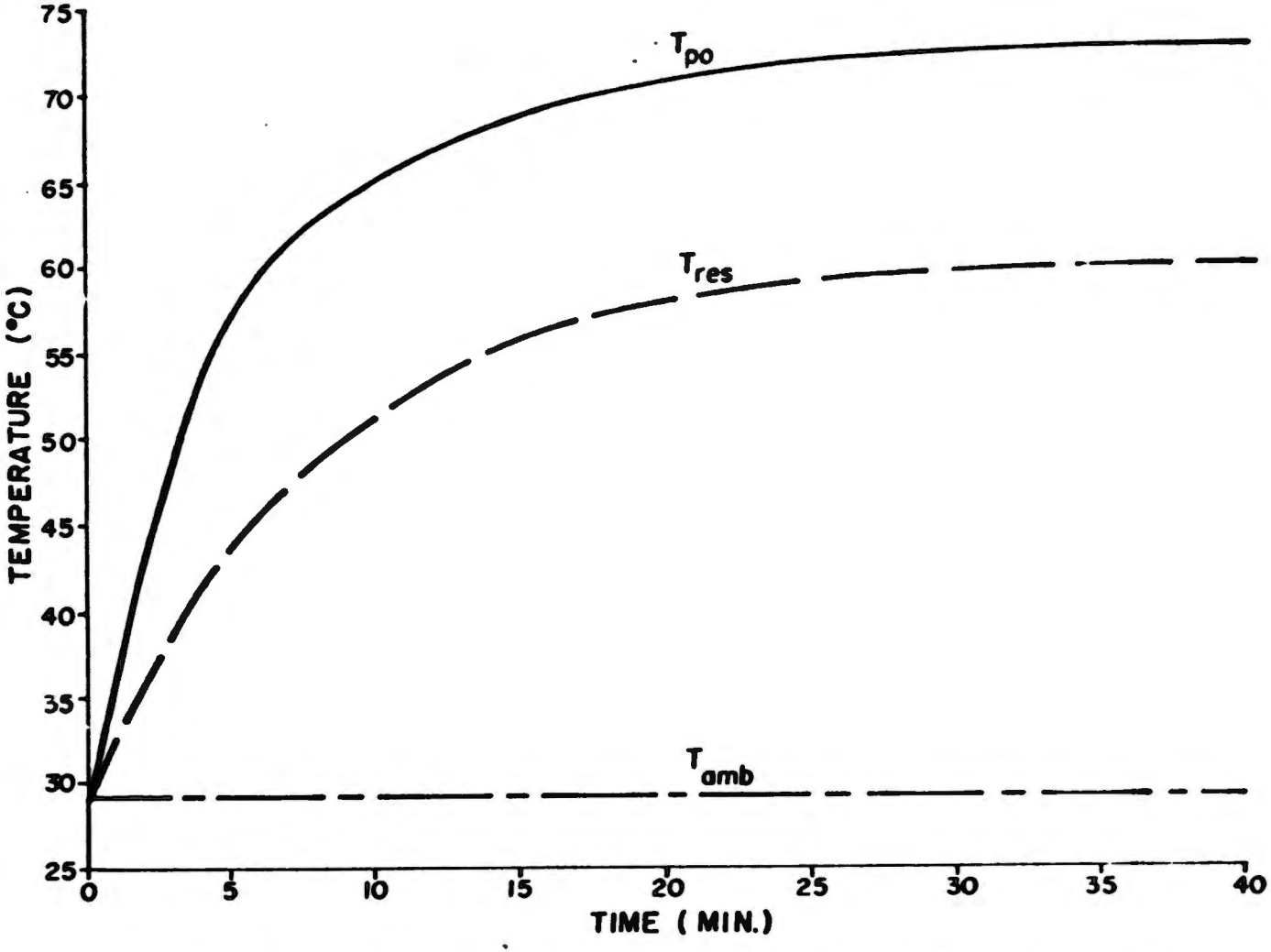

Fig. 3-4. Simulated Results for Constant Pump and Motor Efficiencies, Load, Flow Rate, Spool Displacement, and Viscosity.

spool displacements and varying loads and system flow rates. The fluid viscosity and the pump and motor efficiencies were the only factors that were assumed to remain constant for this simulation. Since duty cycles are commonly only a few seconds long, it is advantageous to analyze only the first cycle and calculate the average heat storage, heat generation, and heat transfer rates for it. Knowing these average values and the duration of the cycle, the reservoir temperature can be calculated for time spans much longer than the duty cycle without high computing costs. The loads and displacements that were used in this simulation are shown in Figs. 3-5(a) and 3-5(b). The simulated response of the reservoir temperature is shown in Fig. 3-6.

Since temperature changes significantly affect fluid viscosity, the assumption that viscosity is constant in any thermal analysis of a hydraulic system is generally unacceptable. Such is the case in this analysis. Incorporating temperature effects on viscosity also requires the removal of the constant pump and motor efficiency assumption. Changes in viscosity create corresponding changes in component efficiencies. Thus, another computer simulation was made for the duty cycle of Figs. 3-5(a) and 3-5(b), and it included the effects of temperature changes on pump and motor efficiencies. Fig. 3-7 illustrates the results of viscosity changes on the reservoir temperature, and Fig. 3-8 shows the effects of temperature and viscosity changes on both pump and motor efficiencies.

As can be seen from Fig. 3-7, warmup time (i.e., time it takes to reach steady-state conditions) for the system as it continuously performs its duty cycle is approximately 60 minutes. This is for an ambient temperature of 85°F (29.44°C), which corresponds to summer operating conditions in the continental United States. Perhaps another point of interest is: What is the temperature response and warmup time for arctic operating conditions? Another simulation was made for the same duty cycle, but an ambient temperature of -20°F(-29°C) was used as the initial conditions for the simulation. For this case, it would take the system approximately 100 minutes to reach a steady-state temperature of 94°F(34.4°C).

From the preceding discussion, it can be seen that thermal modeling of fluid power systems is not an unusually complex mathematical feat. Instead, it is a combination of a relatively straightforward application of basic physical laws and basic test data to yield a simple but accurate method for temperature prediction in fluid power systems. The methods presented here, although they focus upon a specific situation, are sufficiently general to be applicable to any system. Utilization of such methods is of significant value in assessing the performance of systems and in drafting rigorous and unambiguous specifications for procurement by resorting to machine simulation; expensive and time-consuming field trials can be considerably reduced and maximum use is made of test data on components and systems.

- SUMMARY AND CONCLUSIONS -

Fundamental concepts of modern control theory and basic heat trans-

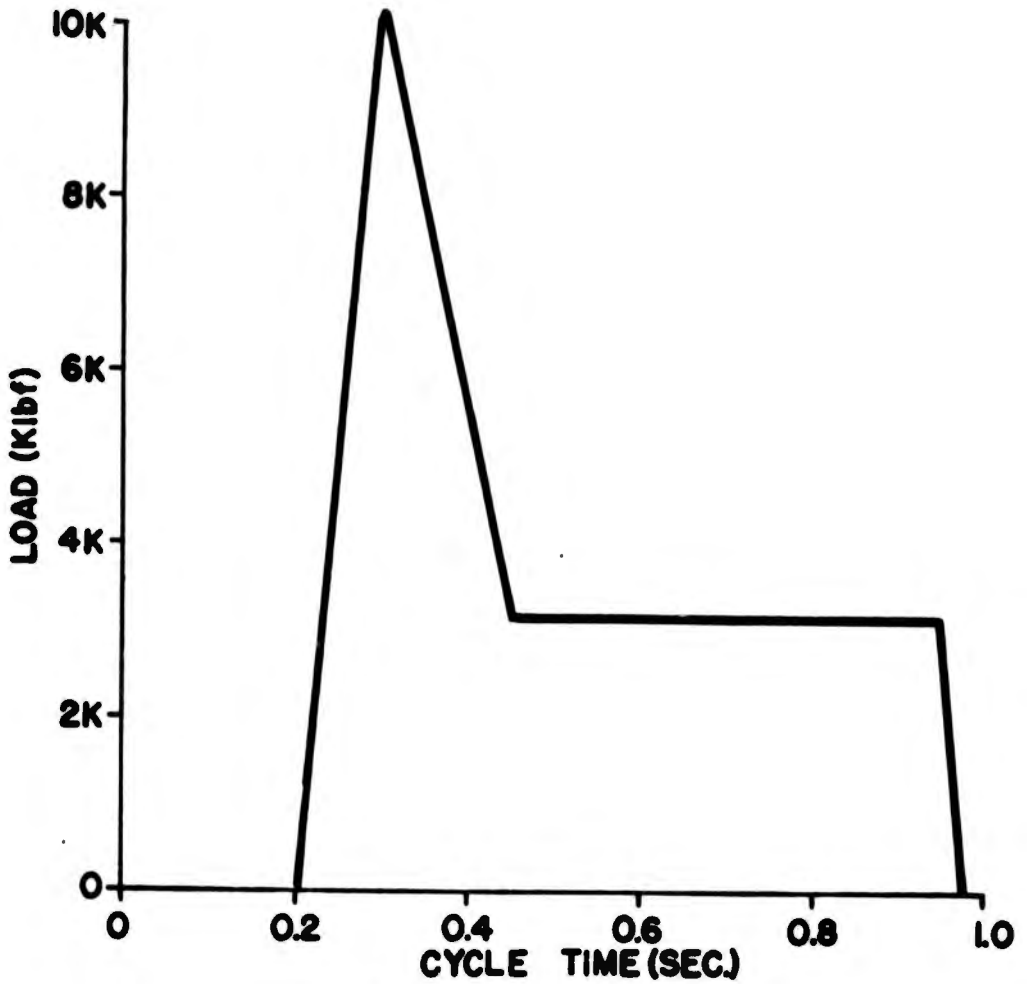

Fig. 3-5(a). Load Versus Cycle Time.

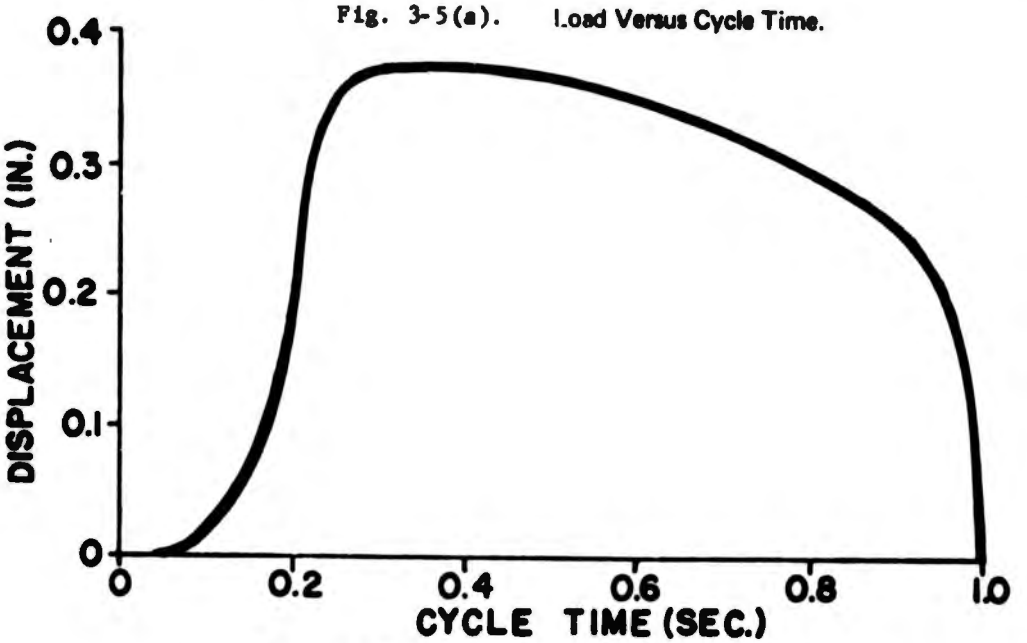

Fig. 3-5(b). Spool Displacement Versus Cycle Time.

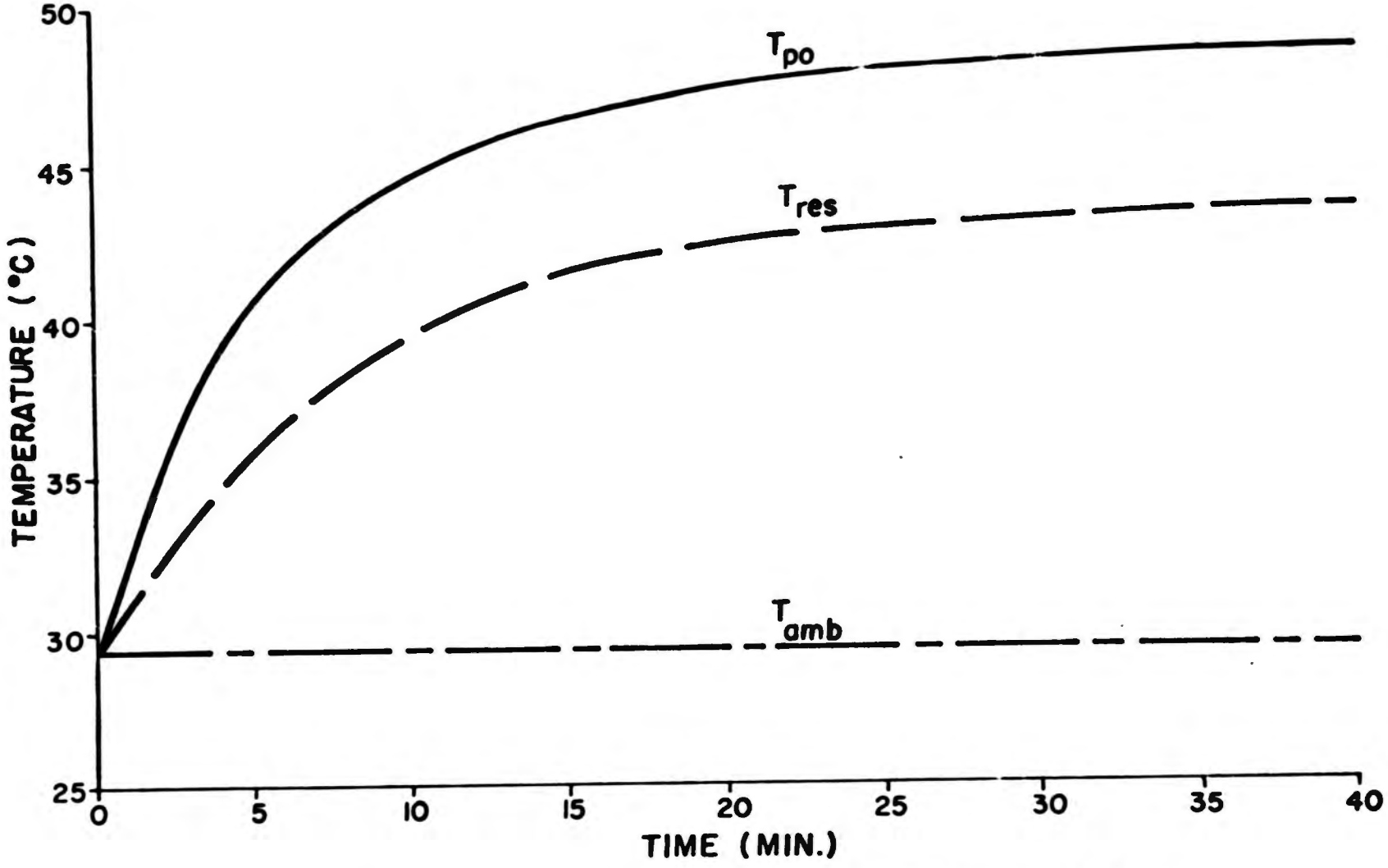

Fig. 3-6. Reservoir Temperature Response for Duty Cycle Operation of the System.

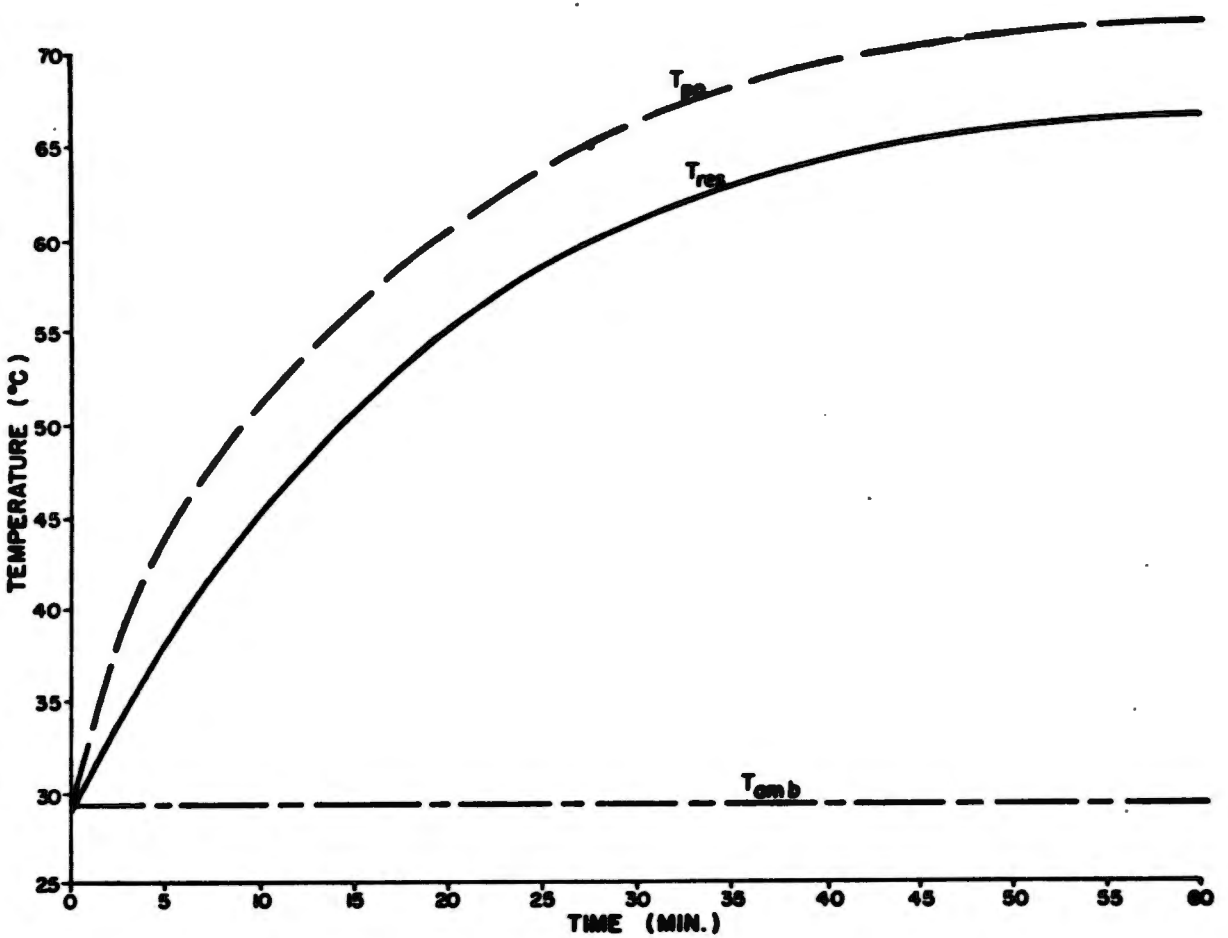

Fig. 3-7. Response of Reservoir Temperature to the Inclusion of Viscosity Change in the System Simulation.

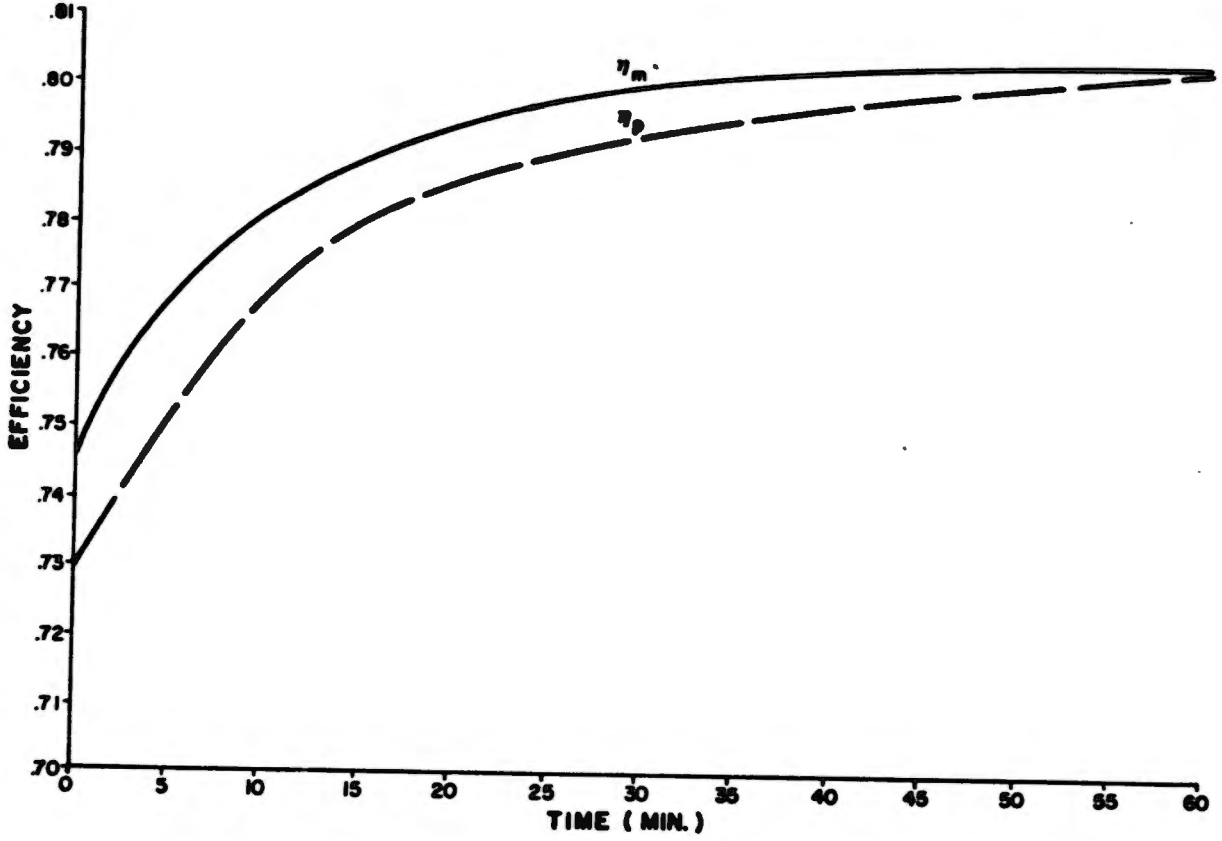

Fig. 3-8. Temperature and Viscous Effects on Pump and Motor Efficiencies.

fer and thermodynamic laws are well suited for the thermal analysis of fluid power systems. Application of these methods to hydraulic systems provides simple but accurate thermal models for components and systems. Such models provide a thorough knowledge of the temperature characteristics of a system. With this knowledge, component inefficiencies can be minimized in design stages, and the generation of high system temperatures and the many ill effects which they produce, can thus be avoided.

Heat exchangers are integral components in many fluid power systems. An analysis for a liquid-to-liquid heat exchanger is presented here on the basis of the arithmetic temperature difference. Treatment of the heat exchanger as a component results in a multi-input, multi-output, non-linear, dynamic thermal model. Solution of this model yields predictions of the AMTD and of the outlet coolant and fluid temperatures. Since this model is non-linear, the only feasible means of solving it, without resorting to linearization techniques, is with a digital computer. Verification of the numerical solution of this model is provided by comparison with experimental test data. The experimental work is in general accordance with the test procedure presented under an earlier phase of the OSU-MERDC contract [11]. The close agreement of the experimental data with the simulated results substantiates the validity of the dynamic thermal model.

A thermal analysis of an open-center system is also presented. A dynamic thermal model is derived and numerically solved for a variety of cases. The most relevant solutions which are discussed include the performance of a duty cycle, temperature effects on viscosity, viscosity effects on component efficiencies, and ambient temperature effects on overall reservoir temperatures. The usefulness of the model that is presented here is that prediction of individual component outlet temperatures are provided in addition to the prediction of the reservoir temperatures.

The lumped parameter analysis that is given here illustrates a practical and simple method for thermal modeling of fluid power systems in general. Although a specific system is considered, the same procedure applies to any hydraulic system. In the case of large and complex systems, individual component analyses are cumbersome in many instances. However, the versatility of this method for thermal modeling allows individual analysis if it is desired, or components can be lumped together, as in general system modeling, to determine their net effect on overall system temperatures. Experimental data can always be used not only to verify the model but also, if necessary, to identify unknown parameters in the model.

- REFERENCES -

1. Parker, J. D., J. H. Boggs, and E.F. Blick, Introduction to Fluid Mechanics and Heat Transfer, Addison-Wesley Pub. Co., Inc., Reading, Mass., 1970.

2. Ebbesen, L. R., "Thermal Analysis of Fluid Power Systems, "Basic Fluid Power Research Program Annual Report No. 6, Paper No. 72-SP-4

Fluid Power Research Center, Oklahoma State University, Stillwater, Oklahoma, 1972.

3. Parker, J.D. and F.C. McQuiston, "Thermal Design of Hydraulic Circuits, "School of Mechanical and Aerospace Engineering, Oklahoma State University, Stillwater, Oklahoma, 1963.

4. Giedt, W.H., Principles of Engineering Heat Transfer, Princeton, New Jersey, 1957.

5. Miller, D.G., "Development and Verification of Thermal Models for Fluid Power Systems, "Report No. R73-SP-1, Fluid Power Research Center, Oklahoma State University, Stillwater, Oklahoma, 1973.

6. Floersch, R.H., D.R. Hahn, and H.R. Sebesta, "Instructions for Performing Optimization and Model Fitting Using DYSIMP," School of Mechanical and Aerospace Engineering, Oklahoma State University, Stillwater, Oklahoma, 1971. (Unpublished)

7. Murali, B.N., L.R. Ebbesen, and H.R. Sebesta, "Optimization of Constrained Dynamic Systems Using the Sequential Unconstrained Minimization Techniques, "Journal of Dynamic Measurement and control, Vol. 94, pp. 319-22, December 1972.

8. Ebbesen,L.R., B. Tomlinson. and H.R. Sebesta, "Instructions for Using the DYSIMP Sub-Program, "School of Mechanical and Aerospace Engineering, Oklahoma State University, Stillwater, Oklahoma, 1970. (Unpublished Report)

9. Blackburn, J.F., G. Reethof, and J.L. Shearer, Fluid Power Control, Massachusetts Institute of Technology, 1960.

10. Iyengar, S.K.R. and D.G. Miller, "Static Analysis of Directional Control Valves Using Analytical and Test Data, "Basic Fluid Power Research Program Annual Report No. 7, Paper No. 73-SP-3, Fluid Power Research Center, Oklahoma State University, Stillwater, Oklahoma 1973.

11. Hydraulic System Control Study (U) Annual Report (Section II) FPRC-2M2, Fluid Power Research Center, Oklahoma State University, Stillwater, Okalhoma (AD 758876) November, 1972.

CHAPTER IV

COMPUTER-AIDED PROCUREMENT
(Service Life)

- INTRODUCTION -

The length of time which a hydraulic system can be expected to remain in service without major repair or maintenance is a primary concern in the procurement of such system. As the degree of sophistication of hydraulic systems increases and more severe duty cycles are imposed on them, field life becomes a much more critical procurement requirement. Thus service life analysis is an important part of the computer-aided procurement concept.

Since a hydraulic system is composed of several components, its service life is determined by the performance of these components. From an engineering standpoint, the service life of a hydraulic component is the operating time during which the degree of performance degradation is acceptable. Ignoring catastrophic failure, service life is directly related to the contaminant wear tolerance of the fluid-exposed elements in the component and the contamination level of the circulating fluid. Therefore, before a realistic analysis of the service life aspects of a hydraulic can be made, information must be available concerning the contaminant sensitivity of the system components and the filtration capability of the filter.

Previous development work in this program has produced test procedures to appraise contaminant sensitivity of the more common hydraulic components as well as filter performance tests [1, 2, 3]. Due to the lack of information concerning average system dynamics, these test procedures were designed to evaluate the components under steady state operating conditions. Since the development of the on-board monitor, it is now possible to efficiently obtain realistic data on the dynamics of the system operating parameters such as pressure, flow, speed, and etc. Therefore, the purpose of this phase of the contract was to determine the influence of the system operating dynamics on the contaminant characteristics of hydraulic component. Such information will permit a much more rigorous evaluation of system service life.

The operating parameter of a hydraulic system which most significantly effects the contaminant sensitivity is the pressure duty cycle. Thus the scope of the work for this phase of the contract included the evaluation of pressure effects upon the contaminant wear exhibited by hydraulic pumps and valves. In addition, filter performance tests were

conducted to evaluate the influence of both ingression rate and flow surge upon the contamination level of a system.

Service life analysis offers the only practical means today of appraising the potential life of fluid power systems. A component which exhibits a low sensitivity to contaminant will have a high wear tolerance and can be exposed to greater contamination levels for a specific period of time than a component having a high sensitivity. The only way to realistically appraise the system service life is to evaluate the contaminant tolerance of the most critical components under the operating environment to which they will be exposed; and to determine the contamination level which will be maintained by the system filter in the same environment.

- INVESTIGATIONS -

The activities pursued in this phase were divided into two basic catagories. The first category was concerned with the influence of system pressure upon the contaminant sensitivity of hydraulic pumps and valves. The second was directed toward the effect of ingression rates, contaminant particle size distribution, and flow surges upon the performance of hydraulic system filters. The work accomplished in each of these areas will be discussed separately.

The contaminant sensitivity of a hydraulic component is reflected by a change in performance when the component is subjected to a specific contaminant environment. The term contaminant wear is also used to describe the deleterious effects caused by all active wear mechanisms which are influenced by entrained particulate contaminant in the fluid. The amount that the performance of a component degrades when exposed to a contaminated fluid environment is a measure of the contaminant wear.

The performance of any hydraulic component can be measured by several different parameters. The performance parameter needed to appraise contaminant wear must be a responsive operating variable which directly or indirectly reflects the contaminant sensitivity of the component. Based on the work accomplished previously on the OSU-MERDC Hydraulic Specification Program, the best performance parameter for a hydraulic pump is the output flow rate. For a relief value the performance parameter is the pressure level maintained by the valve. The performance parameter for a directional control valve is either the pressure drop at a constant spool position and flow rate, or the flow rate at a fixed pressure and spool displacement.

PUMP CONTAMINANT SENSITIVITY

The contaminant sensitivity of a hydraulic pump as reflected by a degradation in the flow rate under a contaminated environment is significantly influenced by the operating pressure imposed on the pump. To

evaluate the effects of both pressure levels and cycling frequency upon the contaminant characteristics of a pump, a number of tests were conducted. Ten gear pumps were obtained from a pump manufacturer for purposes of these tests. With the exception of the pressure imposed upon the pump, each test was conducted in accordance with the test procedure currently under consideration by NFPA (Project T3.9.18). This type of test progressively exposes the pump to increasing sizes of contaminant (from 0-5μM to 0-80μM, classified from ISO contaminant ACFTD) while monitoring the influence of each particle size on the output flow rate of the pump (4).

Test Circuit

Fig. 4-1 shows a schematic of the test circuit used to conduct the cyclic pressure pump contaminant sensitivity tests. The test circuit was the same as that utilized on the steady-state contaminant sensitivity tests for pumps [4] with the addition of the cycle valve driven by a variable speed torque motor through a scotch yoke type linkage. By adjustment of the two variable restrictors shown in Fig. 4-1 the mean pressure and the amplitude of the pressure excursions, were to be established. The frequency of the pressure cycle was varied by the speed of the torque motor.

Test Procedure

A total of seven pump contaminant sensitivity tests were conducted to evaluate the influence of pressure. The conditions to which these pumps were subjected to are listed in Table 4-1. The shape of the pressure wave measured at the pump outlet was approximated sinusoidal. The procedure followed for these pump tests is listed below.

1. The break-in procedure outlined in NFPA T.3.9.1B was used for each pump.

2. The system volume and the quantity of contaminant to be injected was calculated per NFPA T3.9.1B based upon the rated flow at the average pressure shown in Table 4-1.

3. The filter was by-passed, the pressure cycle was initiated and the contaminant slurry was injected.

4. The test was conducted for 30 minutes for each specified contaminant environment.

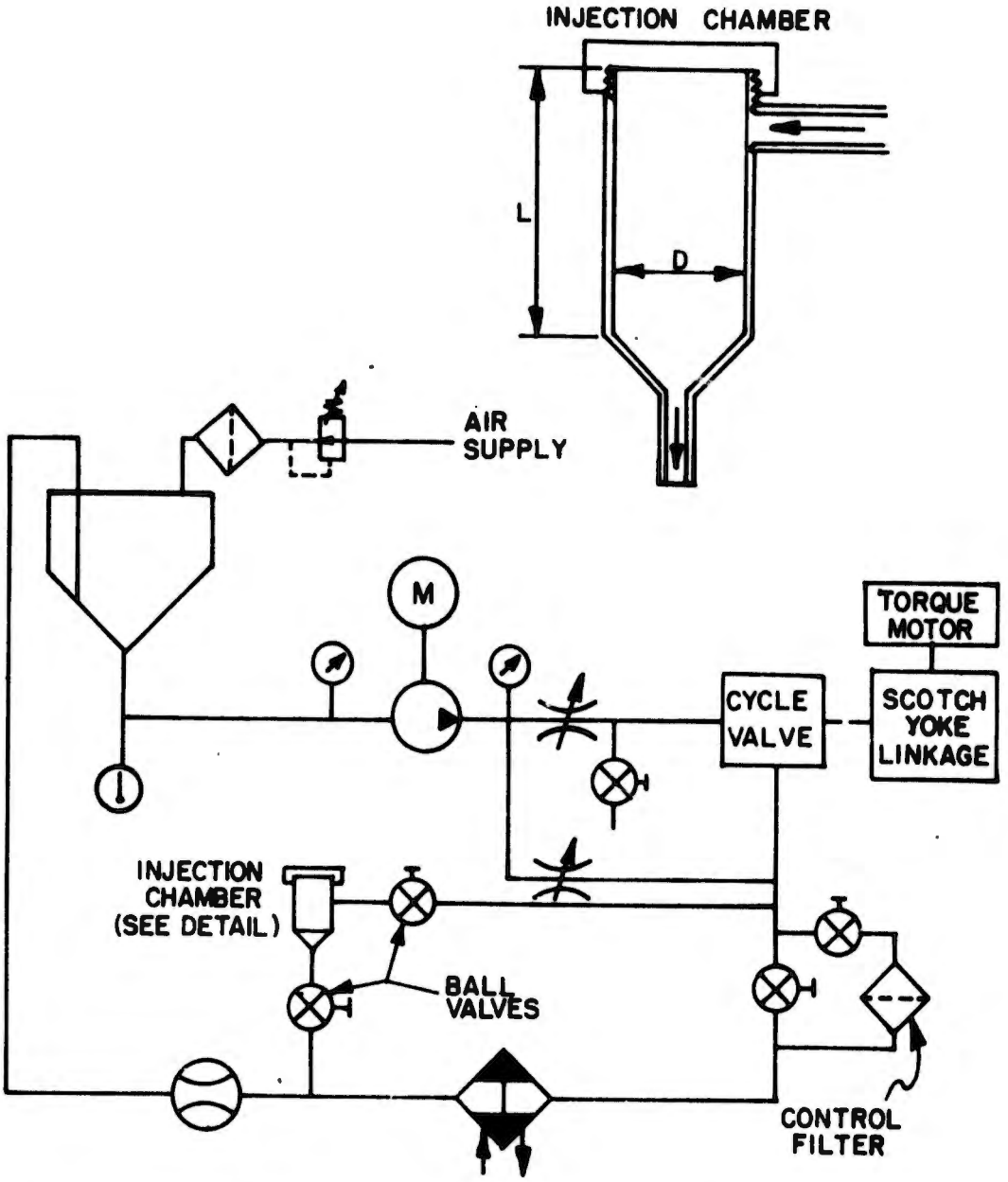

Fig. 4-1. Test Circuit Schematic for Cyclic Pressure Pump Contaminant Sensitivity Tests.

5. After the 30 minute period the pressure cycle was terminated, pressure was adjusted to the specified average pressure, and the system was filtered for 10 minutes.

6. After the filtering period the final flow rate was recorded.

7. Steps 3 through 6 was repeated for each particle size.

Table 4-1

Summary of Test Conditions for Cyclic

pressure pump Contaminant Sensitivity Tests

Pump ID	Speed (RPM)	Average Pressure (Psi)	Pressure Amplitude (Psi)	Pressure Frequency (CPM)
A	2000	1000	-------	---------
B	2000	1500	-------	---------
C	2000	2000	-------	---------
D	2000	2000	2250-1750	1
E	2000	1500	1250-1750	1
F	2000	1500	1000-2000	1
G	2000	1500	1250-1750	2

Test Results

As shown in Table 4-1, three pump tests were conducted at constant pressure to provide a base line for evaluating the cyclic pressure tests. Four tests were conducted with the cyclic pressure conditions indicated in Table 4-1. The results of all seven of these pump tests are shown in Table 4-2. To facilitate a clearer comparison between these test results of three steady pressure tests are plotted in Fig. 4-2, the results of the tests where the mean pressure was 1500 psi are shown in Fig. 4-3, while the 2000 psi mean pressure tests are illustrated in Fig. 4-4.

It can be seen from this data that the mean pressure maintained at the outlet of the pump had a significant effect upon the contaminant wear exhibited. However, it is difficult to conclude from the results of these cyclic pressure tests that there is any significant influence due to the varying nature of the pressure imposed on the pump. While the results of the 2-cycles--per-minute test did indicate a slight improvement in the contaminant tolerance of this pump, the difference was small when compared to the effect of various mean pressures and must be discounted untill additional verification tests are conducted.

Table 4-

Summary of Test Results for Cyclic

Pressure Pump Contaminant Sensitivity Tests

Pump ID		A	B	C	D	E	F	G
Test Pressure(psi) and Conditions		1000	1500	2000	2250-1750 1 CPM	1750-1250 1 CPM	2000-1000 1 CPM	1750-1250 2 CPM
Rated Flow		17.7	17.4	17.2	17.4	17.6	17.6	17.4
Ratio of Final Rated Flow	0-5μm	1.0	1.0	1.0	1.0	1.0	1.0	1.0
	0-10μm	1.0	1.0	1.0	1.0	1.0	1.0	.993
	0-20μm	1.0	1.0	1.0	1.0	1.0	.994	.993
	0-30μm	.994	.994	.994	.994	.994	.994	.993
	0-40μm	.994	.989	.971	.980	.966	.994	.993
	0-50μm	.983	.966	.930	.967	.946	.974	.986
	0-60μm	.960	.937	.895	.914	.923	.940	.946
	0-70μm	.938	.908	.849	.833	.903	.912	.930
	0-80μm	.921	.868	.797	.782	.869	.872	.881

Under the assumption that pressure cycling did not influence the contaminant sensitivity of this pump, the four tests which were conducted at a mean pressure of 1500 psi can be averaged and presented as one test. Also, the two tests which were run at a mean pressure of 2000 psi can

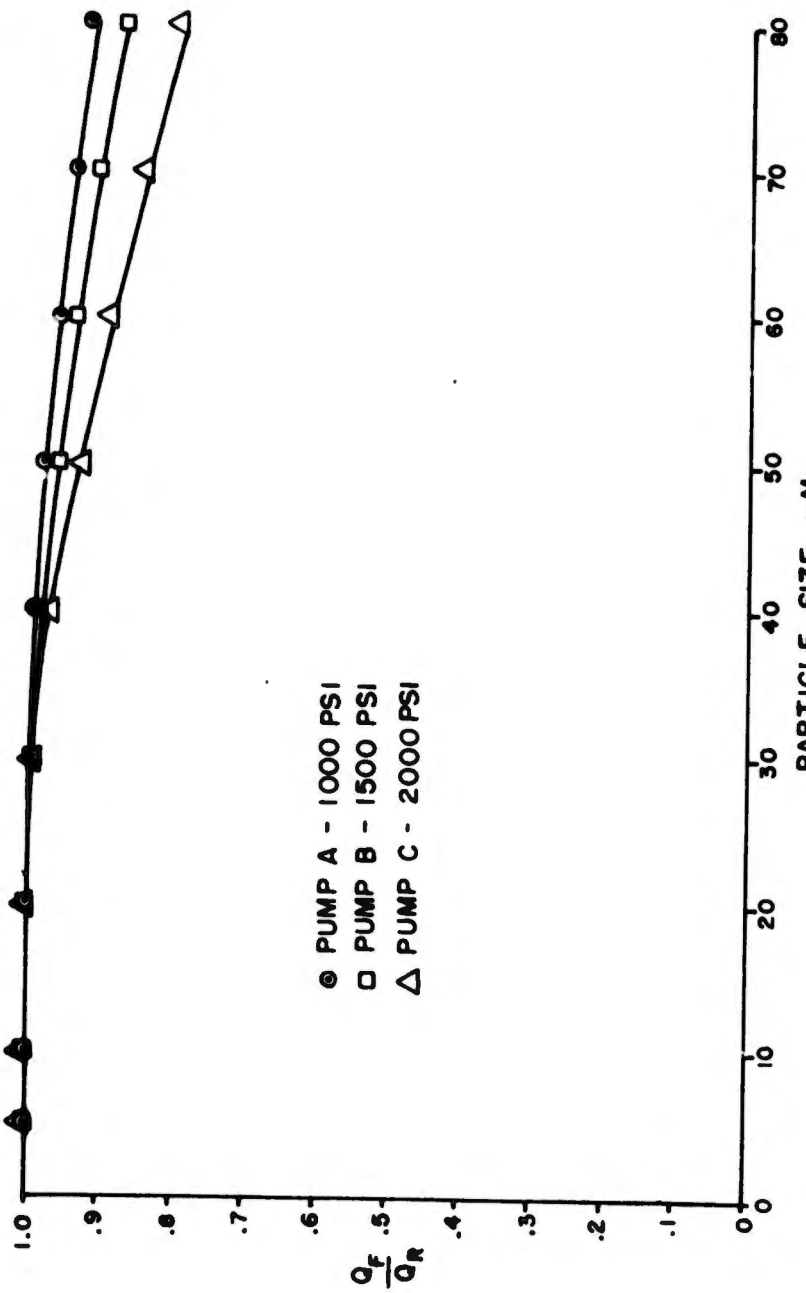

Fig. 4-2. Results of Steady Pressure Pump Contaminant Sensitivity Tests

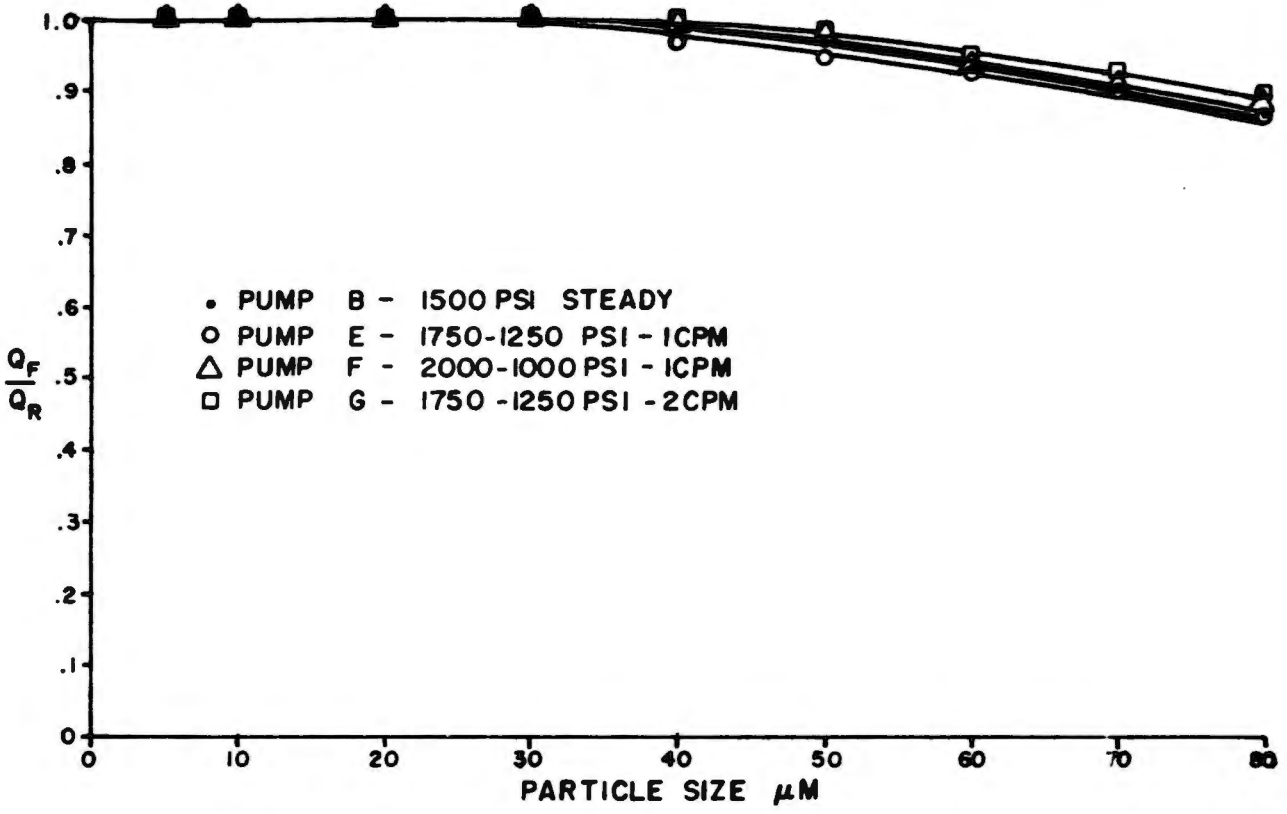

Fig. 4-3. Results of Cyclic Pressure Pump Contaminant Sensitivity Tests (mean pressure = 1500 psi)

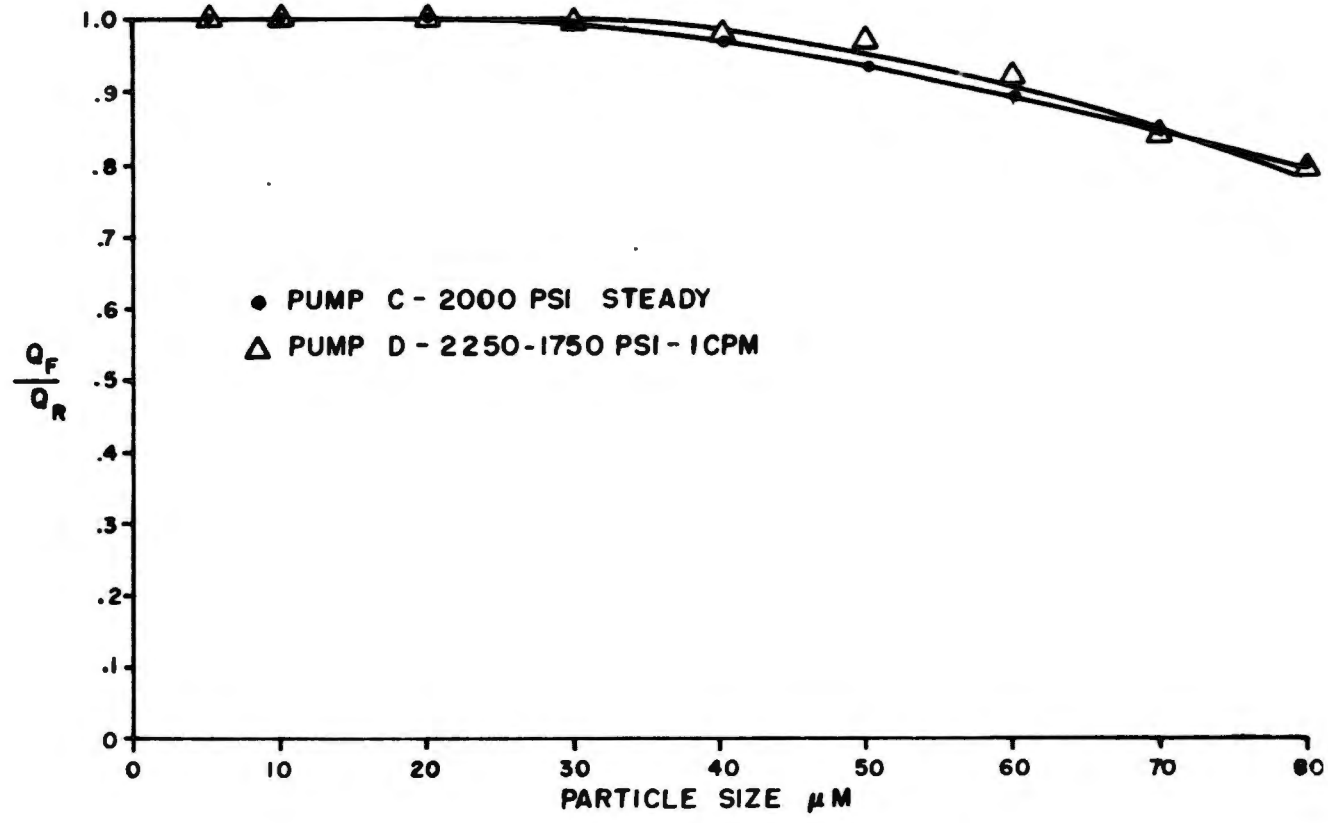

Fig. 4-4 Results of Cyclic Pressure Contaminant Sensitivity Tests (mean pressure = 2000 psi)

be represented by three tests as shown in Table 4-3.

Interpretation of Pump Test Results

Research work conducted at the Fluid Power Research Center and sponsored by the Basic Fluid Power Research program has led to the development of a computer algorithm which processes the laboratory results from a contaminant sensitivity test [4].

Table 4-3

Summary of Average Results from Pump

Contaminant Sensitivity Tests at Various Pressures

Pump ID	Mean Press. (psi)	Aver. rated flow	AVERAGE RATION OF FINAL TO RATED FLOW								
			0-5 µm	0-10 µm	0-20 µm	0-30 µm	0-40 µm	0-50 µm	0-60 µm	0-70 µm	0-80 µm
X	1000	17.7	1.0	1.0	1.0	.994	.994	.983	.960	.938	.921
Y	1500	17.5	1.0	.998	.997	.994	.986	.968	.937	.913	.873
Z	2000	17.3	1.0	1.0	1.0	.994	.976	.949	.905	.841	.790

A computer program which employees this algorithm has been developed by the Fluid Power Research Center, and is currently available at the computing facilities at Ft. Belvoir, Virginia. Basically, this program utilizes the data such as shown in Table 4-3 and the contaminant wear expression [3] given by:

$$\frac{dQ}{dt} = -S(n) \frac{dN}{dt} \qquad (1)$$

Where:

Q = output flow of pump
S = Contaminant Sensitivity
N = Number of particles to which the pump is exposed

The computer program calculates the contaminant wear coefficients (α)

which relate the contaminant sensitivity of the pump to the particle concentration of the fluid. Since most hydraulic components have a different contaminant sensitivity for each particle size range of interest, the sensitivity of a pump is represented by several wear coefficients (αo-5, α5-10, etc). The contaminant wear equation for a pump as given by Eq.(1) expresses the degradation in flow rate with respect to time. Thus, once the wear coefficients have been determined from the laboratory test results, the time for the flow to degrade a specified amount when the pump is exposed to a given contaminant environment in the field can be calculated. However, since the contaminant sensitivity of a pump is influenced by the operating pressure, the contaminant life predicted by the computer will reflect the pressure at which the pump was tested.

A practical way of expressing the sensitivity of a hydraulic component is by the use of the contaminant tolerance profile. The profile is the locus of all log-log[2] particle size distributions which can continuously exist in the exposed fluid and still allow the pump to exhibit an acceptable contaminant life under a given pressure duty cycle. By selecting a service life of 1000 hours and a maximum flow degradation of 20%, three contaminant tolerance profiles can be determined from the data given in Table 4-5 (one profile for each of the pressure conditions). These three 1000 hour tolerance profiles are shown in Fig. 4-5.

It can be seen from Fig. 4-5 that this pump has a lower tolerance level or a greater sensitivity to contaminant when operated at a mean pressure of 2000 psi than when exposed to a mean pressure of either 1500 psi or 1000 psi. To illustrate the influence of pressure in a different manner, the service life of the pump was calculated for each pressure level under a typical field contamination level (based on paper P73-CC-1, Ref. [5]) shown in Fig. 4-5. When exposed to this contaminant environment and subjected to a mean pressure as low as 1000 psi, the pump will have an expected service life of approximately 1600 hours. However, with the same environment and an average pressure of 1500, the service life of the pump will be reduced to about 1000 hours; and finally, at an average pressure of 2000 psi the pumps would last only about 560 hours. This means that if this pump were used in a system which imposed a mean pressure of 2000 psi on it and the system filter maintained a contamination level as shown in Fig. 4-5 the flow rate of the pump would reduce to 20% of its original value in about 560 hours of system operation. It has been determined from industrial opinion that a flow degradation of 20% would be quite noticeable to the operator in the form of slower operation of the system.

Conclusions and Recommendations

It is felt that the results of these pump test have adequately demonstrated the influence of system pressure duty cycle upon the service life of a pump. It was concluded that the peak to peak amplitude of pressure fluctuations had no measureable effect upon the contaminant sensitivity of the pump. However, the sensitivity appeared to be slightly

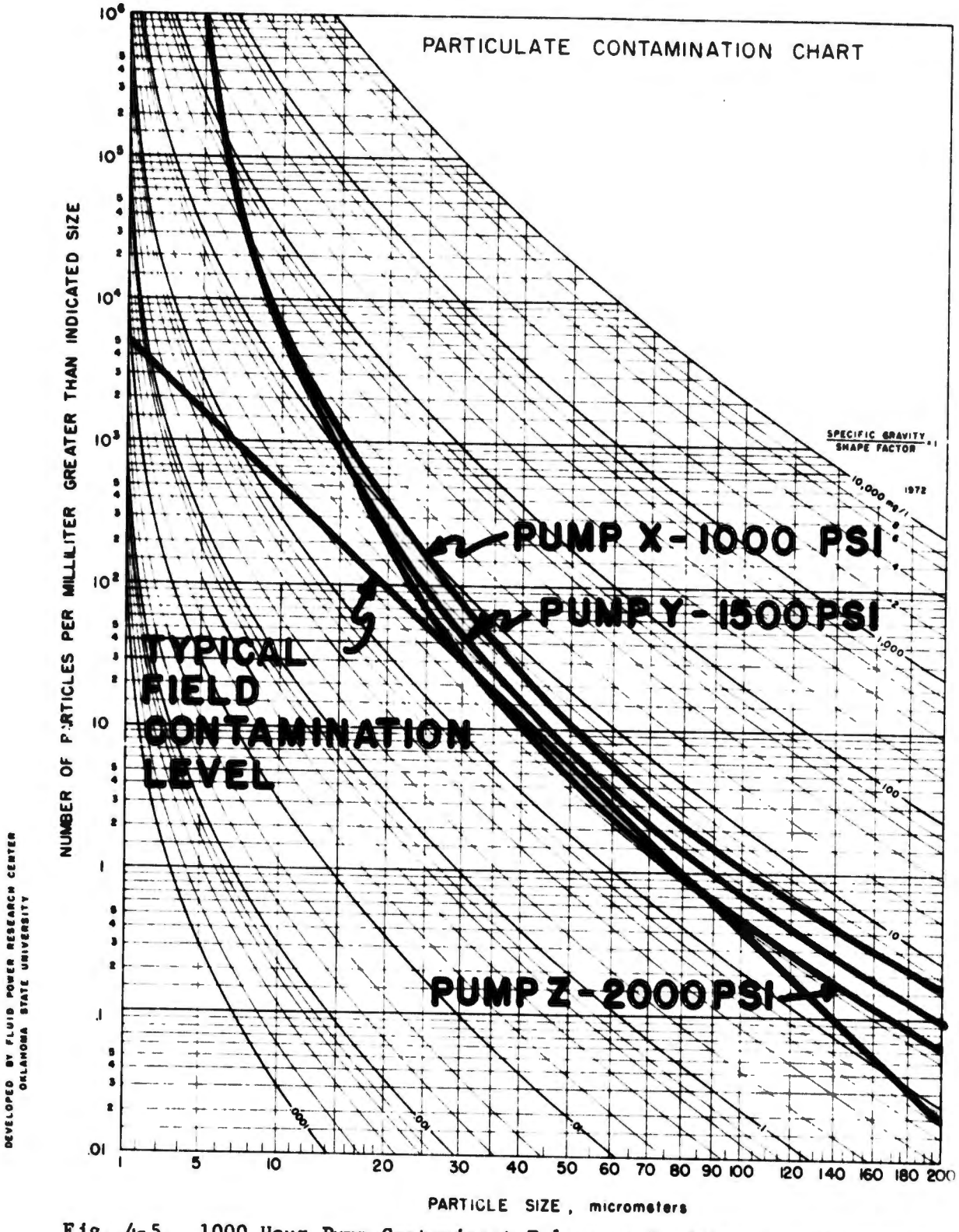

Fig. 4-5. 1000 Hour Pump Contaminant Tolerance Profiles for Various Mean Pressure Conditions.

improved at higher cycle frequencies. Unfortunately, the magnitude of the improvement was not sufficient to support any conclusions in this regard. It is recommended that additional tests be conducted at much higher frequencies (i.e. 10 cycles per minute or 20 cycles per minute) in order to verify this effect. Such tests could also provide additional information concerning the influence of peak-to-peak amplitude variations.

The interpretation placed upon the results of these tests was not meant to label this pump as either a good pump or a bad pump. Instead it was intended to show a subjective evaluation of the service life of this pump under the indicated operating environment (both pressure duty cycle and contamination level). It has been demonstrated however, that information concerning the contamination level which exists in the system fluid and the pressure duty cycle imposed on the pump is necessary in order to realistically appraise the service life of a hydraulic pump.

VALVE CONTAMINANT SENSITIVITY

Almost every hydraulic system which utilizes a positive displacement pump will also incorporate a system pressure relief valve for pressure protection and a directional control valve to direct the pump flow to various parts of the system. While previous work [2,3, & 5] has suggested that the contaminant sensitivity of the system pump will more often determine the protection contamination level needed by the system, the sensitivity of each directional and pressure relief valves should not be omitted from a comprehensive service life appraisal.

The operation of a directional control valve does not easily lend itself to simple incorporation into a contaminant sensitivity test. Not only is such a valve subjected to a pressure duty cycle similar to that of the pump, but it is also exposed to an operational duty cycle which reflects movement of the valve spool by the operator. The directional valve contaminant test procedure previously developed [2] specified that the test be conducted with the valve spool fixed in a position which throttled flow from the inlet to the work port. Therefore, these tests did not incorporate the effect of either the pressure duty cycle or the operational duty cycle.

A system pressure relief valve is only required to operate when the pressure developed in the system exceeds the setting of the valve. Thus such a valve to exposed to a flow duty cycle. The pressure relief valve contaminant sensitivity test developed for MERDC specified that the flow rate through the relief valve be a constant value based upon the rated flow of the valve. Therefore, a flow duty cycle which is normally imposed on a relief valve was not incorporated into this test.

Both the directional valve and the relief valve contaminant sensitivity tests previously conducted provided repeatable information which certainly discriminated between various valves. However, since these tests

did not include the influence of system dynamics their use in the computer-aid procurement concept was not completely realistic. Therefore, tests were conducted during this phase of the OSU-MERDC program to demonstrate the effects of pressure and operational duty cycles on directional valves and flow duty cycle on relief valves.

Test Circuit

The valve contaminant sensitivity test stand at the Fluid Power Research Center (FPRC) was utilized for these valve tests. The concept of the tests involved an attempt to test a directional valve and two relief valves simultaneously. To accomplish this, the circuit as shown in Fig. 4-6 was designed. A four way, open center direction control valve was utilized. This valve was similar in design to those found on mobile construction machinery. Two cartridge type pressure relief valves were installed at the work ports of the directional valve. As can be seen in Fig. 4-6, flow was subjected to the directional valve, and depending upon the spool position, was either directed through the open center passages in the vale or to one of the work ports. From the work ports the flow was forced through one of the two pressure relief valves and was allowed to by-pass the other relief valve through a one way check valve.

In order to simulate different pressure duty cycles, one relief valve was set at 2000 psi while the other had a pressure setting of 1500 psi. The directional valve spool was continuously cycled by the torque motor which was coupled to the spool by a schotch yoke linkage. The spool motion thus achieved was very nearly sinusoidal at 30 cycle per minute. Therefore, these tests subjected the directional control valve to both an operational and pressure duty cycle while the relief valves were exposed to a regulated flow duty cycle.

The performance parameter which was utilized to evaluate the contaminant wear exhibited by the directional valve was metering characteristics. This was accomplished by measuring the flow from the valve inlet to work port at various positions of the valve spool. Valve outlet pressure was maintained at a fixed value during the measurement of the metering characteristics. The performance parameter selected for the relief valve was the pressure versus flow curve. Variations in the magnitude and shape of this curve will reflect any contaminant wear which occurred.

Test Procedure

The test circuit described was designed to function in conjunction with the valve contaminant sensitivity test facility discussed in Refs. [2 & 3]. In this way, the prescribed test procedure exhibited minimum deviation from the static valve contaminant test procedure developed in past work. The following is a summary of the test procedure devised for

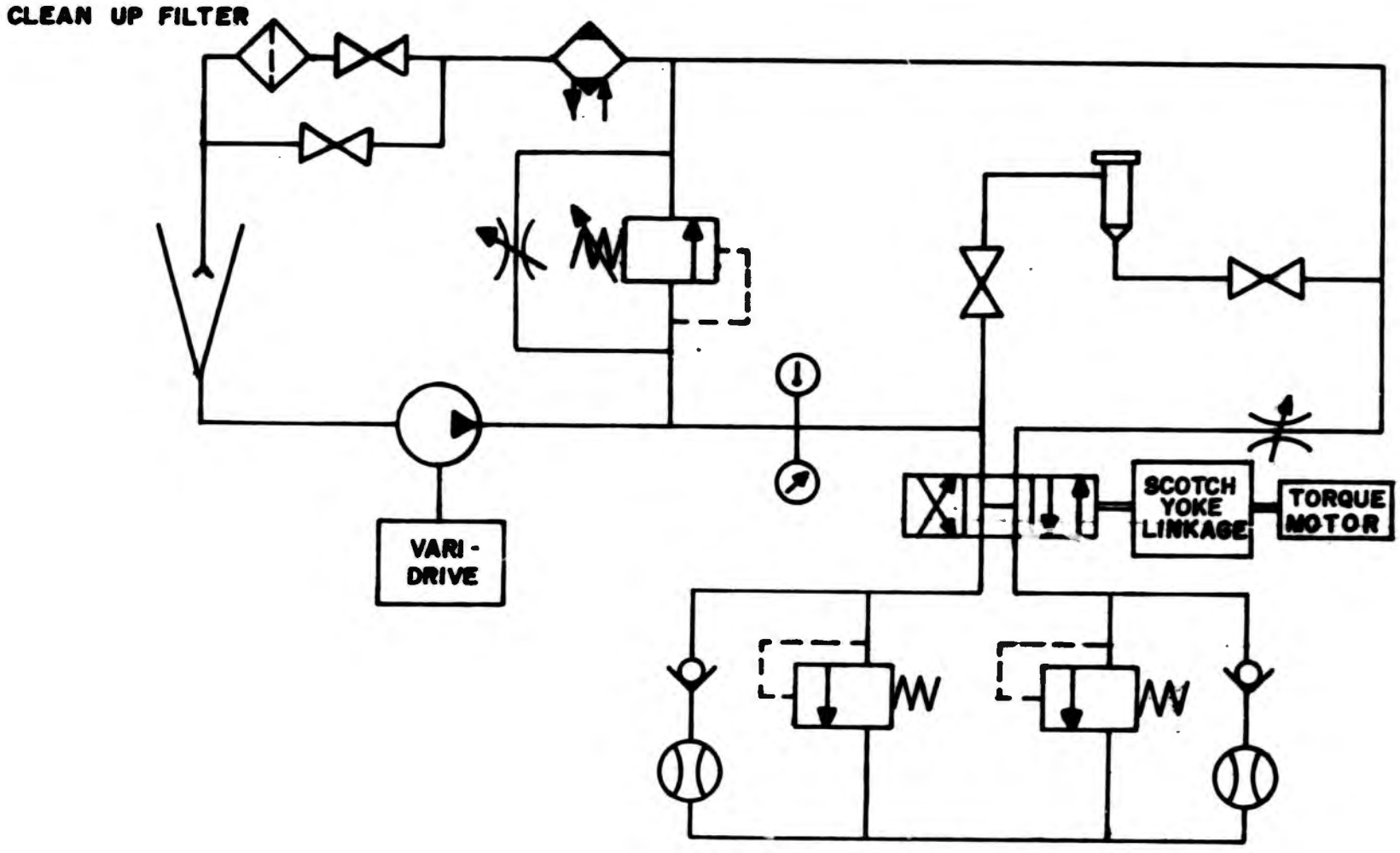

Fig. 4-6. Circuit Schematic for Dynamic Valve Contaminant Sensitivity Tests.

the dynamic valve tests.

1. The valves were installed in a circuit as shown in Fig. 4-6.

2. The system volume was adjusted to be numerically equal to $\frac{1}{4}$ of the test flow rate of 20 GPM.

3. The system temperature was maintained at 150°F $\pm$ 5.4°F while flow was maintained to within $\pm$ 2 percent of the designated value.

4. The system was filtered to a contamination level of less than 1 particles per millilitre greater than 10 micrometres and was validated as described in Ref. [3,4].

5. The cycle rate of the spool was adjusted to 30 cycles per minute. A cycle is constituted of the following: starting with the spool in the center position, displacing it both ways from the center to full displacement is then returning to the centered position.

6. The system filters were switched out of the system and contaminant was added to produce a 300 mg/ℓ of 0-5 micrometre slurry in the test loop.

7. The valve spool was cycled for 30 minutes at the specified flow.

8. The clean-up filters were switched back into the circuit for 30 minutes of cleaning, while the valve spool continued to cycle.

9. After 30 minutes clean up period, the valve spool was positioned at various displacement throughout its cycle to permit measurement of the necessary pressures and flows. At each position of the spool, the system was allowed to stabilize before measurements were recorded.

10. Steps 5 through 9 were repeated for the following particle size ranges: 0-10, 0-20, 0-30, 0-40, 0-50, 0-60, 0-70, and 0-80 micrometres (classified from ISO approved ACFTD).

Test Results

The results from these preliminary dynamic contaminant tests were somewhat disappointing. First of all, it was discovered that the valve contaminant stand which was designed for static testing was structurally inadequate for dynamic testing. The pressure cycling imposed upon this test circuit resulted in many failures which significantly lengthened the test time and seriously strained the schedule for other testing. Also, the degradation reflected by both the directional valve and the relief valves was not sufficient magnitude to complete a realistic service life analysis. That is, the contaminant wear observed after exposing the valve

to a given particle size range was not large enough to assign an accurate value to that particular range. However, a measureable degradation had accumulated by the conclusion of the test.

To illustrate the nature of the contaminant wear or performance degradation which resulted from these tests, plots were made of the flow versus spool position for the directional valve and pressure versus flow for the pressure relief valves. Fig. 4-7 illustrates the initial flow versus spool displacement which was exhibited by the directional control valve used. The two curves shown in Fig. 4-7 represent different downstream pressures which simulate valve load.

The results obtained after subjecting the directional valve to contaminant ranges from 0-5 micrometres to 0-80 micrometres per the test procedure previously outlined indicates that very little degradation had taken place. Fig. 4-8 graphically depicts a subjective evaluation of the degradation; however, as has been pointed out, due to the small amount of change, it was impossible to realistically assign this degradation to a definite particle size range. In Fig. 4-8, the solid line represents the metering curve before contaminant exposure, while the dashed line illustrates the curve after the complete contaminant test.

Fig. 4-9 shows the characteristics of the pressure relief valve. The solid lines in Fig. 4-9 represents the relief valve curve before any contaminant wear had taken place while the dashed line depicts the valve performance after the contaminant sensitivity test. As was the case with the directional valve, the total degradation measured after each particle size range was so small that accurate measurement was not possible. Thus, no attempt was made to perform a service life analysis based upon this data.

Conclusions and Recommendations

Although it would seem that very little could be concluded from the results of these valve contaminant tests, this is not entirely true. The original intention of this work was to demonstrate the influence of the various duty cycles to which valves are subjected by the comparison of the results of these dynamic tests with those obtained on similar valves using a static test. Such a comparison reveals that while the degradation observed during the static tests was both measureable and significant, the same cannot be said for the dynamic tests conducted. This fact alone could indicate that the static tests are more severe but less realistic as a basis for service life evaluation.

In order to understand the difference between the static tests reported in Ref. [3] and the dynamic tests discussed here, the contaminant wear equation (Eq. [1]) must be considered. This equation can be illustrated as follows for any hydraulic component:

$$\frac{dP}{dt} = -S(n)\,\frac{dN}{dt} \qquad (2)$$

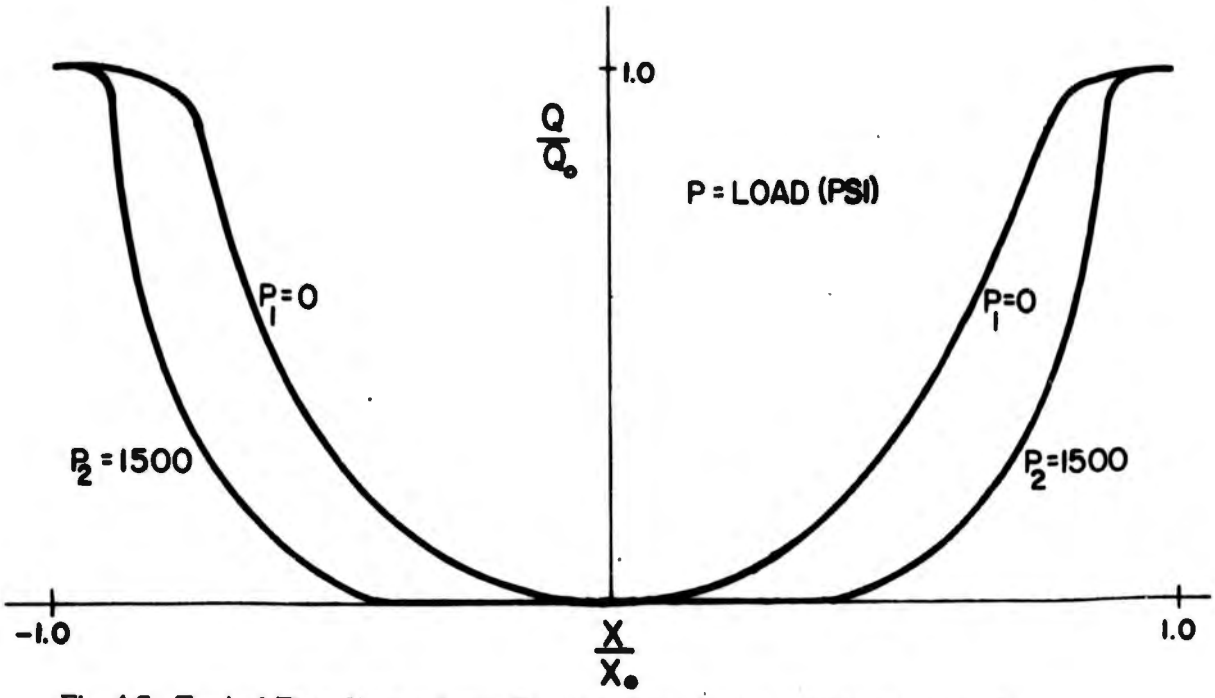

Fig. 4-7. Typical Flow Versus Spool Displacement for the Directional Valve Before Contaminant Exposure.

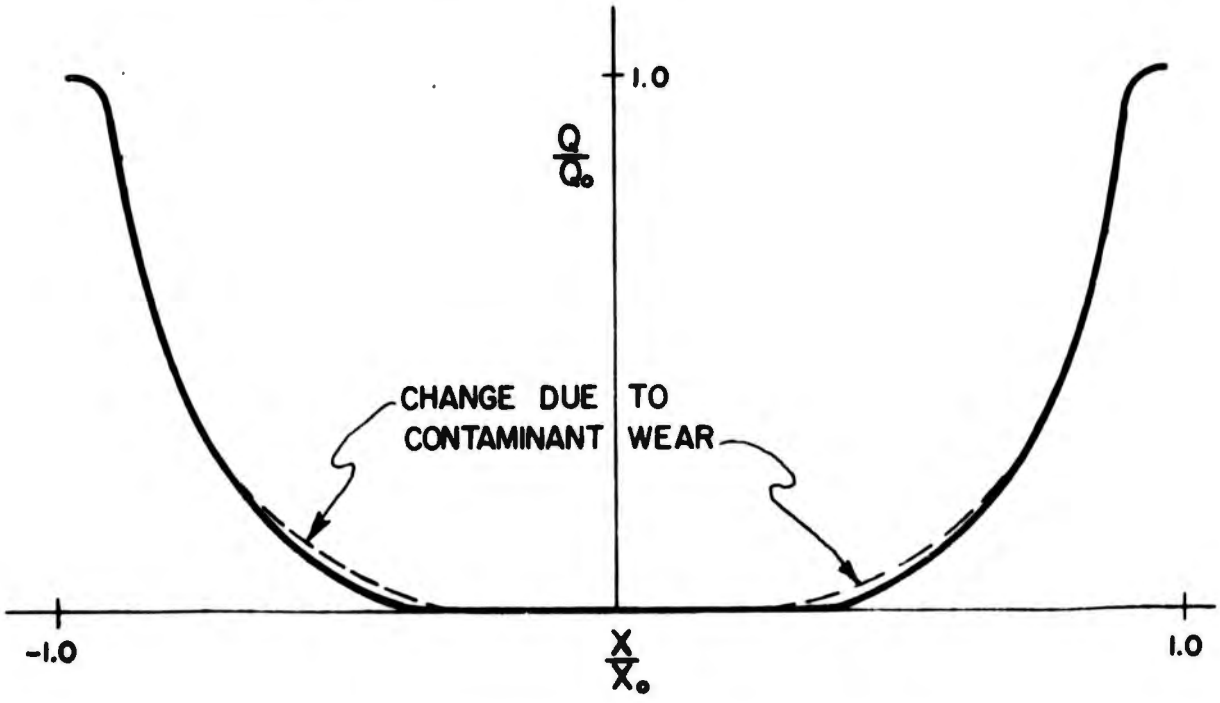

Fig. 4-8. Flow Versus Spool Displacement After Contaminant Exposure.

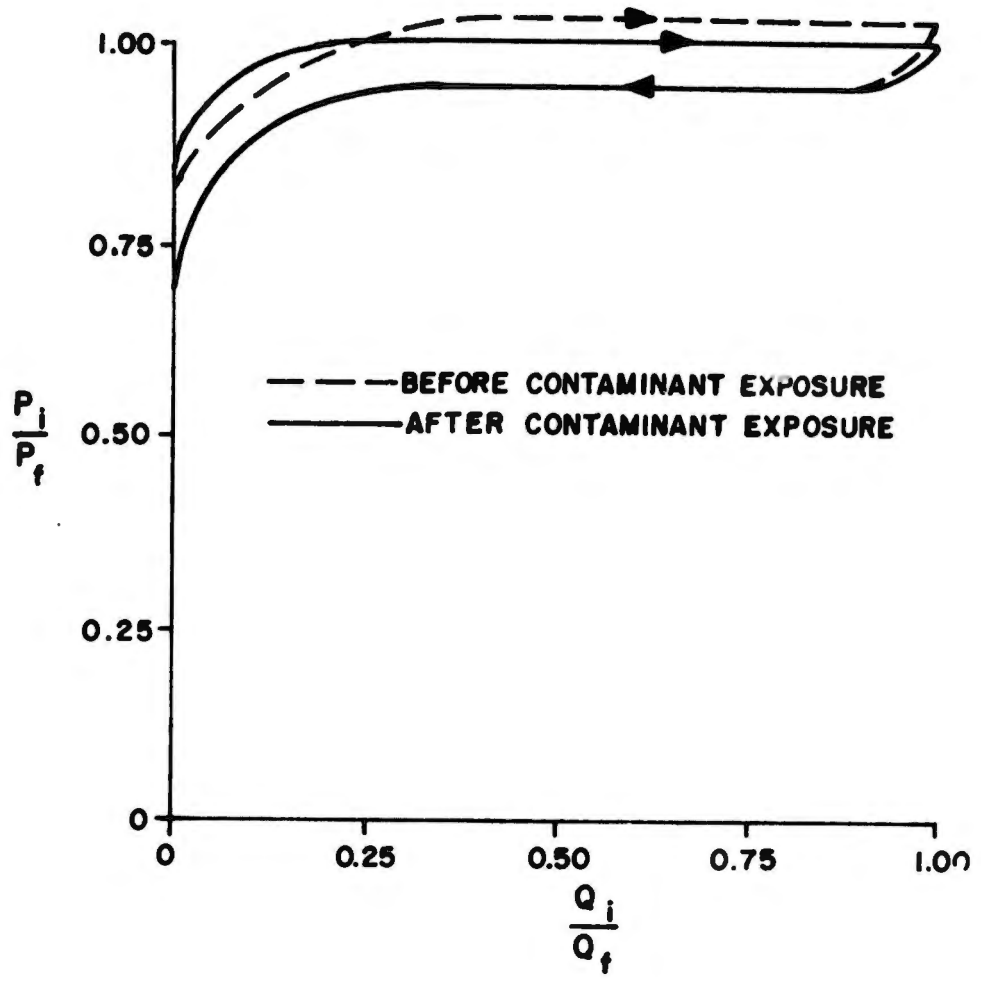

Fig. 4-9. Pressure Versus Flow for Pressure Relief Valve Before and After Contaminant Exposure.

Where: $\frac{dP}{dt}$ = Rate of change of the selected component performance parameter.

S = Component contaminant sensitivity

$\frac{dN}{dt}$ = Contaminant Exposure rate

It should be noted that this equation states that the rate of performance degradation is not only a function of the sensitivity of the component but also the rate at which it is exposed to the contaminant particles. Therein lies the problem experienced in obtaining the results of the dynamic tests. If the rate of the contaminant exposure during the static tests is compared to that maintained during the dynamic tests, it can be shown that the exposure rate is significantly lower for the dynamic case.

In a contaminant test on a hydraulic component the contaminant is entrained in and carried past the wear surfaces by the fluid. Thus, the exposure rate experienced is a function of both the particle concentration in the fluid and the flow rate. In the state tests on directional control valves, the spool was set at a fixed displacement which throttled rated flow from the valve inlet to one work port. Thus, one metering orifice was subjected to contaminant and the area and exposure rate were constant throughout the test. In the dynamic tests the spool was cycled resulting in the use of both work parts and their associated metering orifices by the spool motion, the flow rate was not constant. The average flow rate through one of the metering orifices was approximately 1/3 of that used in the static tests and this average glow rate passed through each orifice for 1/2 of the test time. Therefore, the contaminant exposure rate which characterized the dynamic tests was only about 1/6 of that of the static tests.

Since the test times were the same, if the results of the static tests had shown a 30 to 40% degradation in performance after the complete test, the results after the dynamic test would have only been 5-6%, entirely because of the difference in contaminant exposure rate. The performance degradation results of static tests for these valves (Ref. [3]) was about 30% for the directional valve and 80% for the relief valve. Due to the difference in exposure rate, about 5% and 14% performance degradation could be expected from the directional valve and relief valve respectively during these dynamic tests even if the sensitivity was unaffected by the dynamic conditions. Since the actual results from the dynamic valve tests which were conducted indicated a 2-4% degradation, it can be reasonably concluded that the duty cycles which were imposed during the test had a significant influence upon the results.

Because the results were not sufficient to perform a rigorous service life analysis, it must be recommended that additional testing be conducted to develop a revised test procedure which is capable of providing the necessary data. Based upon the results of these tests as well as the previous static tests, it is felt that such a revised procedure must in-

clude either higher concentrations of contaminant or longer test exposure times in order to compensate for the low exposure rates inherent in these tests. The results of these preliminary dynamic valve contaminant sensitivity tests are sufficiently encouraging to warrant a recommendation for further testing.

CONTAMINATION LEVEL CONTROL (FILTER PERFORMANCE)

The service life of the components in a hydraulic system has been shown to be directly related to both the sensitivity exhibited by the component and the contamination level maintained in the circulating fluid. Since the system filter is required to achieve and maintain a contamination level in the system which is compatible with the contaminant sensitivity of the critical system components, knowledge of the factors which influence its performance are crucial to a service life analysis. Based upon the results of a great many multi-pass filter tests and the theoretical relationships which describes the filtration process [3,4], it can be shown that the ingression rate which is imposed on the system and the flow duty cycle to which the filter is subjected will both influence the resulting contamination level of the system. Furthermore, as a result of the work accomplished during this phase of the OSU-MERDC program, it will be shown that the particle size distribution of the ingressed contaminant can have an effect upon the service life of a filter itself.

In order to present the results of the activities of this phase in an orderly manner, three subdivisions will be utilized--ingression rate effects, surge flow effects and particle size distribution influence.

Ingression Rate Effects

In order to clearly establish the intent of this investigation, some discussion of the term "ingression rate" is appropriate. It makes very little difference to the filter where the contaminant to which it is subjected originates. Although, it is common practice to subdivide the contaminants in a system as to their source (ingressed, generated, or built-in), when viewed at the filter inlet, such discrimination can unnecessarily cloud the issue here. Thus, ingression rate is used in this report to imply all contaminants introduced into the system fluid regardless of their origin.

Theoretical Development

The influence of ingression rate is predicted by the mathematical relationship which describes the contamination level of a hydraulic system [2,3]. This expression for the contamination level downstream of the filter [6] can be written as follows:

$$\frac{d}{dt}(Nd) + \frac{B\mu - 1}{B\mu} \frac{Q}{V} Nd = \frac{R}{B\mu V} \qquad (2)$$

Where:

Nd = Cumulative particle concentration of size greater than μ per unit volume of fluid downstream of the filter.

$B\mu$ = Filtration Ratio

Q = Flow through filter

V = total volume of fluid in system

R = ingression

This equation represents the governing relation for the entire filtration process. This expression does not restrict the magnitude nor the mathematical form of any parameter. It should be noted that Eq. (2) clearly shows that the particle concentration is a function of the ingression rate and flow rate as well as the separation capability of the filter.

By placing the invariant constraints on the parameters of Eq. (2), an analytical solution can be obtained [6]. However, from the great many multi-pass filter test which have been conducted, it has been observed that the time required for the filtration process to reach a steady state is relatively short (minutes). Therefore, the performance of a filter is much more realistically represented by the steady state or stabilized conditions which it will maintain in a system.

The steady state relationship for the downstream contamination level is described by the following expression:

$$\overline{Nd} = \frac{\frac{R}{Q}}{(B\mu - 1)} \qquad (3)$$

It can be noted from Eq. (3) that the magnitude of the steady state downstream contaminant level, Nd, is still influenced by ingression rate, flow rate, and the performance of the filter. Eq. (3) can be graphically illustrated as shown in Fig. 4-10 by the solid lines. In this figure, the filtration ratio has been plotted against the downstream particle concentration exhibited at this size which insures greater accuracy.

The ingression rates shown in Fig. 4-10 are expressed in both number particles per millilitre greater than 10 micrometres and milligrams per litre for convenience only. Since ingression rate, R, is normally expressed in either milligram per minute or number of particles greater than some given size per minute and flow rate can be given in litres per minutes, this is a straightforward conversion of units. In addition, as shown in Fig. 4-10, such units eliminate flow rate and produce more general results.

Test Results

The results of 15 multi-pass type filter tests are included in the verification of the ingression rate influence. Some of these tests were not conducted per the standard multi-pass test procedure [7], in that the injection rate was either higher or lower than the specified 10 mg/ℓ. This deviation from the standard test was deliberate in order to simulate the effects of ingression rates other than 10 mg/ℓ. The contaminant injection rates actually utilized were 1, 5, 10, and 30 mg/ℓ.

A summary of the results from the 15 filter tests is given in Table 4-4. In addition, these results are also plotted on Fig. 4-10 to aid in a visual comparison of the theoretical prediction and the experimental data. As can be noted from Table 4-4, three elements were tests at an ingression rate represented by a R/Q valve of 4320 particles greater than 10μM per millilitre (equivalent to 30 mg/ℓ). Five elements were tested at 1440 (10 mg/ℓ), six elements at 720 (5 mg/ℓ), and only one test was conducted at 144 (1 mg/ℓ). Testing at 1 mg/ℓ was extremely difficult because of the excessive time necessary to load the elements in light of the limitations in size of the test system. All filter elements were taken to a terminal pressure drop of 40 psid at a constant flow rate of 20 gpm. The experimental particle counts which were obtained from these verification tests are shown in Fig. 4-10 as circles for the 30 mg/ℓ tests, squares for 10 mg/ℓ, triangles for 5 mg/ℓ and a diamond for 1 mg/ℓ test.

It is interesting to note that the filters identified as 1, 2, and 3 are the same element from one manufacturer run at different ingression levels. Filters 4 and 5 were represented to be the same by a second filter manufacturer and filters 6 and 7 are supposed to be identical from a third manufacturer. These elements are noted on Fig. 4-10 by their ID number beside the respective data point. The remaining eight elements are all different filters. These "identical" filters are mentioned to illustrate that a change in the ingression rate is not reflected by a change in the filtration ratio. The small differences in β ratio which can be observed in Table 4-4 are due predominantly to element variations and should not be interpreted to reflect ingression effects.

Conclusions and Recommendations

The close correlation between the theoretical and the experimental results demonstrates the capability of the filtration equation to predict the steady state system contamination level from knowledge of the performance of the filter and the ingression rate imposed on the system. It can be seen in Fig. 4-10 that in order to maintain a constant downstream contamination level in the face of increased ingression, a significantly better filter (higher beta ratio) is required. Expressed in another way, the steady state contamination level of a system has been shown to be dependent upon the ingression rate for a given filter application.

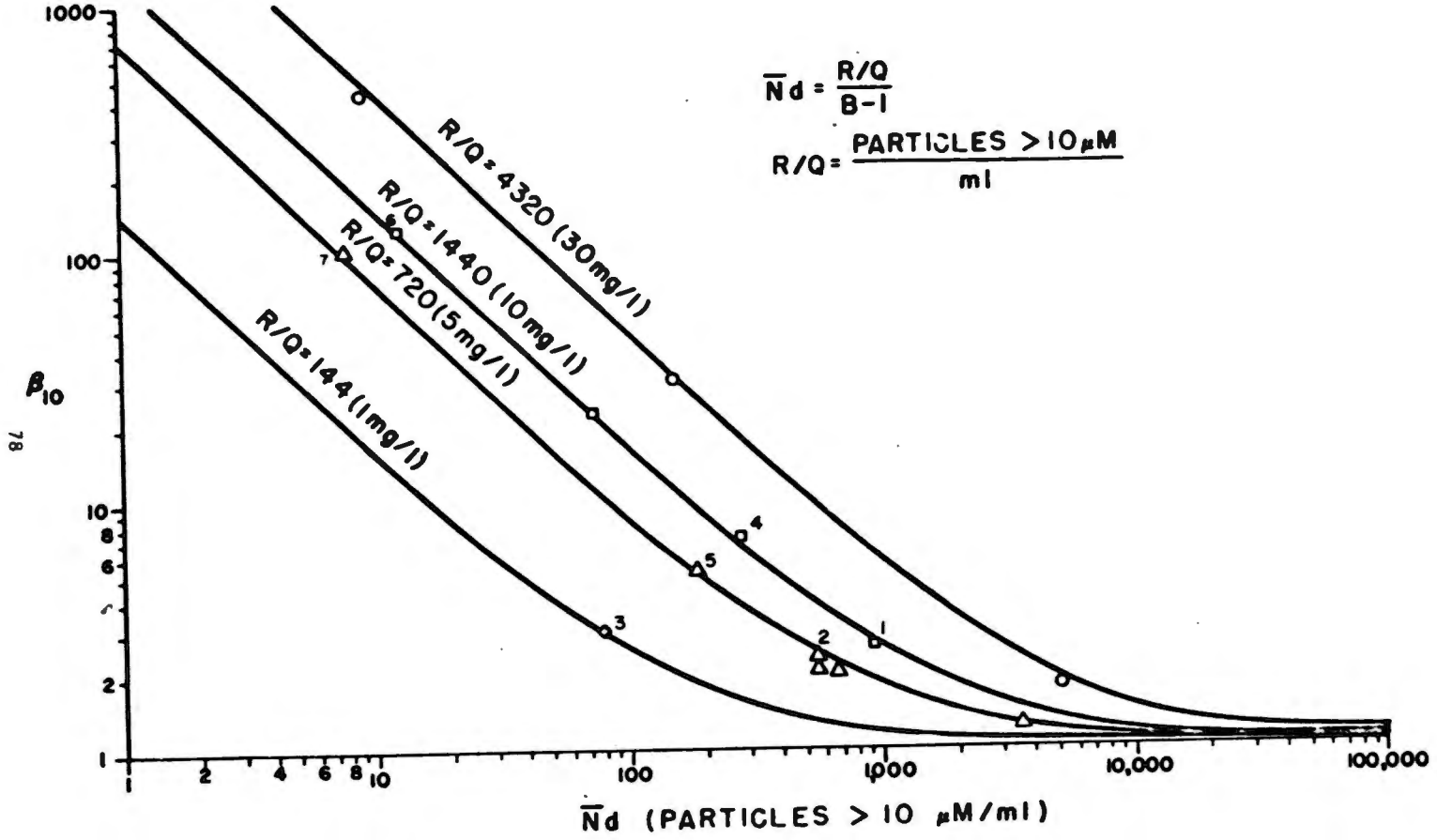

Fig. 4-10. Graphical Representation of steady state filter performance showing theoretical curves and experimental data.

Table 4-4

Summary of Ingression Test Results

		Downstream Particle Count > 10μM/ml			
Filter ID	β_{10}	R/Q = 4320	R/Q = 1440	R/Q = 720	R/Q = 144
1	2.5		928.6		
2	2.1			581.7	
3	2.9				79.2
4	7.0		280.4		
5	5.2			181.5	
6	119.8		12.75		
7	98.0			7.83	
8	2.23			550.0	
9	1.17			3520.0	
10	48.74		31.6		
11	1.72	5069.8			
12	29.71	152.1			
13	1.98			694.8	
14	423.61	8.9			
15	22.85		73.67		

Since it has been adequately demonstrated that the filtration equation successfully accounts for changes in contaminant ingression rates, no more testing is necessary. Once the effects of flow surges are evaluated the relationship can be realistically applied in a service life analysis to predict the contamination level imposed on the system components.

Surge Flow Effects

In an actual hydraulic system, the flow rate through the system is not constant, but it can vary from as low as zero to a rate considerably above manufacturer's recommendations. Based on observations made during both pump contaminant sensitivity testing and multi-pass filter testing, it was concluded that variation in flow through a filter can have a significant effect upon the separation performance exhibited. Before performing a service life analysis of a hydraulic system, information must not only be available concerning the flow duty cycle imposed on the filter but the influence of such flow variation must be determined.

The initial investigation concerning the influence of flow cycling upon filter performance was reported in Ref. [4]. The test method used to simulate flow changes employed the basic multi-pass filter test procedure [7] with a means of sinusoidally varying the flow rate. For these tests the flow was cycled between zero and rated flow of the filter. Also, to simulate different flow duty cycles the frequency of the flow wave was varied between 0 and 1.0 cycles per second. A summary of the results obtained from these tests is shown in Table 4-5. From these results it was clearly shown that the frequency of flow variation had a significant effect on both the separation performance and contaminant capacity of system filters.

However, the flow variations exhibited by hydraulic systems are usually neither sinusoidal nor of constant amplitude. Therefore, additional investigations were conducted to determine the effect of surge flow. A complete mathematical treatement of the effects of flow surges is included in Ref. [8].

Test Procedure

The test fixture used for this work was similar to the standard multi-pass facility with the addition of several parallel by-pass loops around the test element. Likewise, the actual tests were conducted in a manner identical to the standard multi-pass method [7] with the exception of periods of flow surges. Since a ball valve was located in each of the by-pass loops, by quickly opening and closing different arrangements of these valves various magnitudes of flow surges could be imposed upon the test filter.

TABLE 4-5: CYCLE FLOW TEST SUMMARY

Filter	Cycle Rate (CPS)	β_{10} Lowest	Final Gravimetric (mg/ℓ)	Apparent Contaminant Sensitivity (Grams)
A1	0.0	78.00	17.0	13.4
A2	0.1	10.40	51.0	14.9
A3	0.5	6.80	67.2	13.7
A4	1.0	4.80	81.2	15.0
B1	0.0	3.53	45.0	24.1
B2	0.1	2.56	57.8	21.2
B3	0.5	1.91	86.4	25.5
B4	1.0	1.22	150.3	36.8
C1	0.0	2.00	77.4	26.8
C2	0.5	1.30	173.4	37.8
C3	1.0	1.24	183.0	40.1
D1	0.0	47.00	14.2	61.4
D2	0.5	29.20	36.4	90.5
D3	1.0	6.90	46.8	72.7
E1	0.0	2.15	53.4	20.6
E2	0.1	1.49	78.8	22.3
E3	0.5	1.36	134.4	23.0
E4	1.0	1.44	187.6	22.1

The actual test procedure involved continuously injecting AC Fine Test Dust at 10 mg/ℓ at a constant flow rate of 10 GPM. After five minutes, upstream and downstream fluid samples were extracted. Then, the flow samples were extracted. After two minutes at 12.5 GPM the flow was reduced to 10 GPM, held constant for 2 minutes, sampled and sharply increased to about 20 GPM. At 20 GPM, samples were again extracted, the flow was held for 2 minutes, and then reduced to 10 GPM where sampling was repeated. The same procedure was performed an additional time, but the flow was increased to about 30 GPM. After returning to 10 GPM from this third surge, the system was allowed to operate until a pressure increase equal to 5 percent of the net differential pressure was attained. At this point the three flow surge-samplings were repeated. Fig. 4-11 shows typical curves for the flow rate and differential pressure measured during the tests.

Test Results

Filter elements representing four different manufacturers were evaluated according to this test procedure. Each element had a manufacturer's recommended flow rate of 20 GPM and each element was expected to have a different minimum filtration ratio at 10 micrometres. It was assumed that each element type would yield different characteristics when subjected to the flow surges and thus provide a good discriminatory evaluation of the influence of surge flow.

Table 4-6 presents a summary of the results of each flow surge test. It can be noted that, for each filter, the surge magnitude was not exactly equal to 1.25, 2.0, and 3.0 as was planned in the test procedure. These deviations were due to the unique differential pressure characteristics exhibited by each filter. The results obtained for Filter E should be discounted because this filter appeared as if it had collapsed.

Conclusions and Recommendations

Based upon the results of these two sets of tests (sinusoidal flow cycle and flow surge) it must be concluded that both the magnitude and frequency of the variations exhibited by the flow duty cycle imposed on a filter will significantly influence its performance capability. In addition, there is sufficient evidence, as a result of these tests, to conclude that the apparent contaminant capacity can increase from as little as 12% to as much as 74%. Because of the results of these two studies, it is recommended that two things be considered: 1)investigate field flow duty and 2) a standard test or series of tests be formulated which are capable of producing sufficient information to determine the influence of both magnitude and frequency of flow surges.

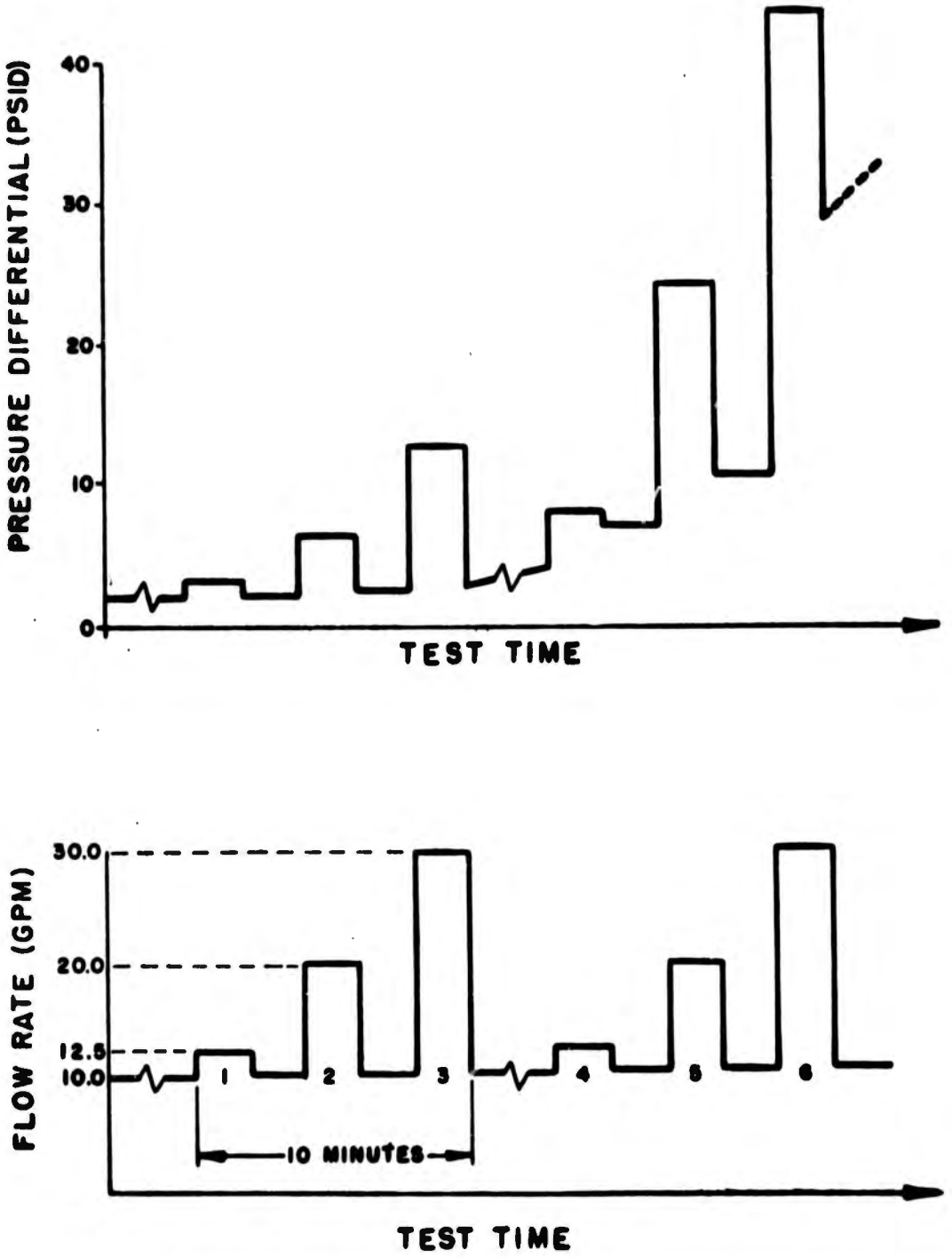

Fig. 4-11: Typical Curves for Flow and Pressure Differential During Surge Test.

TABLE 4-6: Summary of Results of Flow Surge Tests

	Filter	A	B	C	D	E[3]
SURGE #1	Surge Magnitude[1]	1.23	1.25	1.28	1.23	1.26
	β_{10} Before	4.80	95.80	60.60	29.90	54.80
	β_{10} After	7.30	74.60	68.50	21.10	50.80
	β_{10} Reduction[2]	1.52	0.78	1.13	0.71	0.93
SURGE #2	Surge Magnitude	1.80	1.98	2.04	1.81	1.90
	β_{10} Before	6.60	96.30	93.50	35.10	148.60
	β_{10} After	6.70	43.30	31.60	27.20	74.40
	β_{10} Reduction	1.01	0.45	0.55	0.77	0.50
SURGE #3	Surge Magnitude	2.55	2.84	3.02	2.50	2.95
	β_{10} Before	8.40	67.90	94.50	76.00	125.80
	β_{10} After	4.00	10.10	55.60	9.33	25.40
	β_{10} Reduction	0.48	0.15	0.59	0.12	0.20
SURGE #4	Surge Magnitude	1.23	1.28	1.26	1.24	1.25
	β_{10} Before	7.80	18.60	75.60	28.50	2.04
	β_{10} After	8.60	13.10	49.60	25.30	1.05
	β_{10} Reduction	1.10	0.70	0.66	0.89	0.64
SURGE #5	Surge Magnitude	1.90	2.10	2.67	1.88	2.78
	β_{10} Before	5.20	14.70	121.70	16.20	1.05
	β_{10} After	6.60	8.80	41.40	6.01	1.47
	β_{10} Reduction	1.27	0.60	0.34	0.37	1.40
SURGE #6	Surge Magnitude	2.78	3.1[illegible]	4.70	2.70	4.68
	β_{10} Before	9.10	10.70	261.00	21.50	1.00
	β_{10} After	2.09	3.71	40.40	2.62	0.96
	β_{10} Reduction	0.23	.35	0.15	0.12	0.96

1. Surge magnitude is the ratio of the flow rate after the surge to that before.
2. β_{10} reduction is the ratio of β_{10} after the surge to that before the surge.
3. Element E exhibited characteristics of element failure between the third and fourth surges.

Particle Size Distribution Influence

The contaminant capacity of a filter is usually expressed in terms of the number of grams of a specific contaminant to which the filter can be subjected to reach a predetermined pressure drop. It has been shown previously that the contamination level achieved in a system is a function of the ingression rate. From the definition of filter capacity, it should now be obvious that the change period or service life of the filter is also a function of ingression rate.

During the dynamic flow study, it was shown that flow variation can produce significant changes in the capacity of a filter. However, there is one other factor which seriously influences filter service life. This factor is the particle size distribution of the contaminant which is introduced into the system. In order to evaluate the effect of distribution and provide a more realistic appraisal of filter service life, a concept was developed and the results of 24 filter capacity tests were utilized to validate this theory.

Theoretical Considerations

If it is assumed that only those particles of a size which will block the capillary passages of a filter significantly affect the pressure drop versus contaminant added characteristics, these sizes of particles become of particular importance. In order to determine the critical particle sizes, the penetration factor developed in Ref. [6] can be used. These factors are based on the results of over 70 multi-pass filter tests on a broad spectrum of filters. The penetration curves are shown in Fig. 4-12.

In general, the curves depicted in Fig. 4-12, represent the percent contaminant which penetrates a filter exhibiting the designated filtration ratio. However, the increase in pressure drop across the filter is due to contaminant retained insteady of that which penetrates. The retention factor can be calculated from the penetration factor by the following equation:

$$R = 1 - P \qquad (4)$$

Where: R = retention factor
P = penetration factor

In addition, to place all filters on a common basis with respect to capacity, a normalization technique will be employed. Since the capacity tests conducted as part of this effort utilized AC Fine Test Dust (ACFTD), the desired normalization can be accomplished by the following equation.

$$\text{Normalized capacity} = \frac{C_0 - D}{C_0 - 80} \qquad (5)$$

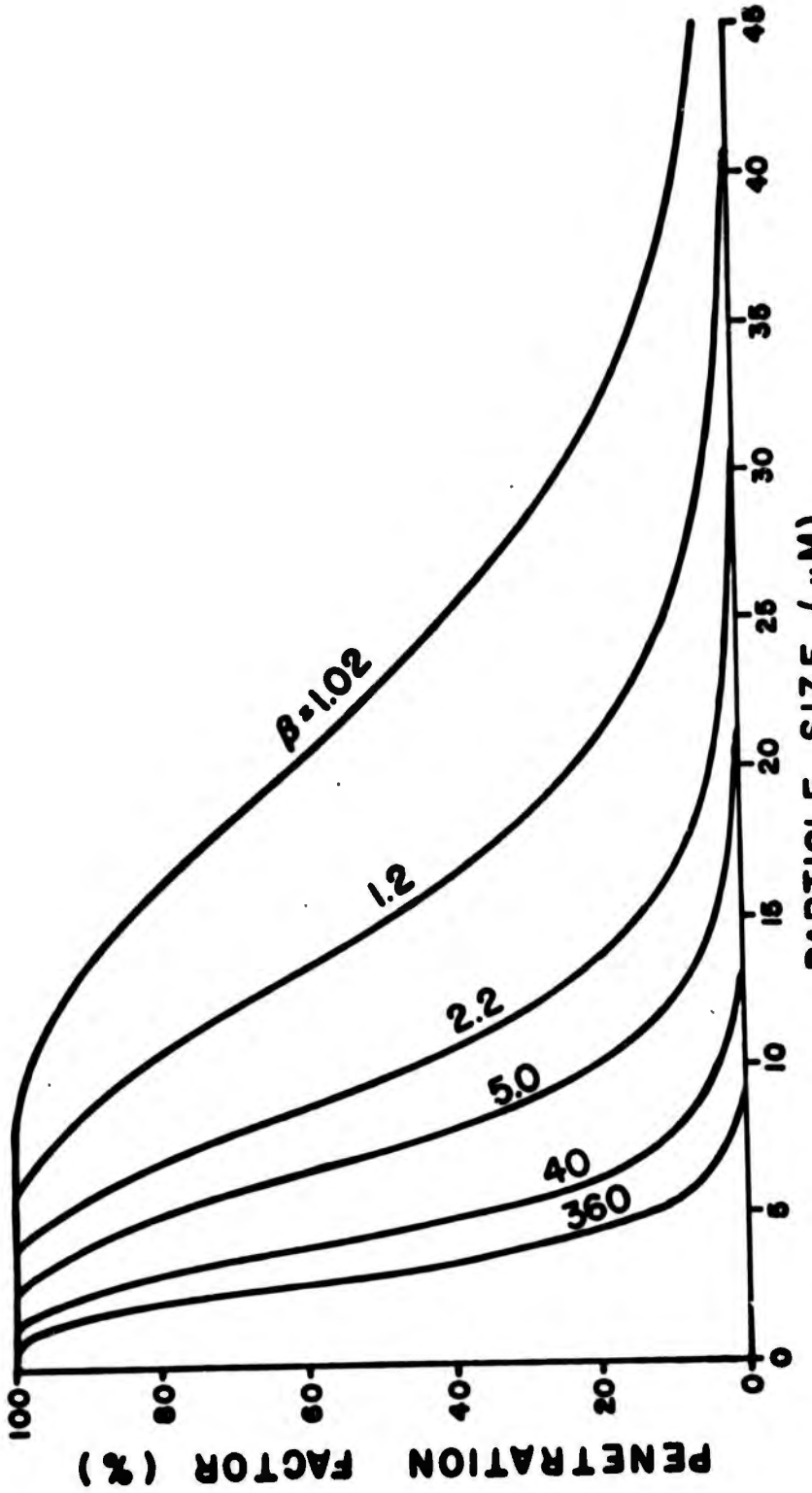

Fig. 4-12. Particle Penetration Graph for a Broad Range of β_{10} Filter Elements.

Where: C_{0-D} = Capacity in grams of contaminant exhibiting a distribution from 0 to D micrometres

C_{0-80} = Capacity in grams wil full ACFTD Distribution

Fig. 4-13 illustrates the theoretical relationship between normalized capacity and particle size distribution derived from the assumption that only those particle sizes for which the filter exhibits a retention factor between 1 and zero contribute to the loading of a filter. To develop these curves, the weight ratio for ACFTD was employed in the following expression.

$$\frac{C_{0-D}}{C_{0-80}} = \frac{W_{0-D}/W_{0-80}}{R_{0-D}} \qquad (6)$$

Where: W_{0-D}/W_{0-80} = Weight Ratio of 0 - D micrometre contaminant in ACFTD

R_{0-D} = Retention Factor for 0 - D Contaminant

Tests were conducted to verify the theoretical curves given in Fig. 4-13. In order to obtain the necessary information, element from five filter manufacturers were used. Also, since a capacity test destroys the usefulness of a filter element for additional testing each capacity value obtained required the use of a separate filter element. Seven elements each of filters numbered 3 and 5 were tested, six elements of filter number 4 were used, while two each were run of filters 1 & 2 for a total of 24 elements.

Test Results

Table 4-7 summarizes the results of the filter capacity tests conducted. The filters used exhibited filtration ratios at 10 micrometres of approximately 1.1, 1.2, 2.5, 7, and 100 as shown in Table 4-7. The multi-pass test filter test circuit [7] was utilized to run these tests. All filters were run at a flow rate of 20 GPM with the multi-pass test requirements adhered to except for the distribution of the contaminant and the sampling specification. Classified AC Fine Test Dust was used to obtain the 0 - D micrometre contaminant distributions.

In order to gain an appreciation for the comparison between theoretical capacity and the capacity obtained experimentally, a plot of one of these filters have been plotted. Fig. 4-14 shows this comparison.

Conclusions and Recommendations

It is felt that the results of the experimental effort agree closely with the predicted (theoretical) results. Thus, it can be concluded that the service life of a filter is influenced by the particle size distribution

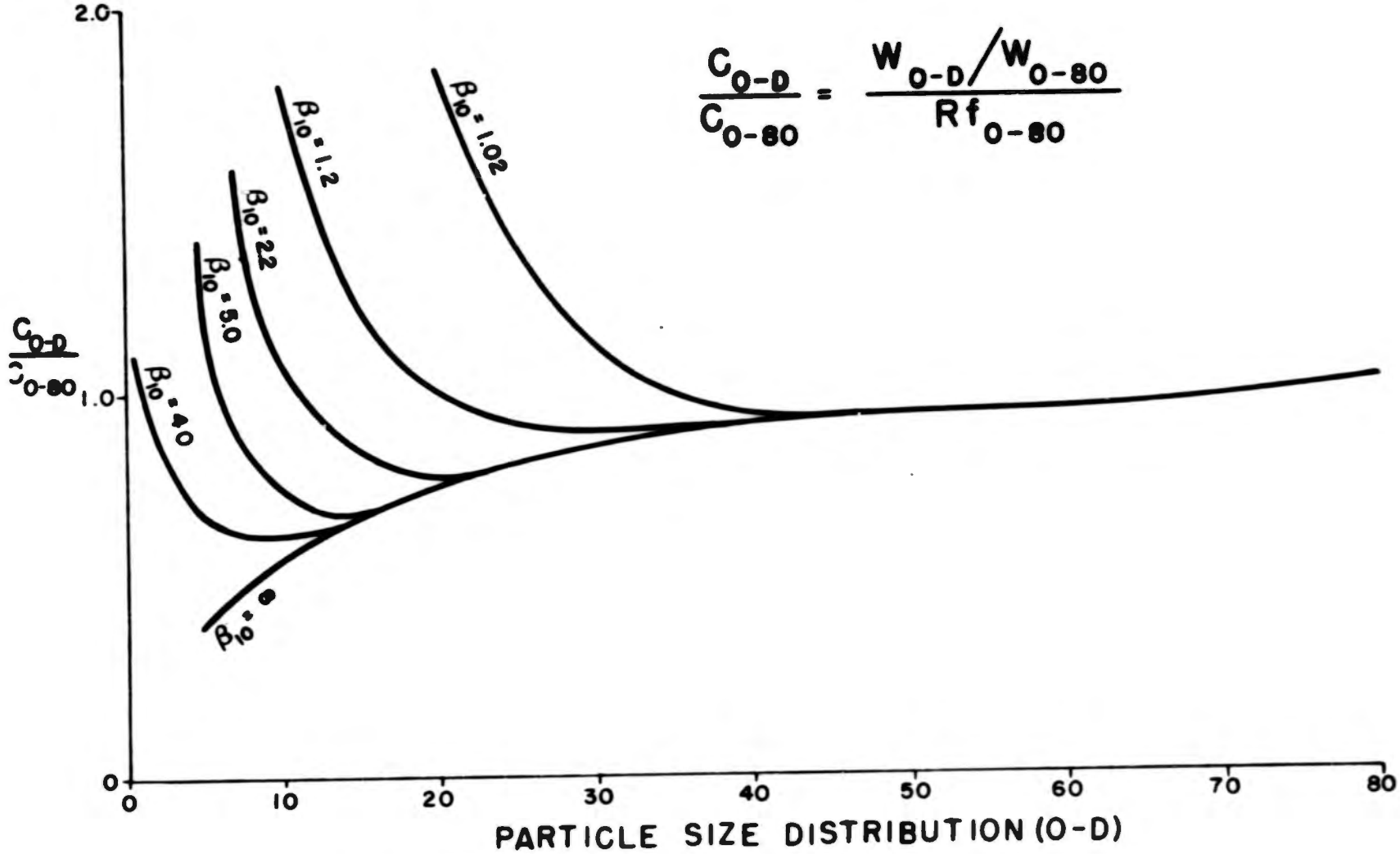

Fig. 4-13. Normalized Capacity Versus Particle Size Distribution.

Table 4-7: **Summary of Filter Capacity Test Results**

Cont. Dist.	Filter #1 β_{10} = 1.1		Filter #2 β_{10} = 1.2		Filter #3 β_{10} = 2.5		Filter #4 β_{10} = 7		Filter #5 β_{10} = 100	
	Act. Cap.	Norm. Cap.	Act. Cap.	Norm. Cap.	Act. Cap.	Norm. Cap.	Act. Cap.	Norm. Cap.	Act. Cap.	Norm. Cap.
0-80	23.3	1.0	48.2	1.0	20.3	1.0	42.5	1.0	36.5	1.0
0-70					20.7	1.02	40.9	0.96	32.4	0.89
0-60					---	---	---	---	---	---
0-50					17.75	0.87	37.3	0.88	30.1	0.83
0-40					19.10	0.94	---	---	30.2	0.83
0-30					13.70	0.67	34.9	0.82	27.8	0.76
0-20					12.80	0.63	27.2	0.64	23.6	0.65
0-10					13.97	0.69	26.0	0.61	23.2	0.64
0-5	104.8	4.5	170.5	3.5	---	---	---	---	---	---

Act. Cap. -- **Actual Capacity**

Norm. Cap. -- **Normalized Capacity**

Cont. Dist. -- **Contaminant Distribution**

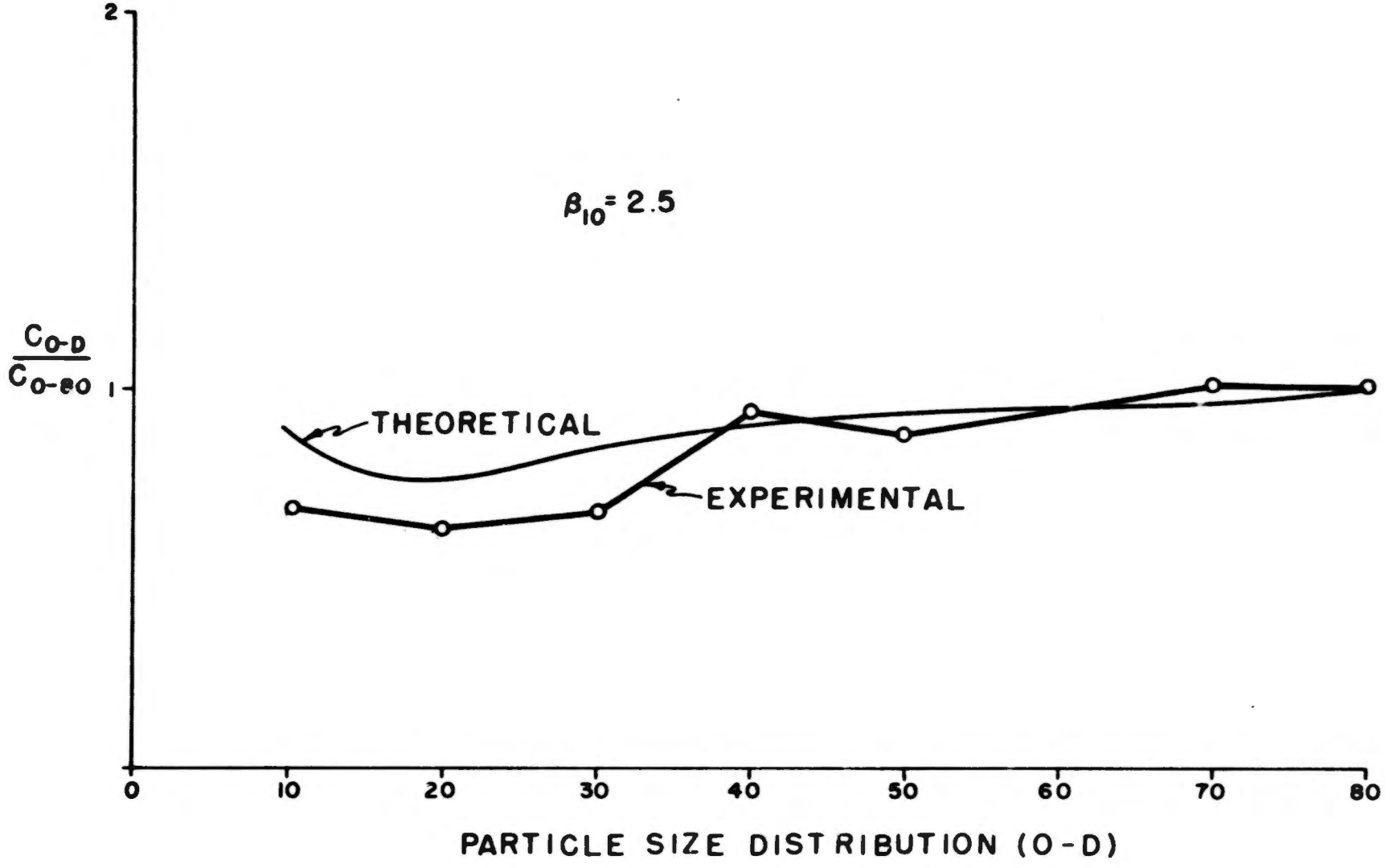

Fig. 4-14. Comparison of Results for Filter No. 3.

of the ingressed contaminant as predicted by Eq. [6].

Because of the close agreement attained between the predicted and experimental results no additional tests are necessary. Therefore, it is recommended the effect of particle size distribution be included whenever possible to evaluate filter service life.

- DISCUSSION -

In the design or procurement of a hydraulic system, service life should be one of the most important criteria. Of course, it is necessary to insure that the system will perform the desired job mission initially and that it does not operate at a temperature which will "cook" seals and/or destroy the system fluid. However, a machine or vehicle which uses a hydraulic system that must be frequently repaired is of dubious value.

It has been shown in this report and numerous previous tests that the service life of a hydraulic system is a function of the contaminant sensitivity of the components (such as pumps and valves), the performance capability of the filter and the severity of the operating conditions. Steady state test procedures to evaluate the contaminant sensitivity of critical hydraulic components which have been developed are valuable from a component control standpoint, but they may be too conservative for a truly rigorous service life analysis. That is, tests which were conducted during this major phase of the contract study to evaluate the influence of the various duty cycles imposed by the system have shown an improvement in the contaminant sensitivity characteristics of the components. Therefore, in general, the variable operating conditions exhibited by a field hydraulic system are apparently less severe, from a component service life point of view, than steady state operation at maximum conditions. Thus, it should be encouraging to those using the results of steady-state tests for procurement proposes to know that their forecast of field service life of components is indeed conservative.

The development work accomplished during the service life phase of the CAP section has shown that variation in flow can have a deleterious effect upon filter performance. Experimental tests indicate that both the filtration ratio and the contaminant capacity by a filter are dependent upon the frequency and magnitude of such a flow duty cycle while the capacity is also influenced, to a less extent, by the particle size distribution of the contaminant introduced in the system. This should not be construed to imply that the results of steady-state filter performance tests cannot be utilized for selection purposes, since a filter which signed or could be designed such that the filter is subjected to very minor flow variations. When this is possible the steady-state filter performance information can be confidently used for protection level prediction. It is recommended however, based upon the test result from this study, that a dynamic flow filter test procedure should be formalized. The data from such a test could be utilized to predict the contamination level of a system in which serious flow surges through the filter cannot be avoided. The first draft of a proposed procedure is

presented in conceptual form in Appendix F for initiating an industrial review of a dynamic flow filter test.

The development of a realistic service life appraisal technique is considered a major objective of the computer-aided procurement program. It is felt that the accomplishments realized during this phase of the OSU-MERDC hydraulics program have made significant contributions toward this goal. Prior to this time, service life analysis was a viable comparison method but was not used confident as a realistic prediction technique. However, with the knowledge and understanding gainad as a result of this work, a rigorous system service life prediction program can be formulated. This is not to say that a field verification effort is not essential in establishing a workable system reliability activity for the U.S. Army. Such a field effort would by necessity collect duty cycle, operational severity factor, and residual life data. This type of information is crucial to the general implementation and overall success of the entire computer-aid procurement program.

- REFERENCES -

1. Hydraulic Specification Program, Phase I, Final Report, Prepared by Fluid Power Research Center, Oklahoma State University, Stillwater, Oklahoma, Contract No. DAAK02-70-C-0093, U.S. Army MERDC, 1970.

2. Hydraulic Specification Program, Phase II, Annual Report, Prepared by the Fluid Power Research Center, Oklahoma State University, Stillwater, Oklahoma, Contract No. DAAK02-71-C-0074, AD-737730, U.S. Army MERDC, 1971.

3. Hydraulic System Controls Study, Section II, Annual Report, Prepared by Fluid Power Research Center, Oklahoma State University, Stillwater, Oklahoma, Contract No. DAAK02-72-C-0172, U.S. Army MERDC, 1972.

4. Basic Fluid Power Reseach Program Annual Report No. 6, Section 72-CC Oklahoma State University, Stillwater, Oklahoma September, 1972.

5. Basic Fluid Power Research Program Annual Report No. 7, Section 73-CC Fluid Power Research Center, Oklahoma State University, Stillwater, Oklahoma, October 1973.

6. Fitch, E.C. and R.K. Tessmann, "Practical and Fundamental Descriptions for Fluid Power Filters," Society of Automotive Engineers, Milwaukee, Wisconsin, September 10-13, 1973.

7. National Fluid Power Association Recommended Standard Multi-pass Method for Evaluating the Filtration Performance of a Fine Hydraulic Fluid Power Filter Element, NFPA/STD T3,10.8.8-1973.

8. Bensch, L.E., "Surge Flow Effects on Filter Performance," Paper No. P73-CC-5, Seventh Annual Fluid Power Research Conference, Oklahoma State University, Stillwater, Oklahoma, October 9-10, 1973.

APPENDIX A

EXAMPLE OF A DNR AND ITS USE FOR SIMULATION

APPENDIX A

EXAMPLE OF A DNR AND ITS USE FOR SIMULATION

In dealing with numerical models, it is too easy to get overwhelmed by the extent of manipulations and the sheer magnitude of the numbers involved. This is particularly so in the case of multi-input, multi-output, non-linear systems. To illustrate the DNR concept, it is necessary to reduce the manipulations and the numerical data to the bare bones, and this is best done on a single-input, single-output, linear, first-order system.

We will derive a classical analytical model and use that to develop a DNR. Consider a simple system comprised of a tank and a capillary resistance as shown in Fig. A-1. Flow Q_1 is directed into the tank, and flow Q_2 leaves the tank. We are interested in determining the pressure in the tank at any point in time after imposing a change in the input flow Q_1. Applying the principle of continuity to the system gives the following equation:

$$Q_1 = Q_2 + Q_{stored} \tag{1}$$

Since a capillary resistance has been specified, the flow Q_2 can be written as follows:

$$Q_2 = K(P_1 - P_2) \tag{2}$$

where K is the resistance of the capillary. The flow stored in the tank, Q_{stored}, is given by the following equation:

$$Q_{stored} = \frac{V}{\beta} \frac{dP_1}{dt} \tag{3}$$

Where: V = volume of the tank
β = bulk modulus of the fluid in the tank

Substituting for Q_2 and Q_{stored} in Eq. (1) gives the following linear, first-order differential equation:

$$Q_1 = KP_1 + \frac{V}{\beta} \frac{dP_1}{dt} \tag{4}$$

In the above equation, the flow Q_1 is the input, and the pressure P_1 is the output.

The equation can be solved analytically if Q_1 is a known function of time. Whatever the nature of the input Q_1, the value of P_1 at any time

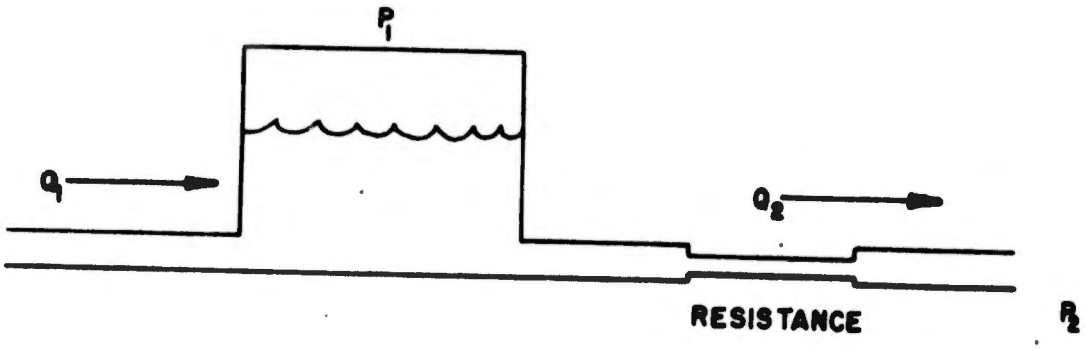

Fig.A-1. Simple First-Order System.

"t" can be explicitly obtained only if the initial conditions for the equation are given. In fact, the same input Q_1 can result in different values of P, at a particular instant, depending on the initial condition. This is shown in Fig. A-2. Thus, merely specifying that the input at any instant, is say Q(t), is insufficient to ascertain the corresponding value of the tank pressure, say $P_1(t)$. However, if the tank pressure at a time just prior to t, say $t - \Delta t$), is given, it effectively establishes the initial condition for the short time period Δt. The combination of $Q(t)$ and $P(t - \Delta t)$ is now sufficient to establish the value of $P(t)$.

Development of DNR

We will assume that a test was conducted on the above linear system and one test run gave inputs (Q_1) and outputs (P), over a period of time, as given in Table A-1. The sampling period os 0.05 but does not have to be constant in order to develop a DNR.

The input Q_1 is augmented with the previous value of the output (i.e. one step earlier in time), and this is shown in Column Z in the table. (Q_1, Z) is known as the augmented input, and Q_1, Z, P_1) forms an augmented input, there can exist one and only one output. The aggregates of all (Q_1, Z, P_1) vectors constitute the DNR of the system. Fig. A-3 graphically depicts the result of augmentation.

Use of DNR for Simulation

The use of the DNR is simplicity itself. Ascertain the augmented-input vector at any point in time, look up the closest augmented input in the DNR, and read off the corresponding output. This gives the output for just one point in time. Generally, however, it is desirable to obtain a complete trajectory of the output, given a time-history of the input and the initial condition. To do this, augment the input at time zero, with the initial condition, and read off the output from the DNR. Use this output as the augmentation for the input at the end of the first time-step. For simplicity, this time-step must be the same as that used in obtaining the DNR from the test data. Continuing in this fashion, the whole output trajectory can be obtained.

To improve accuracy of the simulation, it is advantageous to use an interpolation scheme in ascertaining the augmented-input vector closest to the given value and the corresponding output. Of the many schemes available, the following has been chosen for simplicity and speed.

Using a suitable norm, the points in the augmented-input space in the DNR. within a certain radius of the given augmented input (i.e. a neighborhood) are collected together and a linear equation fitted to the differences in the Q_1, Z, P_1, using one of the points as reference. The

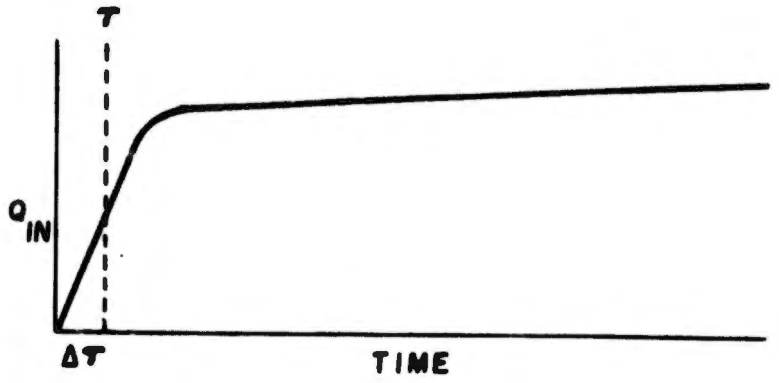

(A)

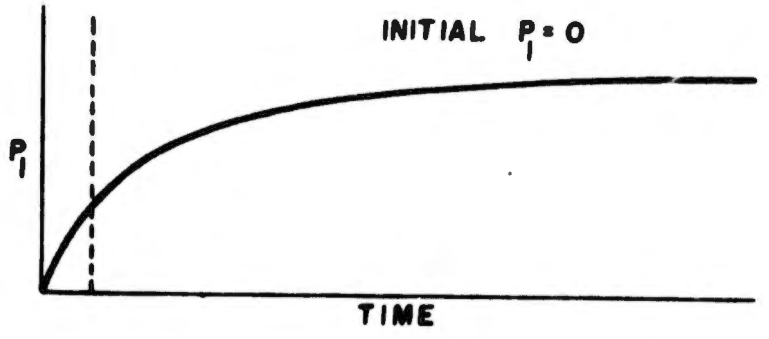

(B)

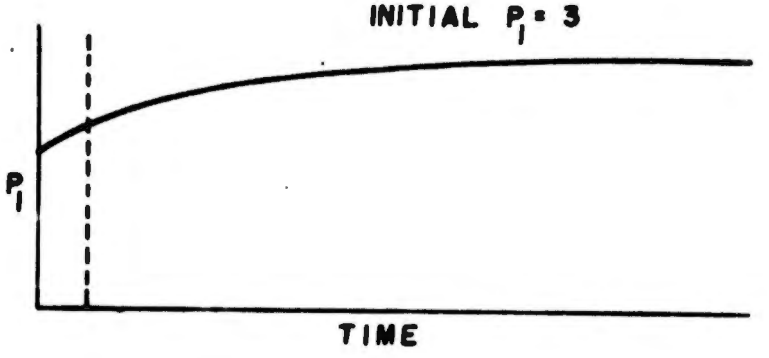

(C)

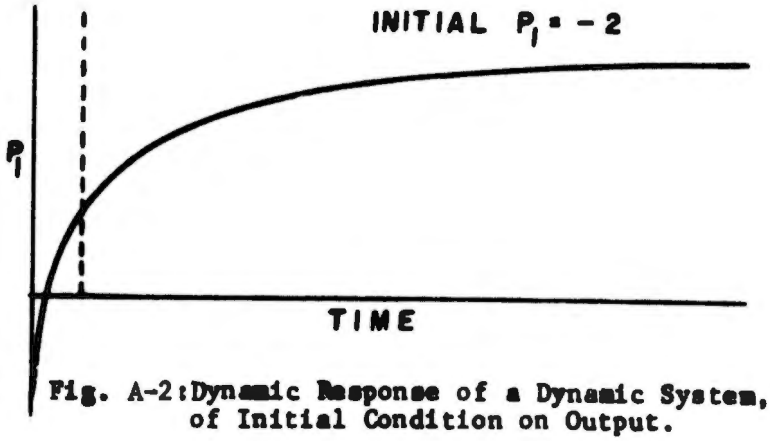

(D)

Fig. A-2: Dynamic Response of a Dynamic System, Showing Effect of Initial Condition on Output.

TABLE A - 1: AUGMENTED INPUT-OUTPUT REPRESENTATION OF SYSTEM

INPUT Q_1	AUGMENTATION Z	OUTPUT P_1
0.0	0.0	0.0
9.9999E-03	0.0	2.4660E-04
2.0000E-02	2.4660E-04	9.6750E-04
3.0000E-02	9.6750E-04	2.1416E-03
4.0000E-02	2.1416E-03	3.7460E-03
5.0000E-02	3.7460E-03	5.7600E-03
6.0000E-02	5.7600E-03	8.1636E-03
7.0000E-02	8.1636E-03	1.0938E-02
8.0000E-02	1.0938E-02	1.4060E-02
9.0000E-02	1.4060E-02	1.7526E-02
1.0000E-01	1.7526E-02	2.1306E-02
1.1000E-01	2.1306E-02	2.5390E-02
1.2000E-01	2.5390E-02	2.9760E-02
1.3000E-01	2.9760E-02	3.4409E-02
1.4000E-01	3.4409E-02	3.9317E-02
1.5000E-01	3.9317E-02	4.4473E-02
1.6000E-01	4.4473E-02	4.9866E-02
1.7000E-01	4.9866E-02	5.5483E-02
1.8000E-01	5.5483E-02	6.1314E-02
1.9000E-01	6.1314E-02	6.7348E-02
2.0000E-01	6.7348E-02	7.3576E-02
2.0000E-01	7.3576E-02	7.9742E-02
2.0000E-01	7.9742E-02	8.5607E-02
2.0000E-01	8.5607E-02	9.1186E-02
2.0000E-01	9.1186E-02	9.6493E-02
2.0000E-01	9.6493E-02	1.0154E-01
2.0000E-01	1.0154E-01	1.0634E-01
2.0000E-01	1.0634E-01	1.1091E-01
2.0000E-01	1.1091E-01	1.1525E-01
2.0000E-01	1.1525E-01	1.1939E-01
2.0000E-01	1.1939E-01	1.2332E-01
2.0000E-01	1.2332E-01	1.2706E-01
2.0000E-01	1.2706E-01	1.3062E-01
2.0000E-01	1.3062E-01	1.3400E-01
2.0000E-01	1.3400E-01	1.3722E-01
2.0000E-01	1.3722E-01	1.4028E-01
2.0000E-01	1.4028E-01	1.4320E-01
2.0000E-01	1.4320E-01	1.4596E-01
2.0000E-01	1.4596E-01	1.4860E-01
2.0000E-01	1.4860E-01	1.5110E-01
2.0000E-01	1.5110E-01	1.5349E-01
2.0000E-01	1.5349E-01	1.5576E-01
2.0000E-01	1.5576E-01	1.5792E-01
2.0000E-01	1.5792E-01	1.5997E-01
2.0000E-01	1.5997E-01	1.6190E-01
2.0000E-01	1.6190E-01	1.6380E-01

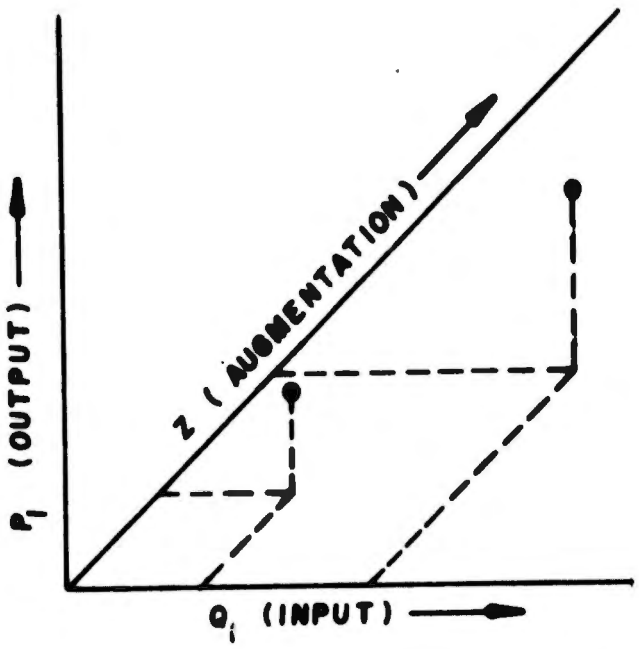

Fig. A-3. Augmentation of Input for a First-Order System.

coefficients, C_1, and C_2 obtained from the least-squares fit for this equation are then used with the augmented input vector to obtain the output, thus:

$$P_1(t) = C_1 \cdot Q_1(t) + C_2 \cdot Z(t) \qquad (4)$$

The value of $P_1(t)$ so obtained is the augmentation $Z(t)$ for the next point i.e. $Z(t + \Delta t)^1 = P_1(t)$.

Fig. A-4 shows the results of a DNR simulation when the input was the same as that given in the original time history. The extremely good fit is reassuring. Figs. A-5, A-6, and A-7 show the output trajectories predicted by the DNR when given various inputs. Fig. A-7 in particular includes an impulse input, and the fact that the simulation responds realistically should be especially noted.

In actual practice, there should be many time histories fed into the DNR. This improves accuracy of the model and reduces computation time too. The calculations of C_1 and C_2 need not be done afresh for each simulation. For a given neighborhood[2] and accuracy of least-squares fit desired, the coefficients can be calculated and stored once for all. Step size changes can also be made by applying the appropriate corrections to these coefficients.

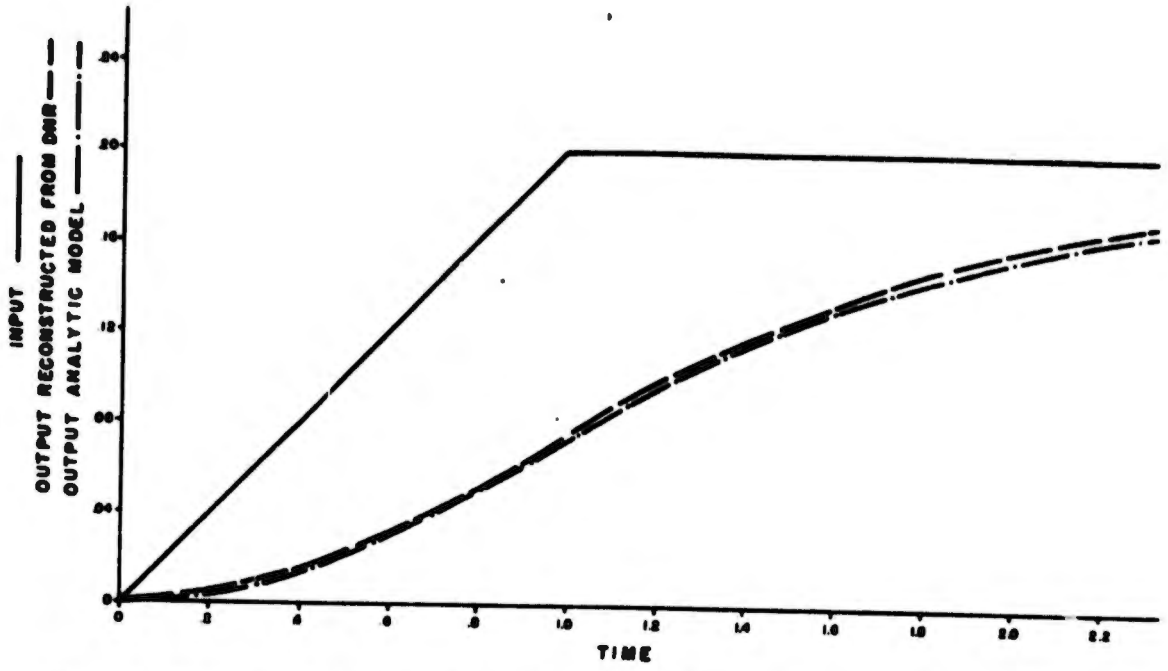

Fig. A-4: Comparison of Analytic Model with DNR Simulation Reconstructed from Analytic Data.

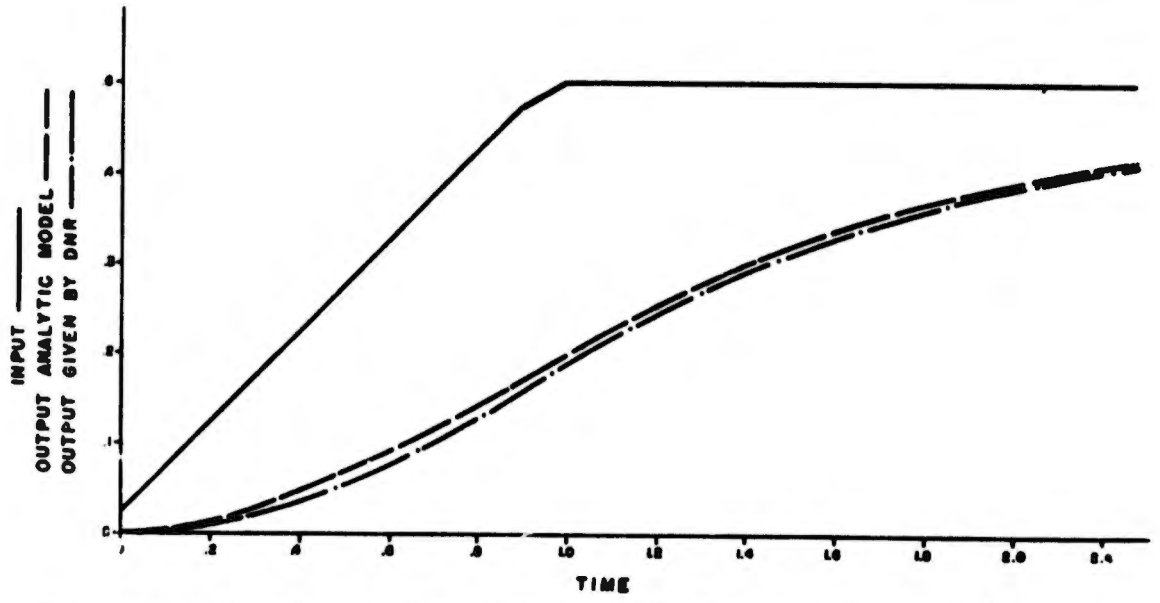

Fig. A-5 : Comparison of Output Given By DNR with Analytic Output. Input #1.

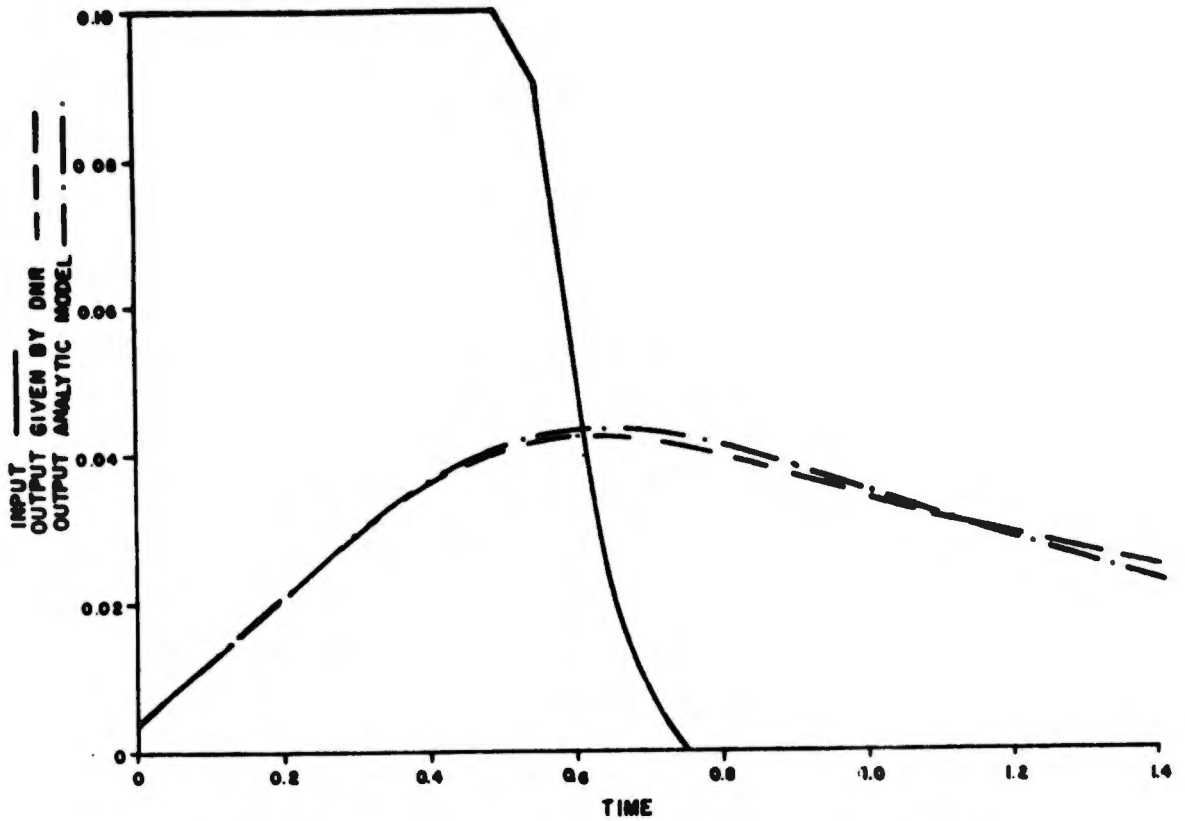

Fig. A-6 : Comparison of Output Given By DNR with Analytic Output. Input #3.

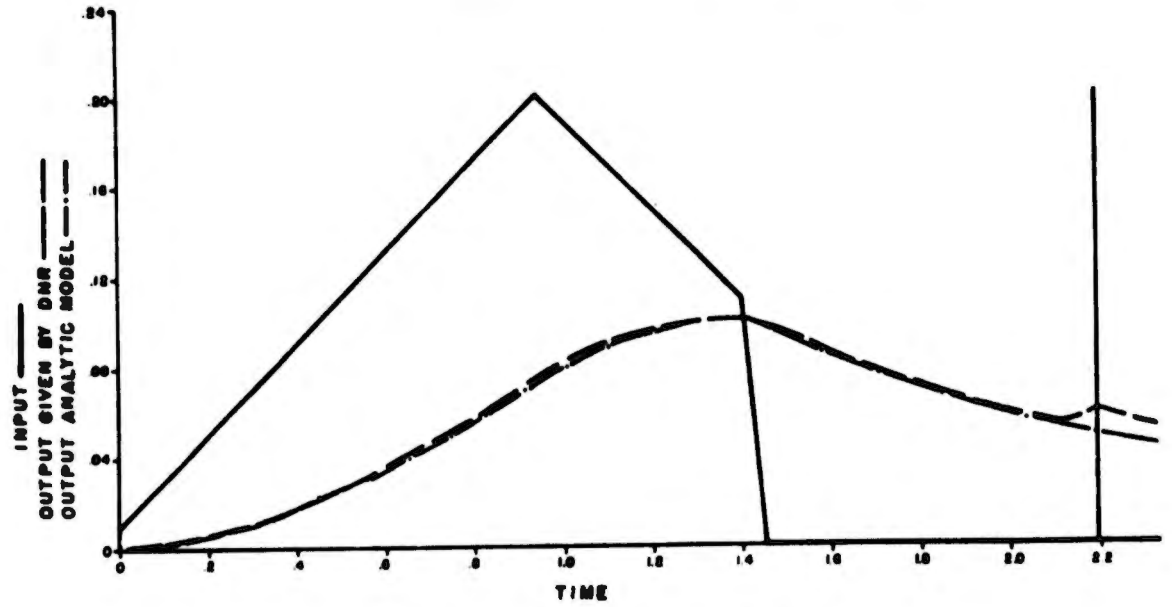

Fig. A-7 Comparison of Output Given By DNR with Analytic Output. Input #2.

APPENDIX B

EXPERIMENTAL TEST FACILITIES USED FOR SYSTEM PERFORMANCE TESTS

APPENDIX B

EXPERIMENTAL TEST FACILITIES USED FOR SYSTEM PERFORMANCE TESTS

The importance of experimental effort in analyzing fluid power systems cannot be overestimated. Test data are invaluable in developing and verifying system and component models. In formulating empirical models--of which DNR is an example -- test data take on added importance, in that there is no simple physical interpretation of the numbers involved, and thus no way of spotting an obviously "wrong" data point. In the case of DNR, the test data, after screening redundant information, is the model of the component or system, and any errors in scaling or transforming the variables, will go through the simulation unchanged and undetected. Poor selection of transducers, recording techniques and test methods can all contribute to degradation of the model, and ultimately, the simulation. Hence, the importance of evaluating the capabilities of the test facilities before using the data for any modeling must not be overlooked. The valve test facility at the Fluid Power Research Center, at Oklahoma State University, was designed to undertake performance and contaminant sensitivity tests on not only valves, but also other fluid power components. As indicated earlier, the development and verification of dynamic models requires special care in the selection of variables to be monitored, transducers to be used, and signal processing techniques to be implemented. To develop completely general models, it is necessary to monitor the variables at all energy ports of a component. For multi-port components like valves, this can pose a severe instrumentation problem. In such cases a judicious selection of variables together with some steady-state measurements of tank port pressures of directional control valves are usually satisfactory for low-order modeling. Similarly, if a constant flow source is available, the inflow to an open center valve need not be monitored, even during a dynamic test. Decisions of this type need to be made before embarking on the tests.

Since the success of the experimental effort depended upon the versatility of the test facilities, a brief description of the set-up is appropriate. The valve test stand is actually composed of two test circuits-performance and contaminant testing. The performance side of the test stand uses a 45 GPM variable displacement pump. A large conical reservoir equipped with level and temperature control supplies fluid to this pump. Two small pumps run by a common motor are utilized to develop pilot pressure for actuating valves, controlling the displacement of the main pump, etc. as well as performing a multiplicity of fluid transfer functions. A secondary conical reservoir is available for fluid storage to supply both the clean (performance) and contaminant test circuits. Both turbine and drag flowmeters are incorporated in the piping so that flow from 0.5 to 70 GPM can be measured by simply opening and closing the

appropriate vales. Pressure taps are also available to fix gauges and transducers. But for minor changes, the fluid power circuitry is the same as reported in an earlier report.[1] However, efforts to validate DNR required constant updating of the instrumentation and also dynamic calibration of certain transducers. A brief description of effort in both areas follows.

- INSTRUMENTATION UPDATING -

In dynamic testing, care must be taken in using automatic recording equipment, to insure that impedances are properly matched. One way of achieving this with minimum effort is to use isolation amplifiers. For all dynamic tests a bank of D.C. amplifiers was used to function as isolation amplifiers. A series-shunt resistance panel was built, to be used in conjunction with the D.C. amplifiers, to perform desired scale changes. Fig. B-1 gives a circuit schematic for the arrangement. Using this setup, it was possible to use a recording oscillograph to continuously monitor, up to five different variables, during a dynamic test. An accurate adjustable D.C. supply was used to adjust the resistances in the series-shunt panel, to obtain the necessary scaling on the recording paper. With calibration and initial adjustments. A considerable amount of time was saved by performing this calibration and adjustment while the stand was warming up.

For the earlier experimental acitivities under the system performance phase, a multi-purpose instrument console, housing the transducer-amplifiers and indicating read-outs, had been used. It was realized that the testing of multi-port components needing the simultaneous measurement of five or more variables, needed a bigger console. To retain portability and flexibility, all signal conditioning equipment was built into two consoles -- one for transducer amplifiers, read-out and recording equipment, and one for diagnostic accessories. While building the console, special care was taken to ensure that there would be no signal interference either between the channels or due to external sources.

Since the directional control valve is the most important control element in many fluid power systems, the measurement of variables associated with it deserve some attention. Thus spool displacement measurement is necessary for almost any type of modeling. For dynamic measurements, this measurement had to be accurate to $\pm$ 0.0005 inches, and also permit continuous recording. DCDT's (Direct Current Differential Transformers) were found to have the follwoing desirable features:

1. Voltage output proportional to the displacement (including change of sign to signify negative displacements)

---

[1] AD 737 730 Hydraulic specification Program U(Phase II) Annual Report, for the U.S. Army Mobility Equipment Research and Development Center, Fluid Power Research Center, Oklahoma State University, Stillwater, Oklahoma, 74074, December 1972

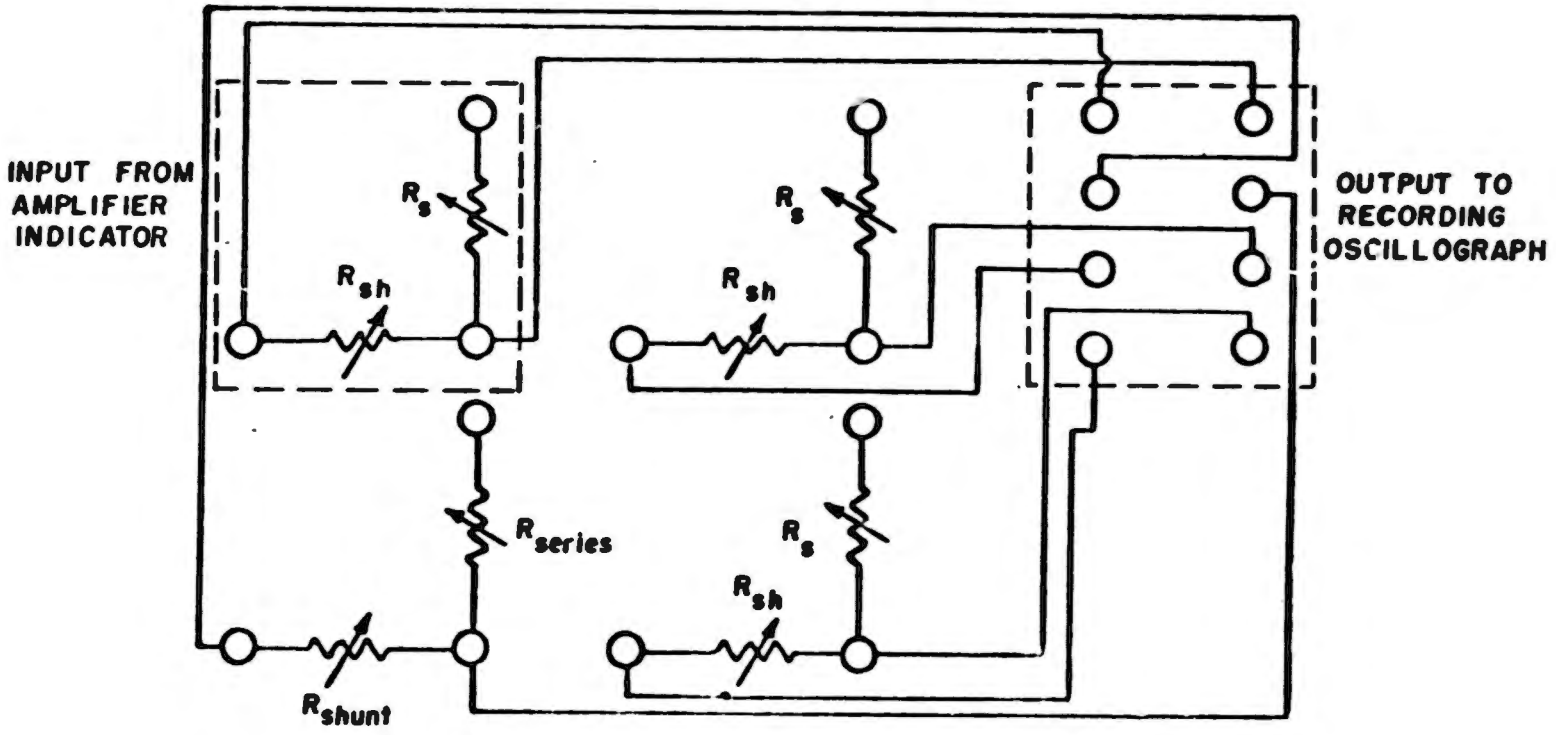

Fig. B-1. Circuit Schematic of Resistance Series-Shunt Arrangement.

2. Practically instantaneous dynamic response.

3. Low noise levels.

Their only disadvantages were that they needed a stabilized D.C. supply and had to be isolated from the recording equipment by a D.C. amplifier. All the pressure and flow vs. displacement curves for the directional control valves tested, used DCDT's for displacement measurement. In using DCDT's it is necessary to ensure that the armature of the DCDT is rigidly attached to the moving part and moves coaxially in the coil. To ensure this, special fixtures, which could be fixed to the valve spool were made. These fixtures had provision for zero adjustment of the DCDT, so that the spool-centered position corresponded to zero output voltage.

Part of the verification program required the acquisition of the data from the Ford backhoe at Hutchinson, Kansas (Cessna Industrial Hydraulics Div.). The measurement of flow required the alteration of the fluid power circuit, so as to permit the installation of a drag flowmeter in the pump delivery line. Pressure taps had to be made at the pump outlet, as well as both sides of actuators. Spool displacement measurement could not be done directly. Consequently, a box was fabricated , to retain the DCDT's, whose armatures were connected by brackets to the vertical rods in the operating linkages. By measuring the dimensions of the linkage arms, it was verified that the movements of the rods and the spools were in the ratio of 1:1. However, due to some play in the fulcrum, and at the connecting pins, a back-lash effect was introduced, and this showed up as a zero-error in the DCDT output voltage. This backlash was measured and compensated for during digital simulation.

To perform tests in the field, selected instruments from the consoles discussed earlier were mounted in a recording van. The instrumentation which was placed in the recording van included, transducer amplifier for pressure measurement, placed on top of the DCDT readout, transducer amplifier for flow measurement, a recording oscillograph and a bank of D.C. amplifiers. Power for operating the recording equipment was developed by a gasoline-engine driven generator, so that the recording van was completely self-contained. The average length of cables from transducers mounted ont the test machine to the recording van was 30 feet and no appreciable deterioration of signals was observed during any of the field tests.

- DYNAMIC CALIBRATION -

Dynamic calibration essentially means recognition of the fact that transducers and instrumentation have dynamic behavior exactly like other systems. This dynamic behavior has to be ascertained before using them for dynamic tests on components and systems, otherwise erroneous data will be used in modeling and simulation. For a variety of transducers the dynamic model is linear and manufacturer's technical specifications are sufficient for this kind of assessment. Thus strain-gauge pressure transducers, DCDT's,

etc. usually have a cut-off frequency specified, and D.C. amplifiers and oscillographs have frequency response plots given for reference. In using this information, it is necessary to estimate the highest frequency in the outputs to be measured during a dynamic test, and if this is within the cut-off frequency of the transducer and recording equipment, the latter can be treated as being instantaneous for all practical purposes, i.e. the static calibration is valid for dynamic operation in the frequency range.

In the case of certain nonlinear instruments, a frequency type specification cannot be given and manufacturers technical specifications are usually inadequate to assess the suitability of the instrument for a particular test. Flowmeters are a notable example of this class of instruments. Since a vast majority of flowmeters are used to monitor only steady or slowly varying flows, manufacturers do not normally give any data on their dynamic behavior. The preceding year's report (Ref. 1) gave a brief discussion of dynamic calibration of flowmeters. A series of tests on both turbine and drag flowmeters were carried out and the conclusion was that drag flowmeters have, in general, performance compatible with dynamic tests on fluid power components [2,3]. Even though their behavior is non-linear, their dynamic performance can be characterized by a cut-off frequency; and, as long as outputs lie within this frequency range, the static calibration is valid for dynamic measurements also.

- REFERENCES -

1. AD758 876. Hydraulic System Controls Study, Section II, Annual Report, for the U.S. Army Mobility Equipment Research and Development Center, Fluid Power Research Center, Oklahoma State University, Stillwater, Oklahoma November 1972.

2. Iyengar, S.K.R., "Dynamic Flow Measurement," Paper P73-SP-6, Basic Fluid Power Research Program, Fluid Power Research Center, Oklahoma State University, Stillwater, Oklahoma, December 1973.

3. Iyengar, S.K.R., "Literature Survey of Unsteady Flow Measurement," Report R73-SP-3, Basic Fluid Power Research Program, Fluid Power Research Center, Oklahoma State University, Stillwater, Oklahoma December, 1973.

APPENDIX C

EXPERIMENTAL DATA AND SIMULATION RESULTS ON FORD TLB 4500 BACKHOE

APPENDIX C

EXPERIMENTAL DATA AND SIMULATION RESULTS ON FORD TLB 4500 BACKHOE

The first part of the tables on the following pages summarize selected test results on components as well as the test machine (the Ford TLB 4500 Backhoe) used to verify numerical modeling. They serve only to indicate the nature of laboratory and field test data and are but a fraction of the data acquired in the course of modeling and verification.

The second part of the tables constitute the computer program developed for low-order simulation using DNR, and typical computer outputs. Here again, only a sample output is provided. It may be noted that the computer program calls for data from a "Direct-Access Storage Device" (DASD). Such a device retains the numerical data for DNR in a very convenient and accessible form, at the same time affording a permanent storage.

A few words of explanation about some of the nomenclature in the tables will give the reader a better appreciation of the information presented. Table C-1 gives the data for the metering tests on the directional valve actuating the boom of the backhoe. Q_{DN} is the flow through the relevant orifice, ΔP, the pressure drop across it and DISP the spool displacement. This data was initially stored as such, on the DASD but subsequently it was found more economical to store just the displacements and the corresponding effective metering areas.

Numerical data is in a form directly usable on a digital computer. However, some test results are best presented graphically. The static characteristics of the directional control valves for the swing and boom actuators were presented earlier (Figs. 2-4 and 2-5). The relief valve in the swing sub-circuit had a static characteristic as depicted in Fig. C-1.

Table C-2 is a typical record of the data collected in the field test on the backhoe. In each test the displacement of the actuating valve spool, the supply flow and the differential pressure across the actuating cylinder were continuously recorded. In some tests the supply pressure was also monitored, and in the rest a cylinder pressure was recorded. Since the displacement of the control rod rather than the spool itself, was measured, a correction had to be applied for the slack in the connecting pin. This accounts for the difference between the DCDT reading and the spool movement. The "volts" under the ΔP refers to the transducer output voltage. A calibration chart for the transducer gave the necessary conversion to psi. Flow was measured with a drag flowmeter

TABLE C-1

FORD BACKHOE BOOM - LABORATORY TEST

18 July 1973

p to A			p to B			A to T			B to T			p to T		
Q_{DN}	ΔP	DISP	Q_{DN}	ΔP	DISP	Q_{DN}	ΔP	DISP	Q_{DN}	ΔP	DISP	Q_{DN}	ΔP	DISP
LPM	psi	in												in
63.5	21.0	.390	0	15.2	0	63.5	21.0	.390	62.5	18.0	.400	61.8	16.2	0
63.0	26.2	.350	8.5	22.5	.200	63.0	16.2	.350	62.5	23.0	.350	61.5	16.8	.100
63.0	30.0	.340	10.5	31.8	.220	63.0	30.0	.340	62.5	33.0	.340	61.2	17.0	.120
62.8	34.0	.330	13.9	48.0	.230	62.8	34.0	.330	62.5	38.0	.330	61.0	17.1	.140
62.5	43.8	.320	16.8	56.0	.240	62.5	43.8	.320	62.2	43.0	.320	58.5	16.9	.160
62.2	61.6	.310	30.7	52.0	.250	62.2	61.6	.310	62.0	48.0	.310	56.5	16.6	.180
61.0	100.8	.300	36.5	51.8	.260	61.0	100.8	.300	61.9	78.0	.300	53.2	18.0	.200
46.5	147.5	.290	42.0	55.1	.270	46.5	147.5	.290	61.7	173.0	.290	51.8	21.9	.210
34.2	180.0	.280	46.2	59.5	.280	34.2	180.0	.280	59.9	443.0	.280	49.4	31.1	.220
27.5	192.0	.270	50.8	64.0	.290	27.5	192.0	.270	58.0	738.0	.270	44.8	44.9	.230
23.8	196.2	.260	53.5	67.5	.300	23.8	196.2	.260	56.5	943.0	.260	36.2	50.9	.240
21.1	200.2	.250	56.5	71.4	.310	21.1	200.2	.250	55.5	1158.0	.250	27.8	45.0	.250
18.9	203.0	.240	58.0	74.0	.320	18.9	203.0	.240	54.2	1413.0	.240	21.0	42.8	.260
15.4	207.1	.230	58.5	74.6	.330	15.4	207.1	.230	51.2	1758.0	.230	16.3	44.4	.270
12.8	210.0	.220	58.5	74.6	.340	12.8	210.0	.220	44.8	1983.0	.220	12.8	49.0	.280
8.0	214.0	.210	58.5	73.9	.350	8.4	214.0	.210	35.0	1993.0	.210	8.5	52.9	.290
0	217.0	.200				0	217.0	.200	25.3	2000.0	.200	0	56.8	.300
0	0	0				0	0	0	16.1	2000.0	.190	0	61.0	.310
									8.5	2000.0	.180			
									0	2000.0	.170			
									0	0	0			

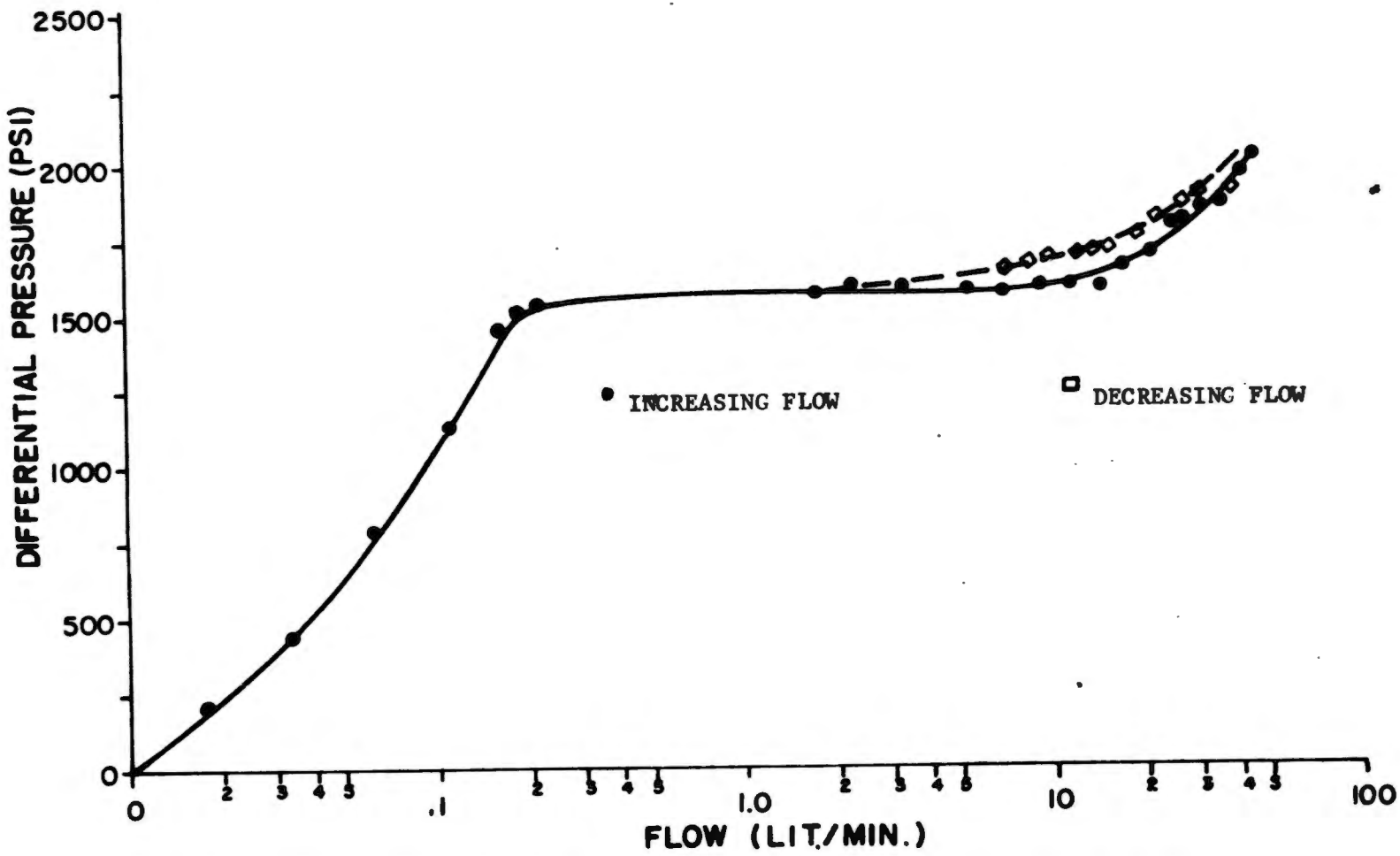

Fig. C-1. Static Characteristics of Relief Valve Integral with Swing Valve.

TABLE C-2

FORD BACKHOE - SWING MODE

Run #7

28 June 1973
FIELD TEST

Time	Displacement		P_{cyl} (B-Port)	ΔP Across Cyl.		Inflow	
	Spool	DCDT				Dayt.	lit/min
(secs)	(ins)	(ins)	(psi)	Volts	psi		
0.0	0	0	250	1.8	0	24.0	51.0
0.1	0	0	250	1.8	0	24.0	51.0
0.2	0	.06	250	1.8	0	24.0	51.0
0.3	.077	.158	250	1.8	0	24.0	51.0
0.35	.379	.46	300	4.0	565	18.0	43.2
0.40	.419	.50	220	7.5	1435	12.0	34.6
0.5	.419	.50	280	7.75	1500	13.0	36.2
0.6	.399	.48	250	7.9	1535	14.0	37.8
0.7	.399	.48	260	7.9	1535	14.0	37.8
0.8	.399	.48	250	7.75	1500	13.4	36.8
0.9	.399	.48	260	6.7	1235	14.0	37.8
1.0	.399	.48	270	6.25	1128	14.0	37.8
1.1	.399	.48	300	5.1	840	15.0	39.2
1.2	.399	.48	320	4.0	565	16.4	41.2
1.3	.399	.48	320	3.0	320	18.8	44.5
1.4	.399	.48	420	2.1	95	19.0	44.8
1.5	.399	.48	1000	.1	- 427.7	18.0	43.2
1.6	.399	.48	1000	.1	- 427.7	18.0	43.2
1.7	.399	.48	580	1.9	45	18.0	43.2
1.8	.399	.48	330	3.0	320	18.0	43.2
1.85	.399	.48	300	3.4	420	18.0	43.2
1.875	.339	.42	300	3.5	440	20.4	46.2
1.9	.098	.18	400	1.4	- 100.6	36.0	64.0
1.925	-.10	-.10	800	0	- 452.8	19.0	44.8
1.95	-.17	-.17	1200	-3.0	- 1207	20.0	46.2
2.0	-.08	-.08	1900	-5.5	- 1836.5	22.0	48.2
2.025	0	.06	1950	-5.6	- 1861.6	21.0	47.2
2.05	.055	.136	1800	-5.25	- 1773.0	22.0	48.2
2.1	0	.036	1730	-4.95	- 1698	23.0	49.8
2.2	0	0	1700	-4.85	- 1673	23.0	49.8
2.3	0	.02	1620	-4.5	- 1585	22.0	48.2
2.4	0	.01	1570	-4.25	- 1522	23.0	49.8
2.5	0	.016	1490	-4.0	- 1460	23.0	49.8
2.6	0	0	1240	-3.0	- 1207	24.0	51.0
2.7	0	0	680	- .65	- 616	24.0	51.0
2.8	0	0	260	2.0	70	24.0	51.0
2.9	0	0	120	4.5	690	24.0	51.0
3.0	0	0	100	5.95	1050	24.0	51.0
			100	6.0	1065	24.0	51.0

and 'Dayt' refers to the output of the transducer amplifier. Once again, a calibration chart had to be used to convert the readings to physical units. Figs. 2-11 and 2-13 show typical traces based on which tables like Table C-2 were generated and stored on the DASD. Note that time is read from right to left on these traces.

Table C-3 is the computer program for the simulation part only, of using DNR for low order modeling. The results of the simulation are contained in Tables C-4 and C-5. The program not only calculates the flows through each of the metering orifices in the control valve, but also the cylinder load and velocity. The last table shows the torque power and efficiency characteristics for the trajectory simulated.

TABLE C-3

```
FORTRAN IV G LEVEL  21                MAIN              DATE = 73037        19/16/57              PAGE 0001

      C*****************************************************************************
      C     THIS PROGRAM PERFORMS A STATIC SIMULATION ON AN OPEN CENTER          01000000
      C     SYSTEM USING DATA FROM DIRECT ACCESS STORAGE DEVICE  20              01100000
      C     THE FOLLOWING QUANTITIES ARE INPUTS:                                 01200000
      C     PS          SUPPLY PRESSURE  (PSI)                                   01300000
      C     DELTP       PRESSURE DIFFERENCE ACROSS WORK PORTS OF VALVE (PSI)     01400000
      C     DISP        SPOOL DISPLACEMENT (INS)                                 01500000
      C     ENSPD       ENGINE SPEED (RPM)                                       01600000
      C                                                                          01700000
      C     THE FOLLOWING QUANTITIES ARE THE OUTPUTS                             01800000
      C     Q1          FLOW FROM PRESSURE PORT TO PORT 'A' (CU.IN/SEC)          01900000
      C     Q4          FLOW FROM PORT 'B' TO TANK PORT  (CU.IN/SEC)             02000000
      C     Q5          FLOW FROM PRESSURE PORT TO TANK PORT (CU.IN/SEC)         02100000
      C     TFLOW       TOTAL SUPPLY FLOW (CU.IN/SEC)                            02200000
      C     EXTLD       LOAD ON CYLINDER (LBS)                                   02300000
      C     VEL         VELOCITY OF CYLINDER (IN/SEC)                            02400000
      C     TORQ        OUTPUT TORQUE OF ENGINE  (LB.FT)                         02500000
      C     HPIN        INPUT  POWER TO HYDRAULIC SYSTEM (HP)                    02600000
      C     HPOUT       OUTPUT POWER OF HYDRAULIC SYSTEM  (HP)                   02700000
      C     EFF         EFFICIENCY OF HYDRAULIC SYSTEM                           02800000
      C                                                                          02900000
      C     OTHER VARIABLES AS FOLLOWS:                                          03000000
      C     FLOW        SUPPLY FLOW MEASURED EXPERIMENTALLY                      03100000
      C     A1          METERING ORIFICE FROM PRESSURE PORT TO PORT 'A'           03200000
      C     A4          METERING ORIFICE FROM PORT 'B' TO TANK PORT               03300000
      C     A5          METERING ORIFICE FROM PRESSURE PORT TO TANK PORT          03400000
      C     CYLDIA      CYLINDER DIAMETER (INS)                                  03500000
      C     ROD         ROD DIAMETER (INS)                                       03600000
      C     AREACL      AREA OF HEAD END OF CYLINDER                             03700000
      C     AREARO      AREA OF ROD END OF CYLINDER                              03800000
      C*****************************************************************************
      C     SUBROUTINES CALLED     NONE                                          05100000
      C*****************************************************************************
0001            DIMENSION PS(70),FLOW(70),DISP(70),DELTP(70),PA(70),PB(70),    09990000
                1TIME(70),TFLOW(70),Q1(70),Q4(70),Q5(70),EXTLD(70),VEL(70),    10000000
                2TORQ(70),HPIN(70),HPOUT(70),EFF(70),TITLE(20)                 10100000
0002            DIMENSION A1(70),A4(70),A5(70)                                 10300000
0003            DEFINE FILE 20(10,421,U,NV)                                    10400000
0004            READ(5,10) TITLE                                               10500000
0005            READ(5,23)R,PTANK                                              10600000
0006       2    FORMAT(I5,F10.4)                                               10700000
0007            READ(20'R) NDATA,(TIME(I),DISP(I),PS(I),DELTP(I),              10800000
                1FLOW(I),I=1,NDATA)                                            10900000
0008            WRITE(6,11)TITLE                                               11000000
0009            WRITE(6,400) (TIME(I),DISP(I),PS(I),DELTP(I),FLOW(I),I=1,NDATA)  11100000
0010       400  FORMAT(///,7X,6HTIME,12X,4HDISP,11X,2HPS,12X,5HDELTP,11X,4HFLOW,/,
                16X,5H(SEC),10X,8H(INCHES),7X,5H(PSI),11X,5H(PSI),8X,9H(LIT/MIN),//
                2,(1H,1PE15.5))
0011            WRITE(6,12)TITLE
0012       10   FORMAT(20A4)                                                   11600000
0013       11   FORMAT(1H1,////,12X,20A4,///)
0014       12   FORMAT(1H1,////,34X,20A4,///)
0015            READ(5,100)CYLDIA,ROD,ENSPD                                    11800000
0016            WRITE(6,1100)CYLDIA,ROD,ENSPD
0017       1100 FORMAT(14X,20HCYLINDER DIAMETER = ,F10.3,2H INCHES,5X,15HROD DIAME
                1TER = ,F10.3,2H INCHES,5X,15HENGINE SPEED = ,F10.3,4H RPM)
0018            WRITE(6,1105) NDATA                                            12100000
0019       1105 FORMAT(14X,23HNUMBER OF DATA POINTS = ,I5)
```

TABLE C-3 (Cont.)

```
FORTRAN IV G LEVEL  21                 MAIN                DATE = 73337        19/16/57                PAGE 0002

0020        100   FORMAT(6F10.3)                                                                    12300000
0021              READ(5,100) (A1(J),A4(J),A5(J),J=1,NDATA)                                         12400000
0022              COEFF=12.204                                                                      12500000
0023              AREACL=3.14159*CYLDIA**2*0.25                                                     12600000
0024              AREARD=(OD**2-3.1415*0.25                                                         12700000
0025              RATIO=AREACL-AREARD                                                               12800000
0026              RATIO=RATIO/AREACL                                                                12900000
                  C   CONVERT SPEED FROM RPM TO RADIANS PER SEC.                                    13000000
0027              SPEED=ENSPD*2.0*3.14159/60.0                                                      13100000
0028              DO 1111 K=1,NDATA                                                                 13200000
                  C   PERFORM CONVERSIONS ON RAW DATA                                             13300000
0029              FLOW(K)=FLOW(K)*1.01608                                                           13400000
                  C   CONVERTS FLOW FROM LIT/MIN TO CU.IN/SEC                                       13500000
0030              PS(K)=PS(K)*1.1                                                                   13600000
0031        1111  CONTINUE                                                                          13700000
0032              WRITE(6,700)                                                                      13800000
0033        700   FORMAT(//,14X,2HQ1,13X,2HQ4,13X,2HQ5,13X,2HPA,13X,2HPB,7X,13HEXTER
                 1NAL LOAD,5X,8HVELOCITY,/,9X,11HICU IN/SEC),4X,11HICU IN/SEC),4X,11
                 2HICU IN/SEC),7X,5H(PSI),10X,5H(PSI),10X,5H(LBS),9X,8H(IN/SEC),///)
                  C   THE FOLLOWING LOOP SOLVES THE OPEN-CENTER SYSTEM                            14100000
0034              SUM1=0.                                                                           14200000
0035              SUM2=0.                                                                           14300000
0036              SUM3=0.                                                                           14400000
0037              SUM4=0.                                                                           14500000
0038              DO 2000 J=1,NDATA                                                                 14600000
0039              IF(A1(J).LE.0.0.OR.A4(J).LE.0.0) GO TO 3000                                       14700000
0040              STORE=(RATIO*A1(J)/A4(J))**2                                                      14800000
0041              PB(J)=((PS(J)-DELTP(J))*STORE+PTANK)/(1.0+STORE)                                  14900000
0042              IF(PB(J).LE.0.0) PB(J)=0.0                                                        15000000
0043              DELPBT=PB(J)-PTANK                                                                15100000
0044              SIGN=DELPBT/ABS(DELPBT)                                                           15200000
0045              A4(J)=COEFF*A4(J)*SQRT(ABS(DELPBT))*SIGN                                          15300000
0046              Q1(J)=Q4(J)/RATIO                                                                 15400000
0047              GO TO 3500                                                                        15500000
0048        3000  CONTINUE                                                                          15600000
0049              A4(J)=0.0                                                                         15700000
0050              Q1(J)=Q4(J)                                                                       15800000
0051              PB(J)=PTANK                                                                       15900000
0052        3500  CONTINUE                                                                          16000000
0053              PA(J)=PB(J)+DELTP(J)                                                              16100000
0054              IF(PA(J).LE.0.0) PA(J)=0.0                                                        16200000
0055              DELPT=PS(J)-PTANK                                                                 16300000
0056              SIGN=DELPT/ABS(DELPT)                                                             16400000
0057              Q5(J)=COEFF*A5(J)*SQRT(ABS(DELPT))*SIGN                                           16500000
0058              TFLOW(J)=Q1(J)+Q5(J)                                                              16600000
0059              FXTLOD(J)=PA(J)*CYLDIA-PB(J)*(AREACL-AREARD)                                      16700000
0060              VEL(J)=Q1(J)/AREACL                                                               16800000
                  C   TORQUE AND POWER CALCULATIONS FOR HYDRAULIC SYSTEM                          16900000
0061              HPOUT(J)=EXTLOD(J)*VEL(J)/6600.0                                                  17000000
0062              IF(HPOUT(J).LE.0.)HPOUT(J)=0.                                                     17100000
0063              HPIN(J)=PS(J)*TFLOW(J)/6600.0                                                     17200000
0064              TORQ(J)=HPIN(J)*550.0/SPEED                                                       17300000
0065              EFF(J)=HPOUT(J)/HPIN(J)*100.0                                                     17400000
0066              IF(EFF(J).LE.0)EFF(J)=0.0                                                         17500000
0067              SUM1=SUM1+HPOUT(J)                                                                17600000
0068              SUM2=SUM2+HPIN(J)                                                                 17700000
0069              SUM3=SUM3+TORQ(J)                                                                 17800000
0070              SUM4=SUM4+EFF(J)                                                                  17900000
```

TABLE C-3 (Cont.)

```
FORTRAN IV G LEVEL 21                MAIN              DATE = 73317        10/16/57                PAGE 0003

0071                  WRITE(6,800) QI(J),PI(J),PS(J),PA(J),PB(J),EXTLO(J),                    17000000
                     1VEL(J)                                                                  17100000
0072          800     FORMAT(5X,1PBE15.4)                                                     17200000
0073          2000    CONTINUE                                                                17300000
0074                  XNDATA=NDATA
0075                  AVSUM1=SUM1/XNDATA
0076                  AVSUM2=SUM2/XNDATA
0077                  AVSUM3=SUM3/XNDATA
0078                  AVSUM4=SUM4/XNDATA
0079                  WRITE(6,13)TITLE
0080          13      FORMAT(1H1,////,30X,20A4,///)
0081                  WRITE (6,1400)                                                          17500000
0082          1400    FORMAT(///,11X,'TIME',9X,'SPOOL',7X,'SUPPLY',7X,'PORT A',7X,'PORT B
                     1',7X,'LOAD',9X,'VELOCITY',15X,'FLOW',/,10X,'(SECS)',7X,'POSITION',
                     29X,'PRESSURE',5X,'PRESSURE',5X,'PRESSURE',32X,'CALCULATED',2X,'MEA
                     3SURED',/,22X,8H(INCHES),7X,5H(PSI),8X,5H(PSI),8X,5H(PSI),7X,4H(LB)
                     4,9X,8H(IN/SEC),4X,11H(CU IN/SEC),2X,11H(CU IN/SEC),///)
0083                  WRITE (6,1500) (TIME(J),DISP(J),PS(J),PA(J),PB(J),EXTLO(J),             18000000
                     1VEL(J),TFLOW(J),FLOW(J),J=1,NDATA)                                      18100000
0084          1500    FORMAT(1H,6X,1P9E13.4)
0085                  WRITE(6,18)TITLE
0086          18      FORMAT(1H1,////,12X,20A4,///)
0087                  WRITE(6,1600)                                                           18400000
0088          1600    FORMAT(18X,' TORQUE, POWER AND EFFICIENCY OF HYDRAULIC SYSTEM',///,
                     18X,4HTIME,15X,10HHORSEPOWER,15X,6HTORQUE,7X,10HEFFICIENCY,/,23X,5H
                     2INPLT,9X,6HOUTPUT,/,7X,5H(SEC),40X,7H(FT LB),6X,10H(PER CENT),///)
0089                  WRITE(6,1700) (TIME(J),HPOUT(J),HPIN(J),TORQ(J),EFF(J),                 18800000
                     1J=1,NDATA)                                                              18900000
0090          1700    FORMAT(1P5E15.3)                                                        19000000
0091                  WRITE(6,33)AVSUM1,AVSUM2,AVSUM3,AVSUM4
0092          33      FORMAT(////,6X,' AVERAGE OUTPUT HORSEPOWER = ',1PE15.3,2X,'AVERAGE
                     1INPUT HORSEPOWER = ',1PE15.3,/,6X,'AVERAGE TORQUE = ',1PE15.3,' FT
                     2 LB',7X,'AVERAGE EFFICIENCY = ',1PE15.3,' %',/,1H1)
0093                  STOP                                                                    80800000
0094                  END                                                                     80900000
```

TABLE C-4

FORD TLB 4500 HACKNEY SWING ROOF SIMULATION RUN 10/28.6.73

CYLINDER DIAMETER = 4.500 INCHES ROD DIAMETER = 1.750 INCHES ENGINE SPEED = 1000.000 RPM
NUMBER OF DATA POINTS = 99

Q1 (CU IN/SEC)	Q4 (CU IN/SEC)	Q5 (CU IN/SEC)	PA (PSI)	PB (PSI)	EXTERNAL LOAD (LBS)	VELOCITY (IN/SEC)
0.0	0.0	5.1301E 01	3.0000E 01	3.0000E 01	-2.6997E 02	0.0
0.0	0.0	5.1301E 01	3.0000E 01	3.0000E 01	-2.6997E 02	0.0
0.0	0.0	5.1301E 01	3.0000E 01	3.0000E 01	-2.6997E 02	0.0
0.0	0.0	5.1301F 01	3.0000F 01	3.0000F 01	-2.6997E 02	0.0
0.0	0.0	5.1301F 01	3.0000F 01	3.0000F 01	-2.6997E 02	0.0
3.6734E 01	2.6083E 01	0.0	1.6507E 03	1.1560E 02	6.7665E 03	1.9308E 00
4.2168E 01	3.5791E 01	0.0	1.7896E 03	1.9156E 02	5.4670E 03	2.6913E 00
3.8377E 01	3.2573E 01	0.0	1.7738E 03	1.6383E 02	5.7707E 03	2.4113E 00
3.8214F 01	3.3734E 01	0.0	1.6361E 03	1.4914E 02	5.3404E 03	2.2767E 00
3.4184F 01	2.9031F 01	0.0	1.5711E 03	1.3608E 02	5.2320E 03	2.1484E 00
3.9461E 01	3.0522E 01	0.0	1.4475E 03	1.4791E 02	4.5222E 03	2.2611E 00
3.8213F 01	3.3734E 01	0.0	1.2491E 03	1.4914F 02	3.6079E 03	2.2767E 00
4.0235E 01	3.4125E 01	0.0	9.5609E 02	1.7609E 02	1.9182E 03	2.5280E 00
4.5934E 01	3.8492F 01	0.0	6.7177E 02	2.2177E 02	2.0291E 01	2.8089F 00
4.7284F 01	4.0134E 01	0.0	4.3819E 02	2.3519E 02	-1.1760E 03	2.9733E 00
1.0158E 02	8.6214E 01	0.0	3.3869E 02	9.6755F 02	-1.1537E 04	6.3867E 00
1.1131F 02	9.4495E 01	0.0	3.5110E 02	1.1563E 03	-1.4029E 04	7.0001F 00
7.6558E 01	6.3762E 01	0.0	5.3513E 02	5.3513E 02	-4.8156E 03	4.6879F 00
4.8537E 01	4.1171F 01	0.0	6.3300E 02	2.4380E 02	-4.3899E 02	3.0499F 00
4.6694E 01	3.7098F 01	0.0	7.5116E 02	2.1116E 02	5.2976E 02	2.8076E 00
4.3941F 01	3.7296E 01	0.0	7.6545E 02	2.0545E 02	7.6116E 02	2.7628E 00
4.5743F 01	3.8825E 01	0.0	7.6014E 02	2.2014E 02	6.6898E 02	2.8762E 00
4.6629F 01	3.9604E 01	0.0	7.2585F 02	2.2585F 02	2.1757E 02	2.9190E 00
4.6604F 01	3.9613E 01	0.0	6.6993E 02	2.2993E 02	-8.9145E 01	2.9693E 00
4.6715E 01	3.9650E 01	0.0	6.4830E 02	2.2830E 02	-1.6444E 02	2.9372E 00
4.5044F 01	3.8762E 01	0.0	6.9432E 02	2.1932E 02	1.6382E 02	2.8700E 00
4.6629F 01	3.9604E 01	0.0	7.2585E 02	2.2585E 02	2.1757E 02	2.9190E 00
4.5764F 01	3.8825E 01	0.0	7.6014E 02	2.2014E 02	6.6898E 02	2.8762E 00
4.3726F 01	3.7129F 01	0.0	8.1882E 02	2.0382F 02	9.3355E 02	2.7500E 00
4.3427E 01	3.6859E 01	0.0	8.4137E 02	2.0137F 02	1.0679E 03	2.7305E 00
4.3427F 01	3.6859E 01	0.0	8.4137E 02	2.0137E 02	1.0679E 03	2.7305E 00
4.3427F 01	3.6859E 01	0.0	8.4137E 02	2.0137E 02	1.0679E 03	2.7305E 00
2.0554F 01	2.5088F 01	3.9263E 00	6.2439E 02	1.0939E 02	1.3331E 03	1.8585E 00
0.0	0.0	-3.3410E 01	3.2500E 02	3.0000E 01	1.0579E 03	0.0
0.0	0.0	6.3809E 01	3.0000E 01	3.0000E 01	-2.6997E 02	0.0
0.0	0.0	5.1301E 01	0.0	3.0000E 01	-4.0497E 02	0.0
0.0	0.0	5.1301E 01	0.0	3.0000E 01	-4.0497E 02	0.0
0.0	0.0	5.1301F 01	5.5100E 01	3.0000E 01	-1.5702E 02	0.0
0.0	0.0	5.1301E 01	1.5000E 02	3.0000E 01	2.7003E 02	0.0
0.0	0.0	5.1301E 01	5.4500E 02	3.0000E 01	2.0479E 03	0.0
0.0	0.0	5.1301E 01	1.0800E 03	3.0000E 01	4.4550E 03	0.0
0.0	0.0	5.1401E 01	1.9550E 03	3.0000F 01	8.3025E 03	0.0
0.0	0.0	5.1301E 01	1.4900E 03	3.0000F 01	6.3000E 03	0.0
0.0	0.0	5.1301E 01	1.4050E 03	3.0000F 01	5.9175E 03	0.0
0.0	0.0	5.1301F 01	1.2300F 03	3.0000F 01	5.1300E 03	0.0
0.0	0.0	5.1301E 01	7.9500E 02	3.0000E 01	3.1725E 03	0.0
0.0	0.0	5.1301E 01	2.5000E 02	3.0000E 01	7.2003E 02	0.0
0.0	0.0	5.1301E 01	7.5000E 01	3.0000E 01	-6.7478E 01	0.0
0.0	0.0	5.1301F 01	3.0000F 01	3.0000E 01	-2.6997E 02	0.0
0.0	0.0	5.1301E 01	0.0	3.0000F 01	-4.0497E 02	0.0
0.0	0.0	5.1301F 01	0.0	3.0000E 01	-4.0497E 02	0.0
0.0	0.0	5.1301F 01	0.0	3.0000E 01	-4.0497E 02	0.0
0.0	0.0	5.1301E 01	0.0	3.0000E 01	-4.0497E 02	0.0
0.0	0.0	5.1301E 01	0.0	3.0000E 01	-4.0497E 02	0.0
0.0	0.0	5.1301E 01	1.3004E 02	3.0000E 01	1.8273E 02	0.0

TABLE C-4 (Cont)

FORD TLB 455D BACKHOE SWING MODE SIMULATION RUN 13/28.6.73

TIME (SECS)	SPOOL POSITION (INCHES)	SUPPLY PRESSURE (PSI)	PORT A PRESSURE (PSI)	PORT B PRESSURE (PSI)	LOAD (LB)	VELOCITY (IN/SEC)	FLOW CALCULATED (CU IN/SEC)	FLOW MEASURED (CU IN/SEC)
0.0	0.0	1.1000E 02	3.0000E 01	3.0000E 01	-2.6997E 02	0.0	5.1301E 01	5.2878E 01
1.0000E-01	0.0	1.1000E 02	3.0000E 01	3.0000E 01	-2.6997E 02	0.0	5.1301E 01	5.2878E 01
2.0000E-01	0.0	1.1000E 02	3.0000E 01	3.0000E 01	-2.6997E 02	0.0	5.1301E 01	5.2878E 01
3.0000E-01	2.3000E-02	1.1000E 02	3.0000E 01	3.0000E 01	-2.6997E 02	0.0	5.1301E 01	5.2878E 01
4.0000E-01	2.3500E-01	1.1000E 02	3.0000E 01	3.0000E 01	-2.6997E 02	0.0	6.2079E 01	6.5291E 01
5.0000E-01	4.1300E-01	1.0700E 03	1.8937E 03	1.1500E 02	6.7665E 03	1.9306E 00	3.0707E 01	3.8438E 01
6.0000E-01	3.9500E-01	1.9200E 03	1.7896E 03	1.9156E 02	9.4670E 03	2.6513E 00	4.2160E 01	5.0845E 01
7.0000E-01	3.9900E-01	1.8040E 03	1.7738E 03	1.6183E 02	9.7707E 03	2.4130E 00	3.8377E 01	3.7116E 01
8.0000E-01	3.9900E-01	1.6610E 03	1.6341E 03	1.4914E 02	9.3409E 03	2.2767E 00	3.6210E 01	3.6099E 01
9.0000E-01	3.9900E-01	1.5950E 03	1.5711E 03	1.3408E 02	9.2329E 03	2.1484E 00	3.4168E 01	3.5286E 01
1.0000E 00	3.9900E-01	1.4740E 03	1.4475E 03	1.4791E 02	4.5226E 03	2.2611E 00	3.5961E 01	3.7116E 01
1.1000E 00	3.9900E-01	1.2760E 03	1.2491E 03	1.4914E 02	3.6079E 03	2.2767E 00	3.6210E 01	3.8641E 01
1.2000E 00	3.9900E-01	9.9000E 02	9.6889E 02	1.7689E 02	1.9182E 03	2.5280E 00	4.0209E 01	4.0472E 01
1.3000E 00	3.9900E-01	7.1500E 02	6.7177E 02	2.2177E 02	2.9291E 01	2.8885E 00	4.5930E 01	4.1794E 01
1.4000E 00	3.9900E-01	4.8400E 02	4.3819E 02	2.3319E 02	-1.1760E 03	2.9733E 00	4.7288E 01	4.3929E 01
1.5000E 00	3.9900E-01	3.5000E 02	3.3065E 02	9.6795E 02	-1.1537E 04	6.3867E 00	1.0158E 02	4.3929E 01
1.6000E 00	3.9900E-01	3.0500E 02	3.5110E 02	1.1963E 03	-1.4029E 04	7.0001E 00	1.1133E 02	4.3929E 01
1.7000E 00	3.9900E-01	3.4900E 02	3.3513E 02	3.3513E 02	-4.8156E 03	4.6879E 00	7.4558E 01	4.3929E 01
1.8000E 00	3.9900E-01	3.8200E 02	3.3383E 02	2.4380E 02	-4.3699E 02	3.0499E 00	4.8907E 01	4.3929E 01
1.9000E 00	3.9900E-01	3.9200E 02	3.5116E 02	2.1116E 02	9.2976E 02	2.8074E 00	4.4650E 01	4.3929E 01
2.0000E 00	3.9900E-01	3.9500E 02	3.8545E 02	2.0545E 02	7.6116E 02	2.7628E 00	4.3941E 01	4.3929E 01
2.1000E 00	3.9900E-01	3.9300E 02	3.8014E 02	2.2014E 02	4.4890E 02	2.8762E 00	4.5743E 01	4.3929E 01
2.2000E 00	3.9900E-01	3.7000E 02	3.2589E 02	2.2589E 02	2.1757E 02	2.9190E 00	4.6425E 01	4.3929E 01
2.3000E 00	3.8700E-01	3.1500E 02	2.6993E 02	2.2993E 02	-8.9145E 01	2.9493E 00	4.6906E 01	4.3929E 01
2.4000E 00	3.8100E-01	2.9300E 02	2.4830E 02	2.2830E 02	-1.6446E 02	2.9372E 00	4.6719E 01	4.3929E 01
2.5000E 00	3.8100E-01	2.8700E 02	2.4252E 02	2.1932E 02	1.6382E 02	2.8708E 00	4.5645E 01	4.3929E 01
2.6000E 00	3.8100E-01	2.7000E 02	2.2545E 02	2.2545E 02	2.1757E 02	2.9190E 00	4.6425E 01	4.3929E 01
2.7000E 00	3.8100E-01	2.8300E 02	2.3014E 02	2.2014E 02	4.4890E 02	2.8762E 00	4.5743E 01	4.3726E 01
2.8000E 00	3.8100E-01	2.9800E 02	2.4382E 02	2.0382E 02	9.3339E 02	2.7500E 00	4.3736E 01	4.3624E 01
2.9000E 00	3.7900E-01	2.8000E 02	2.4137E 02	2.0137E 02	1.0679E 03	2.7305E 00	4.3427E 01	4.3726E 01
3.0000E 00	3.5500E-01	2.6000E 02	2.4137E 02	2.0137E 02	1.0679E 03	2.7305E 00	4.3427E 01	4.4539E 01
3.0625E 00	3.4700E-01	2.4000E 02	2.4137E 02	2.0137E 02	1.0679E 03	2.7305E 00	4.3427E 01	4.5963E 01
3.0950E 00	2.7900E-01	2.6000E 02	2.2439E 02	1.0939E 02	1.3331E 03	1.8585E 00	2.9605E 01	5.9996E 01
3.0750E 00	1.7900E-01	1.1000E 01	3.2500E 02	3.0000E 01	1.0979E 03	0.0	-3.3610E 01	4.7793E 01
3.1100E 00	1.3900E-01	1.5400E 02	3.0000E 01	3.0000E 01	-2.6997E 02	0.0	6.3869E 01	4.6980E 01
3.2000E 00	0.0	1.1000E 02	3.0	3.0000E 01	-4.0497E 02	0.0	5.1301E 01	4.7289E 01
3.3000E 00	-7.4000E-02	1.1000E 02	0.0	3.0000E 01	-4.0497E 02	0.0	5.1301E 01	4.9319E 01
3.4000E 00	-4.3000E-02	1.1000E 02	9.9100E 01	3.0000E 01	-1.5702E 02	0.0	5.1301E 01	4.9624E 01
3.5000E 00	0.0	1.1000E 02	1.5000E 02	3.0000E 01	2.7003E 02	0.0	5.1301F 01	4.9827E 01
3.5500E 00	1.7000E-02	1.1000E 02	5.4500E 02	3.0000E 01	2.0475E 03	0.0	5.1301E 01	4.9827E 01
3.6000E 00	0.0	1.1000E 02	1.0800E 03	3.0000E 01	4.4550E 03	0.0	5.1301E 01	4.9929E 01
3.7000E 00	0.0	1.1000E 02	1.9950E 03	3.0000E 01	8.3925E 03	0.0	5.1301E 01	5.3742E 01
3.8000E 00	0.0	1.1000E 02	1.4900E 03	3.0000E 01	6.3000E 03	0.0	5.1301E 01	5.0946E 01
3.9000E 00	0.0	1.1000E 02	1.4050E 03	3.0000E 01	5.9179E 03	0.0	5.1301E 01	5.1057E 01
4.0000E 00	0.0	1.1000E 02	1.2300E 03	3.0000E 01	5.1300E 03	0.0	5.1301E 01	5.1061E 01
4.1000E 00	0.0	1.1000E 02	7.9500E 02	3.0000E 01	3.1725E 03	0.0	5.1301E 01	5.1061E 01
4.2000E 00	0.0	1.1000E 02	2.5000E 02	3.0000E 01	7.2003E 02	0.0	5.1301E 01	5.1061E 01
4.3000E 00	0.0	1.1000E 02	7.5000E 01	3.0000E 01	-6.7470E 01	0.0	5.1301E 01	5.1061E 01
4.4000E 00	0.0	1.1000E 02	3.0000E 01	3.0000E 01	-2.6997E 02	0.0	5.1301F 01	5.1061E 01
4.5000E 00	0.0	1.1000E 02	3.0	3.0000E 01	-4.0497E 02	0.0	5.1301F 01	5.1061E 01
4.6000E 00	0.0	1.1000E 02	0.0	3.0000E 01	-4.0497E 02	0.0	5.1301E 01	5.1061E 01
4.7000E 00	0.0	1.1000E 02	0.0	3.0000E 01	-4.0497E 02	0.0	5.1301E 01	5.1061E 01
4.8000E 00	0.0	1.1000E 02	0.0	3.0000E 01	-4.0497E 02	0.0	5.1301E 01	5.1061F 01
4.9000E 00	0.0	1.1000E 02	0.0	3.0000E 01	-4.0497E 02	0.0	5.1301E 01	5.1061E 01
5.0000E 00	0.0	1.1000E 02	1.3000E 02	3.0000E 01	1.8273E 02	0.0	5.1301E 01	5.1061F 01

TABLE C-5

FORD TLB 4500 BACKHOE SWING MODE SIMULATION RUN 13/28.6.73

TORQUE, POWER AND EFFICIENCY OF HYDRAULIC SYSTEM

TIME (SEC)	HORSEPOWER INPUT	HORSEPOWER OUTPUT	TORQUE (FT LB)	EFFICIENCY (PER CENT)
0.0	0.0	8.550E-01	4.491E 00	0.0
1.000E-01	0.0	8.550E-01	4.491E 00	0.0
2.000E-01	0.0	8.550E-01	4.491E 00	0.0
3.000E-01	0.0	8.550E-01	4.491E 00	0.0
4.000E-01	0.0	1.345E 00	7.064E 00	0.0
5.000E-01	1.979E 00	8.700E 00	4.570E 01	2.275E 01
6.000E-01	2.196E 00	1.167E 01	6.127E 01	1.882E 01
7.000E-01	2.110E 00	1.049E 01	5.509E 01	2.011E 01
8.000E-01	1.842E 00	9.113E 00	4.786E 01	2.022E 01
9.000E-01	1.703E 00	8.257E 00	4.337E 01	2.063E 01
1.000E 00	1.549E 00	8.031E 00	4.218E 01	1.929E 01
1.100E 00	1.245E 00	7.001E 00	3.677E 01	1.778E 01
1.200E 00	7.347E-01	6.031E 00	3.167E 01	1.218E 01
1.300E 00	1.282E-02	4.977E 00	2.614E 01	2.576E-01
1.400E 00	0.0	3.468E 00	1.821E 01	0.0
1.500E 00	0.0	8.465E 00	4.446E 01	0.0
1.600E 00	0.0	1.021E 01	5.360E 01	0.0
1.700E 00	0.0	7.332E 00	3.851E 01	0.0
1.800E 00	0.0	5.012E 00	2.633E 01	0.0
1.900E 00	2.253E-01	5.358E 00	2.814E 01	4.206E 00
2.000E 00	3.186E-01	5.493E 00	2.885E 01	5.801E 00
2.100E 00	1.957E-01	5.565E 00	2.923E 01	3.516E 00
2.200E 00	9.623E-02	5.416E 00	2.845E 01	1.777E 00
2.300E 00	0.0	5.082E 00	2.669E 01	0.0
2.400E 00	0.0	4.905E 00	2.576E 01	0.0
2.500E 00	7.124E-02	5.097E 00	2.677E 01	1.398E 00
2.600E 00	9.623E-02	5.416E 00	2.845E 01	1.777E 00
2.700E 00	1.957E-01	5.565E 00	2.923E 01	3.516E 00
2.800E 00	3.889E-01	5.686E 00	2.986E 01	6.840E 00
2.900E 00	4.418E-01	5.790E 00	3.041E 01	7.630E 00
3.000E 00	4.418E-01	5.790E 00	3.041E 01	7.630E 00
3.025E 00	4.418E-01	5.790E 00	3.041E 01	7.630E 00
3.050E 00	3.754E-01	3.348E 00	1.759E 01	1.121E 01
3.075E 00	0.0	-5.568E-02	-2.925E-01	0.0
3.100E 00	0.0	1.490E 00	7.827E 00	0.0
3.200E 00	0.0	8.550E-01	4.491E 00	0.0
3.300E 00	0.0	8.550E-01	4.491E 00	0.0
3.400E 00	0.0	8.550E-01	4.491E 00	0.0
3.500E 00	0.0	8.550E-01	4.491E 00	0.0
3.550E 00	0.0	8.550E-01	4.491E 00	0.0
3.600E 00	0.0	8.550E-01	4.491E 00	0.0
3.700E 00	0.0	8.550E-01	4.491E 00	0.0
3.800E 00	0.0	8.550E-01	4.491E 00	0.0
3.900E 00	0.0	8.550E-01	4.491E 00	0.0
4.000E 00	0.0	8.550E-01	4.491E 00	0.0
4.100E 00	0.0	8.550E-01	4.491E 00	0.0
4.200E 00	0.0	8.550E-01	4.491E 00	0.0
4.300E 00	0.0	8.550E-01	4.491E 00	0.0
4.400E 00	0.0	8.550E-01	4.491E 00	0.0
4.500E 00	0.0	8.550E-01	4.491E 00	0.0
4.600E 00	0.0	8.550E-01	4.491E 00	0.0
4.700E 00	0.0	8.550E-01	4.491E 00	0.0
4.800E 00	0.0	8.550E-01	4.491E 00	0.0
4.900E 00	0.0	8.550E-01	4.491E 00	0.0
5.000E 00	0.0	8.550E-01	4.491E 00	0.0

AVERAGE OUTPUT HORSEPOWER = 3.029E-01 AVERAGE INPUT HORSEPOWER = 3.752E 00
AVERAGE TORQUE = 1.970E 01 FT LB AVERAGE EFFICIENCY = 3.909E 00 %

APPENDIX D

OPEN CENTER FOUR WAY VALVE ANALYSIS PROGRAM

APPENDIX D

- OPEN CENTER FOUR WAY VALVE ANALYSIS PROGRAM -

The single, most necessary component in any hydraulic system is the valve which is used to control either the manual or automatic operation of a machine. Such an element is generally termed a directional control valve and is a multi-port device. There are two basic types of these multi-port elements: three-way, or three-port, and four-way valves. Of these two basic types of valves, the most commonly used is the four-way valve. Thus, the discussion below is focused entirely upon four-way directional control valves.

In this class of valves, there are two major categories, which are open and closed center, respectively. The difference between these is the tanking transmission in the center spool position of the valves. When an open center valve is in its center or neutral position, the pressure port of the valve is directly connected to the tank port of the valve, and the incoming supply fluid is returned directly to the reservoir. The attractive feature of such a valve is that energy losses across the valve are minimal at the neutral position. All flow through the valve is subjected to a small differential pressure, and thus only a small portion of the input energy is converted to heat energy before the fluid returns to tank. A system utilizing such a valve is termed an "open center" system. A closed center valve is the opposite of an open center valve, and consequently is not as widely used. A system which uses a closed center valve is called a "closed center" system.

In either case, when an analysis of fluid power system is desired, some method must be available to analyze a four-way directional control valve. With the advent of high speed digital computers, it is advantageous, both timewise and economically, to use a computer an an analysis tool. To hydraulic system designers the wheatstone bridge analogy to solve for unknown pressures and flows in a four-way valve is well known and is particularly well suited for digital computer simulation.

The method that is presented here describes a computer program which provides a steady state analysis of an open center system using the wheatstone bridge analogy for an open center directional control valve. The load across the bridge is a hydraulic cylinder. Appendix E presents a similar analysis for a closed center system. A flowchart of the open center analysis computer program is shown in Fig. D-1. After the initialization of temporary storage values within the program, data is read into the program. The first input data to the program is experimental data, which consists of spool displacements and metering areas for the four bridge orificies and the open center orifice of the valve. This data is stored in arrays for each of the respective orifices. The next set of data

that is read specifies a displacement and an external load on the cylinder Since the program considers only two legs of the bridge to be active at a time and the open center may or may not be active, a check is made of the signs of the specified load and displacement and the appropriate legs of the bridge are solved. For a given displacement, an interpolation scheme is used to calculate the metering areas of each leg of the bridge and the open center orifice.

Linear orifice equations are used to determine initial estimates of unknown flow rates, and pressures within the valve. However, for a correct solution to be obtained, the nonlinear orifice equation for each orifice must be solved simultaneously. A Newton-Raphson technique for solving simultaneous, nonlinear, algebraic equations is used to achieve these results. The Jacobian matrix of the six equations that describe the pressures and flow rates at the various ports of the valve is computed. Inversion and multiplication of this matrix by a vector whose elements are the differences between the linear estimates and the nonlinear calculations based on these estimates provides a simultaneous solution to the nonlinear, algebraic equations. These results are compared with the trial valves obtained from the linear equations. If the error in the calculations is within a limit specified by the user, the remaining unknowns are calculated. If the error is unsatisfactory, the program iterates through the linear and nonlinear calculations until it converges to the specified error limits.

A further safeguard is provided by checking the calculations made for the supply flow. If the tolerance is unacceptable the iteration is done again until it converges to the specified tolerance level. The final solution of bridge equations prints all of the pressures and flow rates for each orifice of the valve as well as the flow rates into and out of the hydraulic cylinder and its output velocity. The entire sequence is repeated until the input data list is depleted.

This program provides a fast and reasonably accurate technique for the calculations of unknown pressures and flow rates for each orifice of an open center directional control valve. The results that are obtained by this program are for static analyses only. Although the program considers the load on the valve to be a cylinder, the case of a rotary motor load could be analyzed by changing part of the input data to the program.

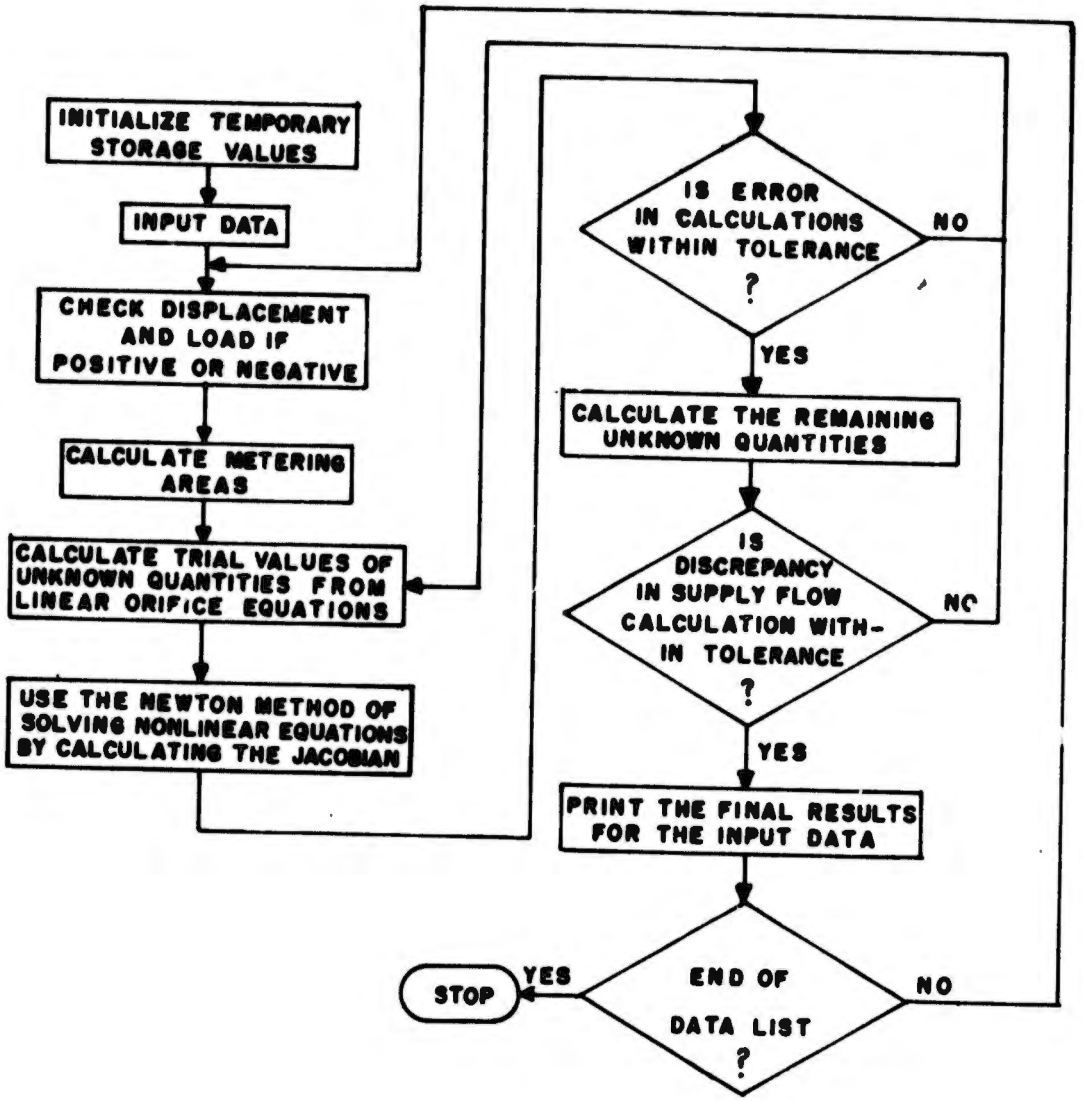

Fig. D-1. Flow Chart of Open-Center System Analysis Computer Program

APPENDIX E

CLOSED CENTER FOUR-WAY VALVE ANALYSIS PROGRAM

APPENDIX E

- CLOSED CENTER FOUR-WAY VALVE ANALYSIS PROGRAM -

It was previously noted that open center directional control valves are more commonly used than closed center valves. However, this does not mean that closed center valves are not used. Many hydraulic systems on mobile equipment, machine tools, and in fluid logic networks rely totally upon a closed center valve as the controlling element in the operation of the system. Systems which employ these hardware elements are "closed center" systems.

In the design stages of such systems a preliminary computer analysis provides insight towards problems which can arise. Thus, system designers can make the necessary alterations to alleviate many problem areas before the hardware is implemented. This served as the motivation for the computer program that is discussed below.

A flow chart of a computer program which performs a static analysis of a closed center system is shown in Fig. E-1. The system that is analyzed by this program consists of a pump, a four-way, closed center directional control valve, a hydraulic cylinder, and a reservoir. This program is similar to the one for the open center system in that it too is based upon the wheatstone bridge analogy of the directional control valve. However, there is a major difference in the methods that are used to solve the nonlinear equations of the bridge analogy. The open center program uses Newton-Raphson technique for solving simultaneous, nonlinear, algebraic equations while the closed center program uses an iterative scheme to converge to preset tolerance levels on the various flows through the legs of the bridge.

The operation of the program begins with the initialization of storage elements. Data is read into the program and consists of spool displacements for each orifice, metering characteristics of the orifices, cylinder loads and dimensions, and fluid density and flow rates. All four legs of the bridge may or may not be active simultaneously, depending upon the magnitude of the input displacement. The metering areas of the orifices are calculated and an iterative process to solve the nonlinear bridge equations is initiated. The flow rates that are calculated for the different legs of the bridge must converge to a specified tolerance before the program can proceed. If the calculated supply flow is not within a preset tolerance, a correction is made for it and the nonlinear bridge iteration scheme is repeated. When the numerical calculations converge to the specified tolerance levels, the various pressures and flow rates of the respective legs of the bridge, the supply pressure and flow rate, and the cylinder flow rates, loads, and velocity are all printed out.

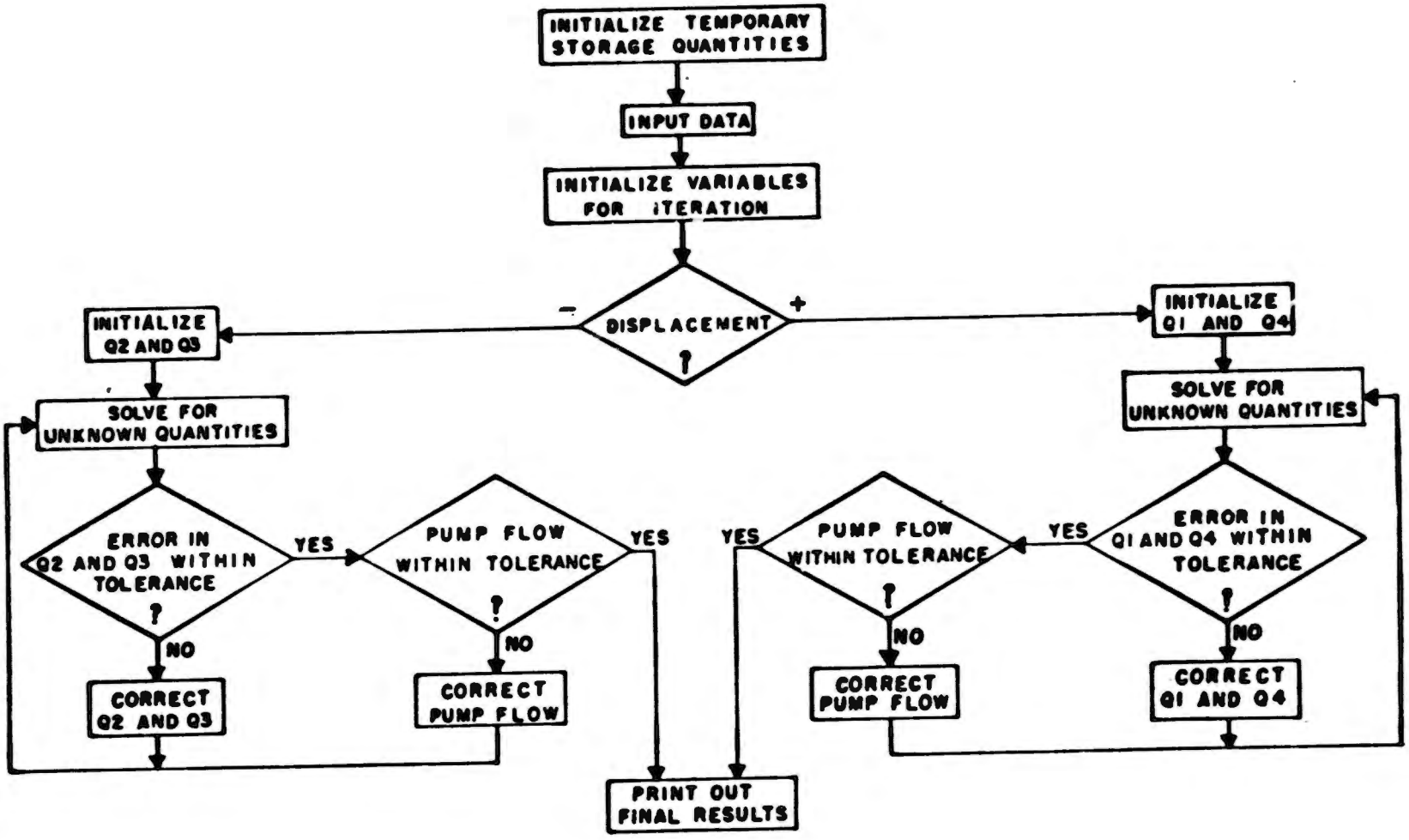

Fig. E-1. Flow Chart for Solving a Closed-Center Valve.

In contrast to the program for the open center system, this program does not utilize a data list for multiple calculations. Only one set input conditions can be handled at a time, and the program must be re-executed for another set of input conditions. With the appropriate modifications in the input data, the case of a hydraulic motor load can be simulated.

The computational ability of this program is attractive in that it does provide a numerical solution to the nonlinear equations which describe the static operation of a four-way directional control valve. The numerical results provided by this program are by far superior to those obtained from equivalent linearized methods. A linearized analysis is generally worked out by hand and is at best a long and tedious process. It is also generally valid only for small perturbations about a steady-state oeprating point. The program described here solves the nonlinear bridge equations in a minimal amount of time and is valid for the entire operating range of the system.

APPENDIX F

FIRST DRAFT OF
DYNAMIC FLOW FILTER PERFORMANCE TEST

APPENDIX F

METHOD FOR DETERMINING THE PERFORMANCE OF A FLUID POWER FILTER ELEMENT UNDER DYNAMIC FLOW CONDITIONS

(OSU-F-6)

1.0 SCOPE: To appraise the performance of a fluid power filter under the influence of cycling flow.

2.0 PURPOSE: To evaluate the multi-pass performance characteristics of a filter when subjected to a cycling flow environment in order to simulate realistic system conditions.

3.0 TEST PROCEDURE

3.1 Modify the standard multi-pass test circuit as specified in NFPA Standard T3.10.8.8-1973 to include a flow by-pass valve as shown in Fig. G-1.

3.2 Install the test filter element in the modified test circuit.

3.3 Perform the standard multi-pass filter performance test as specified in NFPA Standard T2.3.8.8-1973.

3.4 Repeat Step 3.3 with the flow rate cycle given below.

3.4.1 The magnitude of the flow cycle should be from zero to 1.5 times rated flow ($\pm$10%).

3.4.2 The frequency of the flow cycle should not be less than 1.0 cycles per second.

4.0 PRESENTATION OF RESULTS

4.1 Record and report all test data as specified in the parent multi-pass filter test.

4.2 Submit an accurate trace of the flow rate versus time cycle which was imposed on the filter during dynamic testing.

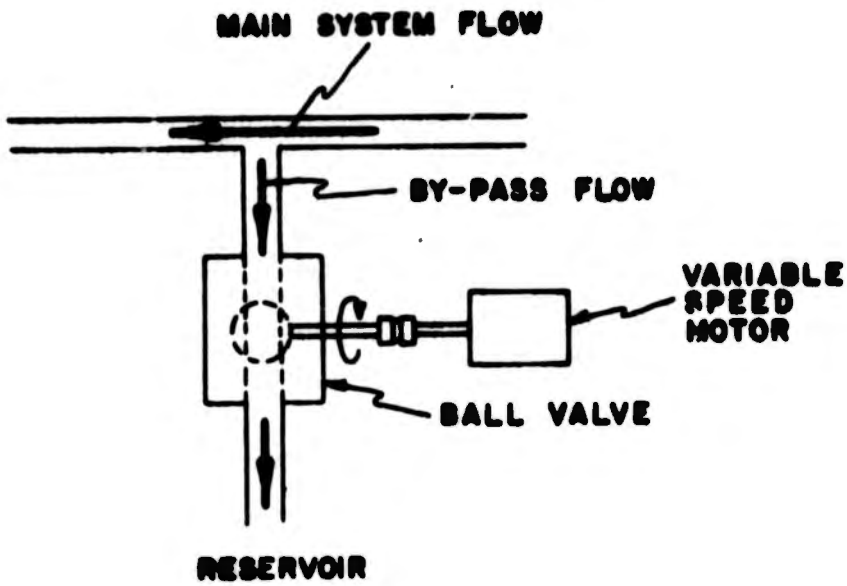

Fig. F-1. Flow By-Pass Valve (Ball Valve).